

**University of Windsor
Scholarship at UWindsor**

Electronic Theses and Dissertations

1974

**An investigation of acoustically controlled
turbulence amplifiers.**

Gary W. Rankin
University of Windsor

Follow this and additional works at: <http://scholar.uwindsor.ca/etd>

Recommended Citation

Rankin, Gary W., "An investigation of acoustically controlled turbulence amplifiers." (1974). *Electronic Theses and Dissertations*. Paper 1103.

This online database contains the full-text of PhD dissertations and Masters' theses of University of Windsor students from 1954 forward. These documents are made available for personal study and research purposes only, in accordance with the Canadian Copyright Act and the Creative Commons license—CC BY-NC-ND (Attribution, Non-Commercial, No Derivative Works). Under this license, works must always be attributed to the copyright holder (original author), cannot be used for any commercial purposes, and may not be altered. Any other use would require the permission of the copyright holder. Students may inquire about withdrawing their dissertation and/or thesis from this database. For additional inquiries, please contact the repository administrator via email (scholarship@uwindsor.ca) or by telephone at 519-253-3000ext. 3208.

AN INVESTIGATION OF ACOUSTICALLY
CONTROLLED TURBULENCE AMPLIFIERS

A Thesis

Submitted to the Faculty of Graduate Studies
through the Department of Mechanical Engineering
in Partial Fulfillment of the requirements for
the Degree of Master of Applied Science at
the University of Windsor

by

Gary W. Rankin

B. A. Sc. The University of Windsor, Ontario, Canada, 1971

Windsor, Ontario, Canada

1974

© Gary W. Rankin

537107

ABSTRACT

The static and dynamic characteristics of shrouded, acoustically controlled turbulence amplifiers are investigated. The static characteristics study includes a variation of shroud diameter, gap length and supply flow conditions.

Existing analytical and empirical relationships are evaluated for the purpose of predicting these characteristics.

It is found that the analytical procedure employed by Bell (Ref. 14) for unshrouded, flow controlled turbulence amplifiers reasonably describes the laminar jet pressure recovery of shrouded turbulence amplifiers. Bell's approximate method for quickly determining the maximum pressure recovered with a laminar jet is modified for operating points which are lower than the maximum. The turbulent jet recovery pressure given by Bell's procedure is not in agreement with the experimental results of this investigation.

A "jump" in the characteristic frequency occurs as the Reynolds number of the emitter tube is increased. The lower characteristic frequency can be predicted by an advanced Helmholtz resonator theory.

It is also shown that the acoustically controlled, unlike the flow controlled, turbulence amplifier can be operated in the proportional mode over a limited range of control variables.

A dynamic characteristic study is performed for

one geometrical shape with varying supply flow conditions.

Both the laminar - turbulent ("switch-off") and the turbulent-laminar ("switch-on") characteristics are investigated.

The "switch on" and "switch off" characteristics of the acoustically controlled turbulence amplifier are more equal and less erratic than the flow controlled turbulence amplifier. The existing theoretical and empirical studies of these response times, originally developed for the flow controlled turbulence amplifier, agree with the present experiments only in general trends.

To my wife and parents

ACKNOWLEDGEMENTS

The author is grateful to Professor W.G. Colborne, Head of the Mechanical Engineering Department, for his interest and continuous support.

The author wishes to express his sincere gratitude to Dr. K. Sridhar for his supervision, generous aid and encouragement throughout the course of this study.

Thanks are also due to Dr. Z Reif and Dr. J. McCorquodale for their efforts in helping the author to better understand the problem.

The technical assistance given by Mr. O. Brady and the staff of the Central Research Shop in constructing the apparatus is gratefully acknowledged. Thanks are also due to Miss Jane Adair and Mrs. D. Abbott for typing the manuscript.

The author wishes to thank his wife, Janice, and his parents for their support and understanding.

The work was financially supported through a Gulf Oil Canada Ltd. Graduate Fellowship and a Bell Canada Centennial Fellowship.

6.

TABLE OF CONTENTS

	PAGE
ABSTRACT	iii
ACKNOWLEDGEMENTS	v
TABLE OF CONTENTS	vi
LIST OF FIGURES	viii
LIST OF TABLES	xi
NOMENCLATURE	xii
CHAPTER I	1
INTRODUCTION	1
CHAPTER II	3
LITERATURE SURVEY	3
2.1 Flow Controlled Turbulence Amplifier	3
2.1.1 Analysis of Static Performance	3
2.1.2 Dynamic Performance	5
2.2 Acoustically Controlled Turbulence Amplifier	6
2.2.1 Analysis of Performance	7
2.3 Jet Sensitivity to Sound	8
2.4 Helmholtz Resonators	12
CHAPTER III	14
EXPERIMENTS	14
3.1 Objectives	14
3.2 Test Facilities	14
3.2.1 Turbulence Amplifiers	14
3.2.2 Test Facility	16

	PAGE
3.3. Experimental Procedure	18
3.3.1 Calibration	18
3.3.2 Setting up the Turbulence Amplifier	19
3.3.3 Static Characteristic Study	20
3.3.4 Dynamic Characteristic Study	22
CHAPTER IV	24
RESULTS AND DISCUSSION	24
4.1 Static Characteristics	24
4.1.1 Emitter Tube Characteristics	24
4.1.2 Output Pressure versus Supply Pressure ²	24
4.1.3 Output Pressure versus Frequency	27
4.2 Dynamic Characteristic Study	34
CHAPTER V	36
CONCLUSIONS	36
CHAPTER VI	38
RECOMMENDATIONS	38
REFERENCES	39
FIGURES	43
TABLES	80
APPENDICES	81
A Dimensional Analysis	81
B Uncertainty Analysis	84
C Equipment Table	91
D Analytical Methods	93
E Experimental Data	107
VITA AUCTORIS	139

LIST OF FIGURES

	PAGE
Fig. 1 Turbulence Amplifier Principle	43
(a) "On State"	43
(b) "Off State"	43
Fig. 2 Basic Helmholtz Resonator	44
Fig. 3 Experimental Turbulence Amplifier and Support	45
Fig. 4 Test Facility	46
Fig. 5 Calibration Curve for (ROTA L10/400-6185) Rotameter	47
Fig. 6 Calibration Curve for (ROTA L2.5/100-3458) Rotameter	48
Fig. 7 Response Time Definitions	49
Fig. 8 Supply Flow Rate Versus Supply Pressure	50
Fig. 9 Output Pressure Versus Supply Pressure	51
(a) $g = 3.81 \text{ cm.}$	51
(b) $g = 2.54 \text{ cm.}$	52
(c) $g = 1.27 \text{ cm.}$	53
Fig. 10 Non-Dimensional Laminar Pressure Recovery	54
Fig. 11 A Test of the Polynomial Fit	55
Fig. 12 Non-Dimensional Gap for Transition Versus Reynolds number	56
Fig. 13 Output Pressure versus Frequency at Constant Supply Pressure	57
(a) $dc = 2.54 \text{ cm.}, g = 3.81 \text{ cm.}$	57
(b) $dc = 2.54 \text{ cm.}, g = 2.54 \text{ cm.}$	58
(c) $dc = 2.54 \text{ cm.}, g = 1.27 \text{ cm.}$	59

	PAGE
(d) $dc = 1.27 \text{ cm.}, g = 3.81 \text{ cm.}$	60
(e) $dc = 1.27 \text{ cm.}, g = 2.54 \text{ cm.}$	61
(f) $dc = 1.27 \text{ cm.}, g = 1.27 \text{ cm.}$	62
(g) $dc = 0.95 \text{ cm.}, g = 3.81 \text{ cm.}$	63
(h) $dc = 0.95 \text{ cm.}, g = 2.54 \text{ cm.}$	64
(i) $dc = 0.95 \text{ cm.}, g = 1.27 \text{ cm.}$	65
Fig. 14 Strouhal Number Versus Non-Dimensional Shroud Diameter and Gap Length	66
Fig. 15 Output Pressure Versus Control Sound Pressure Level at the Characteristic Frequency	67
(a) $dc = 2.54 \text{ cm.}$	67
(b) $dc = 1.27 \text{ cm.}$	68
(c) $dc = 0.95 \text{ cm.}$	69
Fig. 16 Proportional Mode of Operation	70
Fig. 17 Non-Dimensional Turbulent Pressure Recovery Data	71
Fig. 18 Output Pressure Versus Frequency for Different Reynolds Numbers	72
(a) $dc = 0.95 \text{ cm.}$	72
(b) $dc = 2.54 \text{ cm.}$	73
Fig. 19 Characteristic Frequency Variation with Reynolds Number	74
Fig. 20 Comparison of Characteristic Strouhal Numbers with Jet Sensitivity Information	75
Fig. 21 Effects of Control Sound Variables on Response Time	76
Fig. 22 Multiple Traces of Switching	77

PAGE
78

Fig. 23 Hayes Multiple Trace

Fig. 24 Response Time Variations With Supply
Pressure

79



x

LIST OF TABLES

I Summary of Test Program

Page

80

NOMENCLATURE

- A Area, (m^2)
B end correction for the Helmholtz resonator neck (m)
B.N.L. background noise level (db.)
c speed of sound (m/sec.)
D Non-dimensional cavity diameter dc/ds
d diameter (m)
f frequency of sound (Hz.)
G non-dimensional gap length g/ds
g gap length (m)
h effective depth of Helmholtz Resonator (see Equ. D.4.1) (m)
K laminar jet matching parameter
L non-dimensional length ℓ/ds
 ℓ . length (m)
N number of vent holes
P gage pressure (N/m^2)
Q flow rate ($\text{m}^3/\text{sec.}$)
Re Reynolds number of the supply tube $\frac{U_s}{v}$
St Strouhal number $\frac{f ds}{U_s}$
T temperature ($^{\circ}\text{C}$)
T ℓ .d. laminar - turbulent delay time (m.sec.)
Tf. laminar - turbulent fall time (m.sec.)
Tt.d. turbulent - laminar delay time (m.sec.)
Tr. turbulent - laminar rise time (m.sec.)
U average velocity (m/sec.)
V volume (m^3)

β momentum correction factor
 λ wavelength (m)
 δ displacement thickness at the nozzle exit (m)
 μ dynamic viscosity (kg/sec.m.)
 ν kinematic viscosity (m²/sec.)
 ρ density of fluid ($\frac{\text{kg}}{\text{m}^3}$)

Subscripts

a ambient
c control
char. characteristic
c.l. centerline
m.s. maximum sensitivity
n Helmholtz resonance neck
o output
r Helmholtz resonance
s supply
v venthole

CHAPTER I

INTRODUCTION

In general the principle of the turbulence amplifier is based upon the fact that a normally laminar jet can be made turbulent by subjecting it to certain external disturbances. The method employed to disturb the laminar jet is one criterion used to distinguish between different types of turbulence amplifier.

The basic configuration of the turbulence amplifier consists of two, small diameter, tubes located on a common centerline, with a gap between them, as shown in Fig. 1(a). The longer tube serves as a supply tube (emitter) from which a laminar jet is directed across the gap towards a second (collector) tube. This laminar jet will naturally become turbulent at some distance downstream and therefore the gap spacing must be less than this natural laminar length. The laminar jet hitting the collector causes a relatively high pressure to be recovered. This condition is referred to as the "on" state of the turbulence amplifier.

The presence of a control signal disturbance causes the laminar-turbulent transition position to move towards the emitter. Usually, only a small disturbance is needed to cause the laminar-turbulent interface to be shifted to a stable position close to the emitter exit as shown in Fig. 1(b). Because the turbulent jet spreads more than the laminar jet the pressure that is recovered at the receiver is considerably less. This condition is referred to as

the "off" state of the turbulence amplifier.

The most common methods used to disturb the laminar jet are by impinging a control jet onto the main jet, transversely, near the emitter exit or by subjecting the main jet to sound at this position. These types of turbulence amplifiers are referred to as "flow controlled" and "acoustically controlled" respectively.

Another distinct classification can be made depending upon whether the main jet is enclosed in a protective cover referred to as a "shroud".

The main objective of this study is to investigate some of the characteristics of "shrouded, acoustically controlled" turbulence amplifiers. These characteristics may be discussed in terms of two types, static and dynamic.

The static characteristics involve the determination of the output pressure variation with such variables as the supply pressure, gap length, shroud diameter, control sound pressure level and frequency.

The dynamic characteristics involve measurement of the switching times from the "on" to the "off" state and vice versa for certain static characteristic settings referred to as operating conditions.

CHAPTER II

LITERATURE SURVEY

The material presented in this section summarizes briefly the existing literature which is pertinent to the study of acoustically controlled turbulence amplifiers.

2.1 Flow Controlled Turbulence Amplifier

Auger (Ref. 3) introduced the turbulence amplifier in 1962. In this and his subsequent papers (Ref. 4 and 5) emphasis was on describing the basic principle of the device and possible means of control (including acoustic). He also listed several advantages, disadvantages and possible applications. However, no rational analytical or experimental procedure was given to predict the operating characteristics of the device.

Because of the relative ease with which an operable turbulence amplifier could be constructed, a variety of devices were manufactured, marketed and applied. These included both planar and axisymmetric, shrouded and unshrouded configurations.

2.1.1 Analysis of Static Performance

Oels, Boucher and Markland (Ref. 30) were the first to publish results of a systematic experimental study of axisymmetric, shrouded and unshrouded turbulence amplifiers. They presented some design guidelines concerning the emitter length to diameter ratio L_s and the maximum output pressure available.

Verhelst (Ref. 41) presented an experimental design procedure for choosing the operating conditions of an amplifier of certain fixed geometry. However, if the geometry was changed a new set of experimental curves was required to determine the operating points and predict the amplifier performance.

Bell (Ref. 13 and 14) was the first to consolidate theory and experiment to produce an analytical procedure that reasonably describes the unshrouded, flow controlled turbulence amplifier. He separated the turbulence amplifier into its characteristic sections considering the tube flows, laminar jet, turbulent jet and receiver pick up. To model the flow in the tubes (emitter, collector and control) of the amplifier, which in most cases is developing, he used Hornbeck's (Ref. 26) open form solution. To avoid the open solution he interpolated from a table given by Hornbeck.

For the laminar jet he used Schlichting's (Ref. 34) point source model, employing centerline velocity matching to approximate the jet issuing from a source of finite size.

For the turbulent jet he used the Goertler jet model (Ref. 34) with the condition that the virtual origin was at the jet exit. This was to account for the fact that the control jet which caused the jet to become turbulent was located at a distance of 2 nozzle diameters downstream, and the exact position where the turbulent jet began, after the control, was not accurately known.

Bell calculated the blocked load output pressure in the receiver knowing the centreline velocity of the jet at the mouth. This decision was based on previous work cited in his paper.

The only characteristic which could not be predicted analytically was the natural laminar length of the jet. To aid in determining this value he presented his experimental results and those of two other investigators. Other researchers such as Gradetsky (Ref. 22), Vaz (Ref. 40), Marsters (Ref. 27) and McNaughton and Sinclair (Ref. 28) have studied this problem and can be consulted for further information.

The computer program that was written to perform calculations using Bell's analytical procedure is given in Appendix D.1.

2.1.2 Dynamic Performance

Several early investigators (Ref. 3, 4, 5, 25 and 41) quoted approximate values for the switching times of flow controlled turbulence amplifiers.

Siwoff (Ref. 35) demonstrated that by "inbuilding" an edge between the emitter and collector such that this edge almost touches the laminar jet, the switching time could be reduced.

Hayes (Ref. 23) was the first to perform a comprehensive experimental study of the geometrical and flow variables affecting the response time. He also developed an analytical

model to predict the switching times of turbulence amplifiers. The resulting equations for the model are presented in Appendix D.2.

Experiments indicated that the shroud geometry of the amplifier affected the switching times considerably. The laminar-turbulent switching time was not equal to the turbulent-laminar time. This difference increased as the gap length was made larger or the shroud diameter smaller. It was also noticed that the turbulent-laminar switching time was quite erratic. This uncertainty increased with gap length and decreased with shroud diameter.

Abramovich and Solan (Ref. 1) found experimental correlations for the laminar-turbulent and turbulent-laminar switching times for a jet and described how these could be applied to the flow controlled turbulence amplifier. The correlations obtained are given in Appendix D.3.

2.2 Acoustically Controlled Turbulence Amplifier

Auger (Ref. 5) noticed that his turbulence amplifier was sensitive to sound at frequencies of approximately 8 KHz and the sensitivity to sound increased with a larger gap between the emitter and collector. He dealt mainly with applications of the device in the remainder of the paper.

Generally, in the literature, two attitudes were prevalent regarding the sensitivity of the turbulence amplifier to sound. The first one involved the identification of the problem areas of a flow controlled turbulence amplifier

(response to external noise) (Ref. 12 and 23). The other involved a direct use of the phenomenon as an acoustic-fluidic transducer or a switch. In this survey emphasis is given to the papers concerning the second attitude mentioned.

Also, some investigators studied the bistable fluid amplifier as an acoustic-fluidic switch (Ref. 15, 21, and 39). However, these references will not be discussed as they do not pertain to the turbulence amplifier.

2.2.1 Analysis of Performance

In 1968 Gradetsky (Ref. 22) experimentally studied two acoustically controlled turbulence amplifiers. He measured the output pressure drop with control sound over a frequency range from 200 - 10,000 Hz. At the same time the sound pressure level inside the cavity was measured. He noticed that the output pressure dropped appreciably at resonance conditions inside the cavity. However, these resonant frequencies did not correspond to those predicted using the basic Helmholtz formula (without the correction factors).

Nomota and Shimada (Ref. 29) studied what can best be described as an electric-fluidic transducer based upon the principle of acoustic control of a laminar jet. They showed that the laminar jet could be sensitive to frequencies up to 50 KHz. The sound pressure levels used in the study were not measured. Also it was noted that the acoustically controlled turbulence amplifier switching time was small, without giving any numerical values.

Beeken (Ref. 11) described the commercial form of an acoustically controlled turbulence amplifier and an acoustic generator. He mentioned possible methods of using these devices in various applications.

Tryburcy (Ref. 37) did a more comprehensive study of displacement and proximity sensing applications. A generator and sensor similar to Beeken's were used. He studied the maximum separation distance and the sensitivity of the devices as a combined unit.

2.3 Jet Sensitivity to Sound

As mentioned by Rayleigh (Ref. 32) the acoustical sensitivity of jets has been the subject of scientific study since 1858 when Leconte first noticed the "jumping" nature of a coalgas flame in response to certain notes being played on a musical instrument. Initially, the phenomenon was associated only with burning jets. However, it was shown by Tyndall that combustion was not a necessary condition for the phenomenon. Rayleigh's personal contribution was to theoretically show that inviscid plane jet flows are always unstable.

Subsequent to these early investigations, a considerable amount of work was done on both two-dimensional and axisymmetric jets. Although there is a similarity of behaviour in both cases, emphasis is on the axisymmetric case in the remainder of this section because of the present experimental arrangement. Papers concerning the instability of axisymmetric jets due to

very small internal disturbances are included because of their direct relationship to the instability caused by sonic disturbances.

Batchelor and Gill (Ref. 7) solved the inviscid stability equations for an axisymmetric parallel jet. They determined that a point of inflection in the velocity profile is a necessary condition for any disturbance in the jet to be amplified. Such a point always exists downstream in a jet. This condition occurs closer to the nozzle exit for a flat velocity profile than for a parabolic one.

Viilu (Ref. 42) experimentally determined, using flow visualization, that for a real jet, a minimum Reynolds number exists below which the jet is always stable to small disturbances. He found this value to be approximately 11.

Freymuth (Ref. 20), using a hot-wire technique, experimentally studied the growth of small sonic disturbances in a jet issuing from a nozzle with a flat velocity profile except for the boundary layer. He noticed that transition of the jet to a turbulent state begins very near the nozzle exit. The effects of jet supply pressure, compressibility, viscosity and sound frequency were investigated in terms of nondimensional parameters. The characteristic length and velocity used were the local momentum thickness and the centerline velocity respectively. The only term which had an important effect on the transition was the Strouhal number. The wavelength of the vortices produced in the jet increased as the Strouhal number decreased.

Becker and Massaro (Ref. 9) used smoke photography, stroboscopic observation and a light scattering technique to study a jet emerging from a nozzle. The displacement thickness at the nozzle exit (δ) could be determined from the experimental correlation shown below:

$$\frac{\delta}{ds} = \frac{0.9}{\sqrt{Re}} \quad --- 2.1$$

They noticed that as the jet velocity increased, the maximum sensitive frequency increased in a stepwise manner. They attributed this to resonance effects in the supply tube. A correlation for the Strouhal number of maximum jet sensitivity and the Reynolds number was found and is given below:

$$St = \frac{fmsds}{U_s} = 0.012\sqrt{Re}; \quad 1000 < Re < 10,000 \quad --- 2.2$$

Their Strouhal number was based on the frequency of sound for maximum sensitivity to the sound, the jet average velocity and the diameter of the jet.

They also measured the growth and frequency of the vortices that occur in the jet due to natural causes and found that the above correlation also held for this case. Hence, the effect of sound is maximum when the sound wavelength is approximately equal to that of the vortices which occur naturally (λ_n). A correlation for λ_n was found as well as for lb , the wave-breaking length defined as the distance from the nozzle exit to the first vortex.

These expressions are given below:

$$\frac{\lambda_n}{ds} = \frac{43}{\sqrt{Re}} \quad 2.3$$

$$\frac{\ell_b}{ds} = \frac{107}{\sqrt{Re}} \quad 2.4$$

It was also noted by observing equations 2.1 and 2.2, choosing ℓ_b as the characteristic length in the Strouhal number that this value would be a constant and independent of Reynolds number. It was then speculated that because a parabolic velocity profile has a constant ratio of displacement thickness to nozzle diameter, the Strouhal number based on the diameter of the jet should be the constant.

A discussion of the jet issuing from a square-edge orifice was also given. In this case it was pointed out that in the flow through an orifice there would be an eddy between the shoulder and the separating flow rounding the shoulder. The eddy size would be proportional to the width of the orifice wall. They postulated that this wall dimension might determine the displacement thickness at the jet exit and hence be independent of orifice diameter.

Such a case was studied by Beavers and Wilson (Ref. 8) and they found the Strouhal number based on orifice diameter to be a constant value of 0.63 over a Reynolds number range of 600 to 3200.

Bell (Ref. 12) studied the sensitive frequency range of round tubes of various ℓ_s/d_s . However, he did not

determine the particular frequencies associated with maximum sensitivity. Jet sensitivity was indicated by the decrease in total pressure measured on the centerline of the jet at the downstream end of the laminar jet length. He found an upper Strouhal number limit of approximately 0.5. The lower limit increased with Reynolds number.

2.4 Helmholtz Resonators

The Helmholtz resonator shown in Fig. 2 essentially consists of a relatively large cavity with a narrow opening (neck) connecting the fluid inside to the surrounding medium. When the opening is subjected to an acoustical signal the frequency of which corresponds to the natural frequency of the resonator, the amplitude of the sound signal inside the cavity increases above that of the impressed sound.

A theoretical model of the resonator was developed about one hundred years ago, according to Rayleigh (Ref. 32) and is given below.

$$f = \frac{c}{2\pi} \sqrt{\frac{A_n}{V c l n}}$$

--- 2.5

This is essentially a lumped parameter model assuming that the only mass being accelerated is in the neck of the resonator. The fluid inside the volume is considered as a spring and the resonant frequency is considered to be independent of the shape of this cavity volume.

Not long after this formula was developed it was found to be in considerable error in predicting the resonant

frequency when the length of the neck was short. This was attributed to the fact that the fluid just inside and that just outside of the neck was also undergoing some acceleration. A correction factor was added as indicated below, (Ref. 36)

$$f_r = \frac{c}{2\pi} \sqrt{\frac{A_n}{V_c (\ell n + B)}} \quad \text{--- 2.6}$$

It was shown that for necks approaching the configuration of an orifice in a plate the value of

$$B = \frac{\pi d n}{4} \quad (\text{Ref. 36}).$$

Alster (Ref. 2) showed that the shape of the resonator does affect the resonant frequency and developed a complicated theoretical formula to account for this. The general formula that was developed has the restrictions that any dimension of the resonator $\ll \frac{\lambda r}{4}$ and $h \ll dn$.

The particular expression for a circular cylinder with a centred lateral hole along with the definitions of terms used are given in Appendix D.4.

CHAPTER III

EXPERIMENTS

3.1 Objectives

Although acoustically controlled turbulence amplifiers can be obtained commercially, little work has been published on a systematic experimental investigation of this device.

The present investigation aims to provide information of primary importance to the operation of shrouded, acoustically controlled turbulence amplifiers. This involves the determination of:

- (a) the effect of the shroud on the output pressure with no sound.
- (b) the control sound frequency to which the device is most sensitive (denoted as the characteristic frequency) as a function of the shroud geometry and flow variables.
- (c) the effect of the sound pressure level on the output pressure of the device at the characteristic frequency.
- (d) the dynamic switching times .

3.2 Test Facilities

3.2.1 Turbulence Amplifiers

To accomplish the objectives described in the previous section three turbulence amplifier shrouds were designed and fabricated. An axisymmetric, as opposed to a planar, geometry was chosen because of the manufacturing ease and availability of theoretical analyses.

The shrouds are identical except for the diameter and made of plexiglass. Each consisted of two sections, a barrel and an end plate. A schematic diagram with pertinent dimensions is shown in Fig. 3.

The barrel was made so that it fit tightly over the emitter tube at the lowest position. To allow for fine alignment of the emitter and collector the hole for the emitter tube, in the barrel, was drilled slightly larger than the emitter outside diameter over approximately 7/8 of the length of the hole.

In order to provide a means of moving the barrel for alignment two sets of thumb screw tighteners were attached to the end plate with an angle of 120° between them. The other ends of the thumb screws were rigidly attached to the settling chamber which is described later.

In order to vary the gap length between the emitter and the collector the hole for the collector was machined slightly larger than the tube. A set screw was provided for fastening the collector.

A modified DISA subminiature hot-wire (5 micron dia.; 0.45 mm. length) was mounted such that the hot-wire was on the centerline of the collector, approximately 0.25 mm. in front of the mouth. The hot-wire was also held in position by a set screw fastener.

3.2.2 Test Facility

Figure 4 shows a schematic diagram of the general experimental facility that was used to test the amplifiers. Air from the building compressed air facility was passed through a 3 micron filter, pressure regulators, needle valve and rotameters before entering a large settling chamber (approximately 15.24 cm. dia.; 50.8 cm. length) which contained screens, flow straighteners and pressure taps connected to an inclined manometer for measurement of the supply pressure (P_s). A bellmouth entrance led to the inlet of the emitter tube of the turbulence amplifier. Further information concerning the settling chamber, bellmouth and emitter tube construction can be found in Ref. 40.

The output pressure (P_o) was measured by connecting the collector tube to a second inclined manometer.

The control sound was provided by passing the signal from a sine wave oscillator through an electronic switch, power amplifier and speaker. The frequency of this signal was measured with an electronic counter. A speaker was mounted on a tripod (not shown in Fig. 4) in such a way that it was aligned with the control hole opening of the turbulence amplifier and approximately 5cm. in front of it. A trigger signal, needed in the dynamic response tests, was taken from the electronic switch.

The sound measuring equipment consisted of a standard B&K microphone (Type 4138), preamplifier (Type 2618) and measuring amplifier (Type 2607). The microphone was held

in position approximately 3mm. in front of and 2mm. to the side of the control opening. The microphone was secured by means of a specially designed holder (not shown in Fig. 4) which fastened onto the settling chamber. The holder allowed positioning of the microphone at various positions in front of the control opening. A traverse of the area around the control opening indicated a uniform sound field, hence, the position of the microphone mentioned previously, was found to be acceptable.

The signal from the measuring amplifier was displayed on one channel of a dual beam oscilloscope. The second channel was connected to a DISA Type 55M10 hot-wire anemometer for the dynamic tests..

In order to provide a controlled acoustic environment for the turbulence amplifier the items shown within the dashed lines in Fig. 4 were kept inside a "soft" room enclosure. The tubes and wires required for the auxiliary equipment, that was kept outside of the room, were passed through a small hole in the enclosure. This hole was then plugged with plasticine. The "soft" room enclosure was a modified "walk-in" refrigerator. The inside dimensions were 2.79 m. by 3.38 m. by 2.29m. high. The walls, ceiling, floor and door of the refrigerator consisted of thin sheets of steel separated by approximately 7.62 cm. of styra-foam insulation. In addition to the existing structure approximately 7.62 cm. of polyurethane foam was adhered to the inner walls and ceiling of the refrigerator and also around the refrigeration unit which occupied one corner of

the room. The same thickness of foam was laid on the floor, however, it was not adhered in order to facilitate movement of the tripod and settling chamber. Both the tripod and settling chamber were sitting solidly on the main floor of the refrigerator with polyurethane foam around them.

A complete list of the standard equipment and instruments mentioned in this section is given in Appendix A along with the pertinent information concerning them.

3.3 Experimental Procedure

The material in this section naturally falls into the following categories; calibration, setting up the turbulence amplifier with alignment of the emitter and collector, static characteristics and dynamic characteristics. The geometrical variables and a summary of the test programme are given in Table I.

3.3.1. Calibration

The three types of equipment which are considered in this section include the rotameters, sound measuring equipment and the hot-wire.

Two rotameters were used in this study, the ROTA L10/400 - 6185 and the ROTA L2.5/100 - 3485. Both of these were calibrated by installing a precision wet test meter in series with them. The calibration curves for these two rotameters are shown in Fig. 5 and 6.

The sound measuring equipment which required calibration included the B&K microphone, preamplifier, and measuring amplifier combination. The procedure that was used

is a standard one given in Ref. 6 using the B&K Type 4220 Pistonphone and therefore will not be repeated here. This calibration was performed each time the equipment was used.

In this study it was not necessary to calibrate the particular hot-wire anemometer to obtain a relationship between velocity and voltage because velocity was not actually measured. Only time readings were taken, hence, it was only necessary that the hot-wire and anemometer respond fast enough. Therefore, the standard procedure given in Ref. 18 for adjusting and measuring the time constant was performed. The time constant measured was approximately 2 microseconds.

3.3.2 Setting up the Turbulence Amplifier

A standard procedure was developed for setting up the turbulence amplifier shroud on the test stand and aligning the emitter and collector. This procedure was followed for each turbulence amplifier to assure consistency.

After a particular shroud was fitted onto the common emitter tube, the exit of the emitter tube was observed under a microscope to determine if any dirt particles were present. Any such particles were brushed away using a small, clean paint brush of the type artists use.

The emitter tube-shroud assembly was then bolted onto the settling chamber using vaseline as a sealant.

The dimensions C and D in Fig. 3 were measured using a vernier caliper and the dimension E calculated to obtain the required gap setting. This value was then set by positioning the collector tube and fastening it with a set

screw. For the static characteristic study the hot-wire hole was plugged so that the inside surface was smooth. For the dynamic characteristic study the hot-wire was positioned at a small (but safe) distance from the mouth of the collector (approximately 0.25 mm.). It was centered over the opening by observing the setting under a microscope.

In both cases the end plate was then attached to the shroud by means of three screws, two of the screws were used to secure the adjustable thumb screws to the shroud as shown in Fig. 3.

The supply pressure was then increased until the output pressure dropped, indicating that the jet had become turbulent. The collector tube and shroud were moved by means of the adjustable thumb screws until the output pressure rose above the value before the drop. The supply pressure was increased again until another output pressure drop occurred. This procedure was repeated until it was not possible to increase the output pressure by any further adjustment of the alignment.

This was an extremely tedious procedure, taking as long as 3 hours to be reasonably sure that the proper alignment had been achieved.

3.3.3. Static Characteristic Study

(A) Output Pressure versus Supply Pressure

For all the geometrical combinations given in Tables I, the ouput pressure P_o and supply

flow rate were measured for different values of supply pressure P_s . This was done until P_o dropped and began to increase again.

Results from these tests were used to obtain the P_o versus P_s plots and select the different operating conditions for P_s .

(B) Output Pressure versus Sound Variables (Constant Re)

With P_s set at a particular value, P_o was measured for different values of the control sound frequency f and pressure level P_c . For all the geometrical combinations, the conditions used were: $P_s = 660 \text{ N/m}^2$ ($Re = 895$); $P_c = 90, 100, 110, \text{ and } 120 \text{ db}$; and $170 < f < 18000 \text{ Hz}$.

This portion of the investigation was done with the specific aim of holding the Reynolds number constant, so that the effects of shroud geometry could be brought out more clearly.

(C) Output Pressure versus Sound Frequency (Different Re)

For a given value of P_c , P_o was measured for different values of f and P_s or Re in order to study the Reynolds number effects. However, this type of experimentation was carried out for two geometrical configurations only. With the $d_c = 0.95 \text{ cm.}$ and $g = 1.27 \text{ cm.}$ configuration $P_c = 110 \text{ db.}$ and for the $d_c = 2.54 \text{ cm.}$ and $g = 3.81 \text{ cm.}$ configuration $P_c = 100 \text{ db.}$

It should be noted that the ambient pressure, temperature and noise level were measured at the beginning of all the tests mentioned above.

3.3.4 Dynamic Characteristic Study

This study was conducted only for the $dc = 2.54$ cm. and $g = 3.81$ cm. geometrical combination.

The dynamic characteristic study consisted of the measurement of four response times, characteristic of the turbulence amplifier. These times are the laminar-turbulent delay time $T_{l.d.}$, laminar-turbulent fall time $T_f.$, turbulent-laminar delay time $T_{t.d.}$ and the turbulent-laminar rise time $T_r.$ and are defined in Fig. 7. These definitions are similar to those used by Hayes (Ref. 23).

The response times were measured by photographing the trace of the hot-wire signal and the microphone signal which were simultaneously displayed on the screen of the dual-beam scope. At least three traces were photographed for each experimental condition studied. Slides were made from the film and displayed on a screen for measurement.

Such measurements were taken at a supply pressure of 1120 N/m^2 ($Re = 1244$), with control sound pressure levels of 100, 95 and 90 db. Five frequencies were chosen for study, the characteristic frequency (3100 Hz) and two frequencies on each side of this (2200, 2600, 3700 and 4400 Hz).

To investigate the effects of Reynolds number, measurements were also taken at a frequency of 3100 Hz and

sound pressure level of 100db for additional supply pressures of 1220 N/m^2 ($\text{Re} = 1332$), 1030 N/m^2 ($\text{Re} = 1153$) and 834 N/m^2 ($\text{Re} = 991$).

CHAPTER IV

RESULTS AND DISCUSSION

In some of the figures discussed in this chapter a few data points have been omitted in order to avoid overcrowding. However, this omission does not affect the interpretation of the results.

4.1 Static Characteristics

Because of the large number of readings the university I.B.M. 360-65 computer and the on line Calcomp 565 plotter were used to reduce and plot the experimental data.

4.1.1 Emitter Tube Characteristics

The variation of the supply flow with the supply pressure is shown in Fig. 8 along with Bell's prediction. This characteristic is not of much importance to this study as the emitter tube was not altered throughout the experiments. However, it does serve to show that the analytical procedure given by Bell for predicting the emitter tube characteristics holds for this case with about 7.5% difference from the present experimental data.

4.1.2 Output Pressure versus Supply Pressure

The dimensional plots of the output pressure versus the supply pressure for the various diameter shrouds used and a gap setting of 3.81 cm. is shown in Fig. 9 (a). Bell's analytical procedure was used to calculate the laminar recovery pressure for this case and is shown as a dashed line. It should be noted, however, that the supply pressure

at which transition occurs cannot be predicted from the analytical procedure.. Similar plots for gaps of 2.54 and 1.27 cm. are shown in Fig. 9(b) and 9(c) respectively.

It can be seen that the laminar pressure recovered compares reasonably well with the analytical result having a maximum difference of approximately 12%.

To obtain a reasonable estimate of the output pressure for a given turbulence amplifier Bell suggested an approximate graphical method (Ref. 14). He plotted P_o/P_s versus R_e/KGL_s , using only those values of P_o/P_s near the P_o versus P_s peak. In this method it is assumed that the amplifier is to be operated near the peak. In some cases this may not be desirable. It was decided to attempt to obtain a correlation for the laminar pressure recovery without the above mentioned restriction.

A plot of P_o/P_s versus R_e/KGL_s was made as a first attempt. This graph is shown in Fig. 10. In the present investigation L_s is a constant and the jet matching parameter K only varied 2.5% according to Bell's procedure. Hence both were considered constant. The lines through the data points are Bell's prediction for each gap length. Obviously, these scaling parameters are not adequate to describe the phenomenon.

It was decided to attempt a correlation of the form
 $P_o/P_s = A R_e^B G^C$. Multiple linear regression yielded:

$$A = 1.14 \times 10^{-4}$$

$$B = 1.2$$

$$C = -0.27$$

A plot of this correlation along with the data points indicated that the exponent $C = -0.27$ is adequate to merge the three curves in Fig. 10 into one. Further the Reynolds number dependence is not of the form indicated above.

An attempt to fit a curve of the form

$$G^{+0.27} \frac{Po}{Ps} = A + BRe + CRe^2 + DRe^3 + \dots \quad --4.1$$

was undertaken using a standard I.B.M. program package. A second order polynomial was indicated with no further improvement obtained by going to a third order. The constants were

$$A = -0.2$$

$$B = 8.3 \times 10^{-4}$$

$$C = 1.22 \times 10^{-7}$$

A plot of the experimental $G^{0.27} Po/Ps$ versus the $G^{0.27} Po/Ps$ estimated by the equation is shown in Fig. 11 indicating that the agreement is good.

Although the different laminar-turbulent transition lengths cannot be predicted analytically, they can be compared with correlations and the data found by other investigators. A method of indicating this comparison is to plot G for transition versus Re . This plot is shown in Fig. 12 and contains curves found for free and shrouded jets.

It can be seen that even for the unshrouded free jet, large discrepancies exist not only in the magnitudes but in the shapes of the curves. The free jet transition depends upon a large number of variables such as the entrance conditions of the supply jet, ambient noise and the method of measurement. These are not taken into account in a simple plot of the type shown in Fig. 12. It would be expected that the present data would best be described by Vaz's (Ref.40) correlation, due to the fact that the settling chamber, bellmouth and supply tube used in that experiment were also used in the present study. However, a large discrepancy exists in this particular comparison also, indicating that the shroud has a significant effect.

4.1.3 Output Pressure versus Frequency

(A) Effects of Geometrical Variables ($Re = \text{constant}$)

The dimensional plots of output pressure versus the sound frequency at various control-sound pressure levels and a constant supply pressure of 660 N/m^2 ($Re = 895$) for all the geometrical configurations tested are shown in Fig. 13. The straight dashed line is the value of P_0 for the turbulent jet obtained from Bell's procedure. It can be seen that in some of the plots there are two and in others, there is one substantial frequency range where the output pressure drops significantly. Also it is noticed that as the control sound pressure level is reduced, the sensitive frequency range becomes narrower and in some cases disappears.

The following points can be investigated using the information from these plots:

- (1) the variation of the characteristic frequency (defined in Section 3.1) with the geometrical variables dc and g .
- (2) the effects of the control sound pressure level on the output pressure at the characteristic frequency.
- (3) a comparison between the "off" state (turbulent jet) pressure recovery and that obtained using the analytical procedure of Bell.

The characteristic frequency is defined as the frequency at which the output pressure drops the greatest percentage of the undisturbed level. In each of the plots in Fig. 13 this is just the frequency at which ρ_0 is the lowest value. To reduce the error in obtaining $f_{char.}$ for each geometrical combination the value of $f_{char.}$ was obtained for each sound pressure level plot that had a significant drop and then averaged. This value was then expressed in terms of a Strouhal number ($f_{char.} ds$) and the geometrical terms in $G = g/ds$ and $D = dc/ds$. The plot of Strouhal number versus D for various G values is shown in Fig 14. The lines shown are the Strouhal numbers calculated using the frequency obtained from the theoretical formulas for Helmholtz resonators given in the literature survey and Appendix D.2 (Equ. 2.5, 2.6 and D.2.1) using the appropriate velocity and emitter diameter. It can be seen that G has no significant effect as the three points

for different G values at each value of D lie approximately at the same point.

Comparison with the theoretical formulae show that the simple expression (Eqv. 2.5) overestimates the Strouhal number. The addition of the theoretical correction factor B(Eqv. 2.6) overcompensates so that lower values are predicted. The theoretical formula of Alster (Eqv. D.2.1) agrees quite well with the experimental data, even though the effect of the vent holes is ignored. The maximum deviation occurs at $D = 6.94$ with a difference of 12%. This may be expected as Alster points out that errors occur when $\lambda r./4$ is less than the largest dimension of the cavity. Although the condition is not violated in this case it is being approached.

A standard way of showing the effect of the control signal on a flow controlled turbulence amplifier is to plot P_o versus P_c at the operating Reynolds number and characteristic frequency.

Plots similar to this are obtained for the present investigation by taking cross plots of the P_o versus f plots shown in Fig. 13 at the characteristic frequency in each case. The cross plots are shown in Fig. 15. The dashed line in each case indicates the output pressure with only the background noise level present. The output pressure is unaffected by the control signal until a certain level of control is reached. The output pressure then decreases with increasing control to a value which does not change for further increases.

It was not possible to obtain the entire curve for all of the geometrical configurations due to the upper limit imposed by the speaker used and the lower limit set by the loss of accuracy in measurement of the control sound pressure level near the background noise level. However, some general observations can be made.

It is known that the transition from the "on" state to the "off" state of a flow controlled turbulence amplifier requires only a small change in the control pressure signal and it is difficult to maintain an intermediate position between "on" and "off". Also within this range the output has been noticed to consist of large, erratic fluctuations. These characteristics have led to the use of the flow controlled turbulence amplifier only as a digital device.

As can be seen from Fig. 15, the output pressure decreases gradually as the control sound pressure level increases. It was also noted qualitatively that there were no large erratic output pressure fluctuations.

The above discussion leads to the possibility of operating the acoustically controlled turbulence amplifier as a proportional device. To do so the output pressure versus control pressure plot should have a straight portion. The lines passing through the data points in Fig. 15 indicate that this is approximately true for certain geometrical configurations and sound pressure level ranges. More data points would increase the confidence in this observation and hence additional

experimentation was done for one particular case. The results are shown in Fig. 16 which indicate that for the $d_c = 0.95$ cm. and $g = 1.27$ cm. geometry with $P_s = 660$ N/m² ($Re = 895$) and $101 < P_c < 112$ db. a proportional mode of operation is possible. The gain is -9.64 N/m² per db. The gain obtained by expressing the sound pressure as a root mean square pressure in N/m² is -18.5.

In order to compare the "off" state turbulent pressure recovery with the analytical procedure mentioned previously it must be insured that the jet is fully turbulent. The criterion used to determine whether this condition is satisfied is to observe the change in the output pressure at the characteristic frequency as the control sound pressure level is increased (see Fig. 15). If there is no substantial change the jet could "reasonably" be assumed as fully turbulent. The value of the output pressure for 120 db. was then taken as the "off" state pressure. The corresponding values for the geometrical configurations which complied with this criterion were recorded and Bell's non-dimensional parameter $\frac{G^2 P_o}{41.0 P_{c,l}}$ was calculated using an experimental value of $P_{c,l} = 1/2 \rho (2U_s)^2$. Figure 17 shows this parameter as a function of D along with the constant value predicted from the analytical procedure. Unlike the unshrouded flow controlled turbulence amplifier case, the present data lie consistently above the predicted value. This could perhaps be

explained by the assumed location of the virtual origin in the analytical procedure or by the effects of the shroud. However, the number of data points are considered insufficient for further analysis at this time.

(B) Effects of Reynolds Number ($P_c = \text{constant}$)

The dimensional plots of the variation of P_o with f for two geometries at various Reynolds numbers are shown in Fig. 18. The line indicating the analytical turbulent "off" pressure is not shown as only one sound pressure level is used in each case.

The characteristic frequencies at various Reynolds numbers were taken following the definition mentioned previously and plotted against Reynolds number as shown in Fig. 19. The line going to a Re of 400 is shown dotted to indicate that a characteristic frequency was not evident at $P_c = 110$ db. When P_c was increased to 120 db. a characteristic frequency was found.

It is seen that a frequency "jump" occurs for each geometry considered. This is a result of the definition used to determine the characteristic frequency. When the output pressure drop at any frequency becomes larger than the one at the characteristic frequency, this new frequency becomes the characteristic. At the discontinuity, the pressure drops for both frequencies would be the same, hence, $f_{\text{char.}}$ would be double valued at this Reynolds number.

The lower two frequencies correspond to those found from Alster's Helmholtz equation for a circular cylinder with a lateral hole (Equ. D.2.1). The upper frequency is not a harmonic of the lower. Neither supply tube resonance nor resonances related to the cavity could satisfactorily account for the higher characteristic frequency.

By calculating characteristic Strouhal numbers from the frequency data this information can be compared to the upper and lower limits of jet sensitivity to sound found in Ref. 12. Although the investigation cited was not detailed it can serve as a reasonable estimate of the sensitivity of jets emitting from tubes of large L_s . Figure 20 indicates this plot. The upper and lower limits are denoted by cross hatched lines. The solid lines join the data points of the characteristic frequencies taken from Fig. 19. It can be seen that almost all the Strouhal numbers lie within the limits.

A plot of Becker and Massaro's correlation (Equ. 2.2) is drawn on Fig. 20. Although there is an order of magnitude agreement of Strouhal number values, the Reynolds number dependence indicated by the experiments is opposite to that of the correlation. It is believed that this discrepancy could be attributed to some modes of cavity resonance. It is worth recalling that the lower characteristic frequency is related to a Helmholtz type resonance.

4.2 Dynamic Characteristic Study

The variation of the switching times with the control sound frequency and pressure level is shown in Fig. 21. It can be seen that within the experimental range and accuracy, the four response times are almost independent of the control sound variables. Perhaps a possible exception is that the turbulent-laminar rise time T_r has a very weak dependence on the frequency. Further, the laminar-turbulent delay time decreases slightly but consistently with an increase in the control pressure level.

The mean of all the experimental values taken for the four response times are given below along with the standard deviation in each case. From these mean values it can be

$$T_{d.d.} = 2.24 \text{ msec. } (S = 0.171 \text{ msec.})$$

$$T_{t.d.} = 2.40 \text{ msec. } (S = 0.287 \text{ msec.})$$

$$T_f = 0.487 \text{ msec. } (S = 0.130 \text{ msec.})$$

$$T_r = 0.606 \text{ msec. } (S = 0.263 \text{ msec.})$$

seen that the two delay times are almost equal and the difference between the fall time and the rise time is not significant. Thus the acoustically controlled amplifier tested has more equal switch "on" and switch "off" dynamics than the flow controlled turbulence amplifiers studied by Hayes (Ref. 24). This point is more emphatically made considering that Hayes found a large increase in the difference between the switch "on" and switch "off" characteristics with increasing gap length. The largest gap considered in Ref. 24 was 2.44 cm.

while the present, as noted previously is 3.81 cm.

From the standard deviations given above an indication of the erratic nature of the response time can be felt. Hayes did not express the erratic behaviour in this manner. He produced multiple traces of switching. The multiple trace photograph of the "on" and "off" switches for the present study are shown in Fig. 22. The lack of erratic behaviour in the position of the rise and the fall portions of the traces can be seen. Hayes multiple trace of the switch "on" dynamics for $dc = 1.27$ cm., $g = 2.44$ cm. and $ds = 0.074$ cm. is shown in Fig. 23. (taken from Ref. 23). The extremely great variation in the position of the rise portion of the trace is evident. Hence the acoustically controlled turbulence amplifier dynamics can be seen to be less erratic than the flow controlled mode of operation.

The variation of the response times with supply pressure are shown in Fig. 24 compared to Hayes theoretical and Abramovich's empirical equations (Ref. 23 and 1 respectively) for the flow controlled turbulence amplifier. Within the range tested the present data agrees with both of the above mentioned relationships in general trends only. Hayes theory predicts the laminar-turbulent delay time T_{ld} , more closely than the other three times. Abramovich's relationship predicts the turbulent-laminar rise Tr. time and the laminar-turbulent delay time T_{ld} , quite well but the other two times are of considerably different magnitude.

CHAPTER V

CONCLUSIONS

(a) Bell's Analytical Approach

- (1) Bell's analytical procedure can reasonably predict the characteristics of the laminar jet in a shrouded, turbulence amplifier. However, for the turbulent jet the results of the procedure are not in agreement with the present experimental data.
- (2) The approximate method put forward by Bell for determining P_o/P_s at an operating point near the peak of the P_o versus P_s curve is extended to include operating points in the laminar portion. The following equation was obtained by curve fitting

$$G^{+0.27} P_o/P_s = - 0.26 + 8.3 \times 10^{-4} Re + 1.22 \times 10^{-7} Re^2$$

(b) Static Characteristics

- (1) A "jump" in characteristic frequency occurs as the Reynolds number of the emitter is increased, the upper characteristic frequency is yet to be predicted.
- (2) The characteristic frequency of a shrouded, acoustically controlled turbulence amplifier may be determined for low Reynolds number using advanced Helmholtz resonator theory such as Alster's (Ref. 2).

- (3) The Strouhal numbers at which shrouded, acoustically controlled turbulence amplifiers respond, fall within the limits of the sensitivity of a free jet given by Bell (Ref 12).
- (4) The acoustically controlled turbulence amplifier, unlike the flow controlled turbulence amplifier can be operated in a proportional mode under certain conditions of shroud geometry and control variables.

(c) Dynamic Characteristics

- (1) Within the experimental range studied, the switching dynamics of the acoustically controlled turbulence amplifier is almost independent of the control sound frequency and pressure level.
- (2) The two delay times (T_{qd} and T_{td}) are almost equal and the fall and the rise time (T_f and T_r) may also be considered equal.
- (3) The switching dynamics of the sound controlled turbulence amplifier tested is less erratic and more equal than a flow controlled turbulence amplifier.



CHAPTER VI

RECOMMENDATIONS

- (1) An analytical and experimental study of the turbulence amplifier should be undertaken which would extend Bell's procedure to account for the effect of a shroud on the laminar-jet length and the turbulent jet output pressure.
- (2) Further work should be done to determine the nature of the frequency "jump" and the higher characteristic frequency that occur when the Reynolds number is increased.
- (3) The many studies that have been conducted concerning the maximum sound sensitivity of jets issuing from short nozzles should be extended to cover those issuing from long, straight bore tubes.

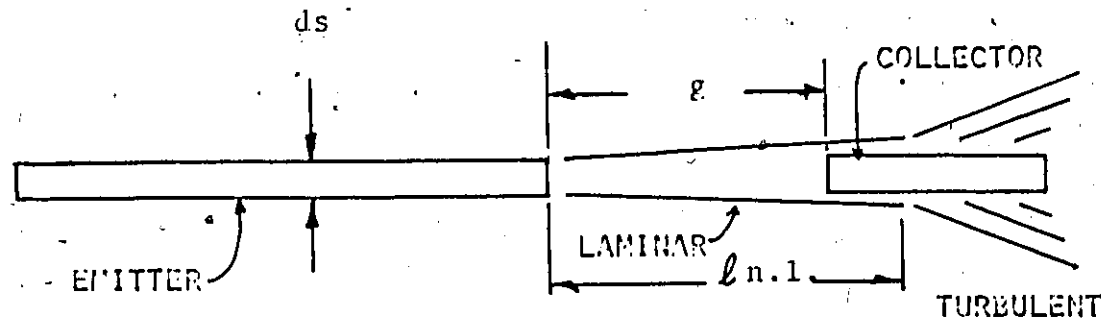
REFERENCES

1. Abramovich, S. and Solan. A., "Turn - on and Turn - off times for a Laminar Jet" A.S.M.E. paper no. 73-Aut-N (1973)
2. Alster, M., "Improved Calculation of Resonant Frequencies of Helmholtz Resonators", Jour. of Sound and Vibration, vol. 24, no. 1, pp. 63 - 85 (1972).
3. Auger, R.N. , "A New"Solid State" Pneumatic Amplifier for Logic Systems," Automatic Control, pp.24-28 (Dec. 1962) .
4. Auger, R.N. , "Pneumatic Turbulence Amplifiers", Instruments and control Systems, vol. 38, pp. 129-133 (March 1965)
5. Auger, R.N. , "Turbulence Amplifier Design and Application", Proc. of the Fluid Amplifier Symposium, Harry Diamond Labs, vol. 1, pp.357-365 (Oct. 1962)
6. B and K Manual for Type 2607 Measuring Amplifier, B and K Naerum, Denmark (Nov. 1970).
7. Batchelor, G.K. and Gill, A.E. , "Analysis of the Stability of Axisymmetric Jets", Jour. of Fluid Mechanics, vol. 14, pt. 4, pp.529-551 (1962).
8. Beavers, G.S. and Wilson, T.A., "Vortex Growth in Jets", Jour. of Fluid Mechanics, vol. 44, pt. 1, pp. 97-112 (1970).
9. Becker, H. A. and Massaro, T.A., "Vortex Evolution in a Round Jet", Jour. of Fluid Mechanics, vol. 31 , pt.3, pp. 435-448. (1968).
10. Beeken, B.B., "Long Range Fluidic Acoustic Sensor", A.S.M.E. paper 72-WA/FLCS - 8 (1972).
11. Beeken, B.B., "Acoustic Fluidic Sensor", Instruments and Control Systems, pp. 75-79, (Feb. 1970).
12. Bell, A.C., "An Analytical and Experimental Investigation of the Turbulence Amplifier", Sc. D. thesis, Mechanical Engineering Department, M.I.T. (1969).
13. Bell, A.C., "An Analytical and Empirical Basis for the Design of Turbulence Amplifiers Part I: Analysis and Experimental Confirmation", A.S.M.E. paper no 72-WA/FLCS-1. (Nov. 1972).
14. Bell, A.C. , "An Analytical and Empirical Basis for the Design

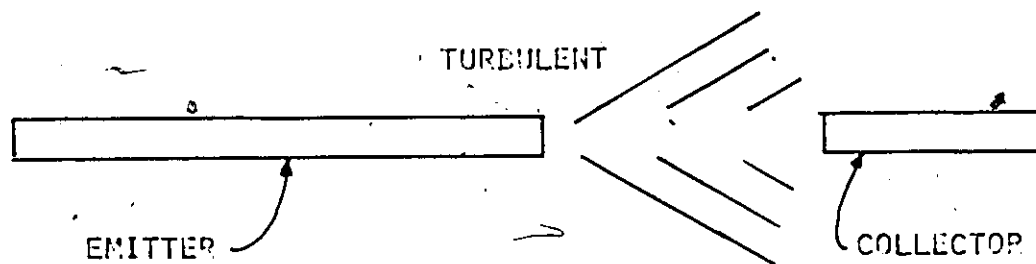
- of Turbulence Amplifiers Part II:- Empirical Relationships and Design Procedure", A.S.M.E. paper no. 72-WA/F&CS-2 (Nov. 1972).
15. Benson, C.A.R. and Hagwood, D., "Electropneumatic Transducer using the Acoustic Switching of Fluid Logic Elements", Jour. of Scientific Instruments, vol. 43, pp. 527-528 (1966).
 16. Brown, G.B., "The Vortex Motion in Gaseous Jets and the Origin of their Sensitivity to Sound", Proc. of the Physical Society of London, England, vol. 47, pp. 703-732 (1935).
 17. Chanaud, R.C. and Powell, A., "Experiments Concerning the Sound Sensitive Jet", J.A.S.A., vol. 34, no. 7, pp. 907-915 (July 1962).
 18. DISA Type 55M System: Service Manual, DISA Information and Documentation Dept., DISA ELEKTRONIK A/S DK-2730, Herlev, Denmark (March 1972).
 19. Fox, M.L., "Direct Fluidic Sensors", Instrumentation Technology, pp. 67-75 (Sept. 1967).
 20. Freymuth, P., "On Transition in a Separated Laminar Boundary Layer", Jour. of Fluid Mechanics, vol. 25, pt. 4, pp. 683-704 (1966).
 21. Gottron, R.N., "Acoustic Control of Pneumatic Digital Amplifiers", Proc. of the Fourth H.D.L. Fluid Amp. Symp., vol. 1, pp. 279-292 (1964).
 22. Gradetsky, Dr. V, Dmitriev, Dr. V. and Sons, M., "Some Design Problems of the Fluidic Digital Elements and Devices", paper T1, Proc. of the Third Cranfield Fluidics Conference, Turin, Italy (May 1963).
 23. Hayes, W., "Static and Dynamic Performance Characteristics of Fluidic Turbulence Amplifiers", Report LTR-CS-9, control Systems Laboratory, N.R.C. (June 1969).
 24. Hayes, W., "The Dynamic Response of Fluidic Turbulence Amplifiers", paper A1, Proc. of the Fourth Cranfield Fluidics Conference Coventry, England (March 1970).
 25. Hodge, J. and Hutchinson, J.G., "Turbulence Amplifiers - Principles and Applications", paper F2, Proc. of the First International Conference on Fluid Logic and Amplification, B.H.R.A. Cranfield, England (Sept. 1965).

26. Hornbeck, R.W., "Laminar Flow in the Entrance Region of a Pipe", Applied Scientific Research, Series A13, pp. 224-232 (1962).
27. Marsters, G.F., "Some Observations on the Transition to Turbulence in Small, Unconfined Free Jets", Report #1-69, Dept. of Mech. Eng., Queen's University, Kingston, Ontario, Canada (Oct. 1969).
28. McNaughton, K.J. and Sinclair, C.G., "Submerged Jets in Short Cylindrical Flow Vessels", Jour. of Fluid Mechanics, vol. 25, pt. 2, pp. 367-375 (1966).
29. Nomoto, A. and Shimada, K., "Ultrasonically Modulated Fluid - State Transducer", Bull. Fac. Science and Eng. of Chou University, vol. II, pp. 76-84 (1968).
30. Oels, R.A., Boucher, R.F. and Markland, E., "Experiments on Turbulence Amplifiers", paper D3, Proc. of the First International Conf. on Fluid Logic and Amplification (Sept. 1965).
31. Powell, A., "Characteristics and Control of Free Laminar Jets", Proc. of First Fluid Amp. Symp., vol. 1, pp. 289-299 (Oct. 1962).
32. Rayleigh, J.W.S., "The Theory of Sound", vol. II, Dover Publications Ltd., New York, N.Y. (1945).
33. Rayleigh, J.W.S., "The Theory of Sound", vol I, Dover Publications Ltd., New York, N.Y. (1945).
34. Schlichting, H., "Boundary Layer Theory", Sixth Ed., McGraw Hill, New York, N.Y. (1968).
35. Siwoff, F., "Improvement of the Static and Dynamic Behaviour of the Turbulence Amplifier by Inbuilding an Edge over the distance between the Emitter and the Collector", paper no. H-2, Third Cranfield Fluidics Conference, Turin, Italy (May 1968).
36. Stephens, R.W.B., and Bate, A.E., "Acoustics and Vibrational Physics", Edward Arnold (Publishers) Ltd., London, England (1966).
37. Tryburcy, J., "Investigations of an Acoustic Fluidic Sensor", paper no. P-22, Fourth International Fluidics Conference, Varna Bulgaria (Oct. 1972).
38. Urifried, H.H., "An Approach to Broad Band Fluid Amplification at Acoustic Frequencies," Proc. of the H.D.L. Third Fluid Amp. Symp., vol. 1, pp. 267-296 (1965).

39. Unfried, H.H., "Experiment and Theory of Acoustically Controlled Fluid Switches", Proc. of the H.D.L. Third Fluid Amp. Symp., vol. 2, pp. 113-127 (1965).
40. Vaz, T.I.N., "An Experimental Investigation into the Response of a Turbulence-Type Amplifier and Laminar/Turbulent Jet Study", M.A.Sc. thesis, University of Windsor, Windsor, Ontario, Canada (1970).
41. Verhelst, H.A.M., "On the Design, Characteristics and Production of Turbulence Amplifiers", paper no. F-2, Second Cranfield Fluidics Conference, Cambridge, England (Jan. 1967).
42. Viilu, A., "An Experimental Determination of the Minimum Reynolds Number for Instability in a Free Jet", Journal of Applied Mechanics, Trans. of the A.S.M.E., pp. 506-508 (Sept. 1962).



(A) "ON STATE"



(B) "OFF STATE"

2
Fig. 1 TURBULENCE AMPLIFIER PRINCIPLE

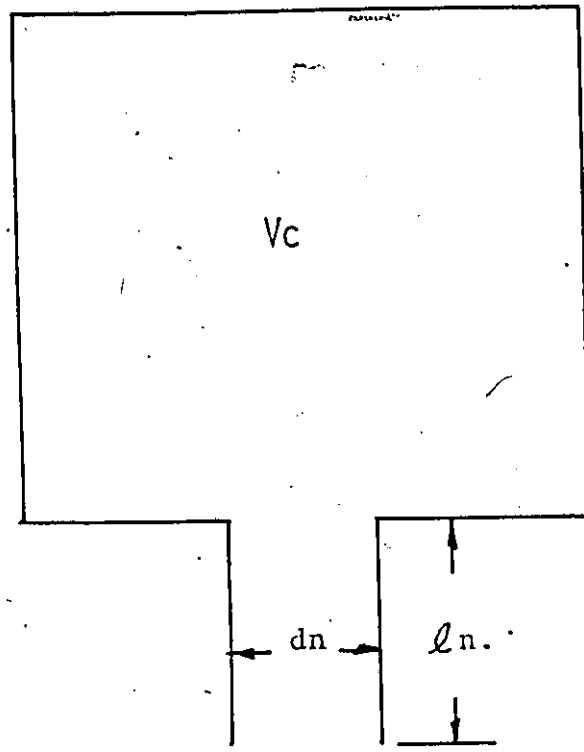


FIG. 2. BASIC HELMHOLTZ RESONATOR

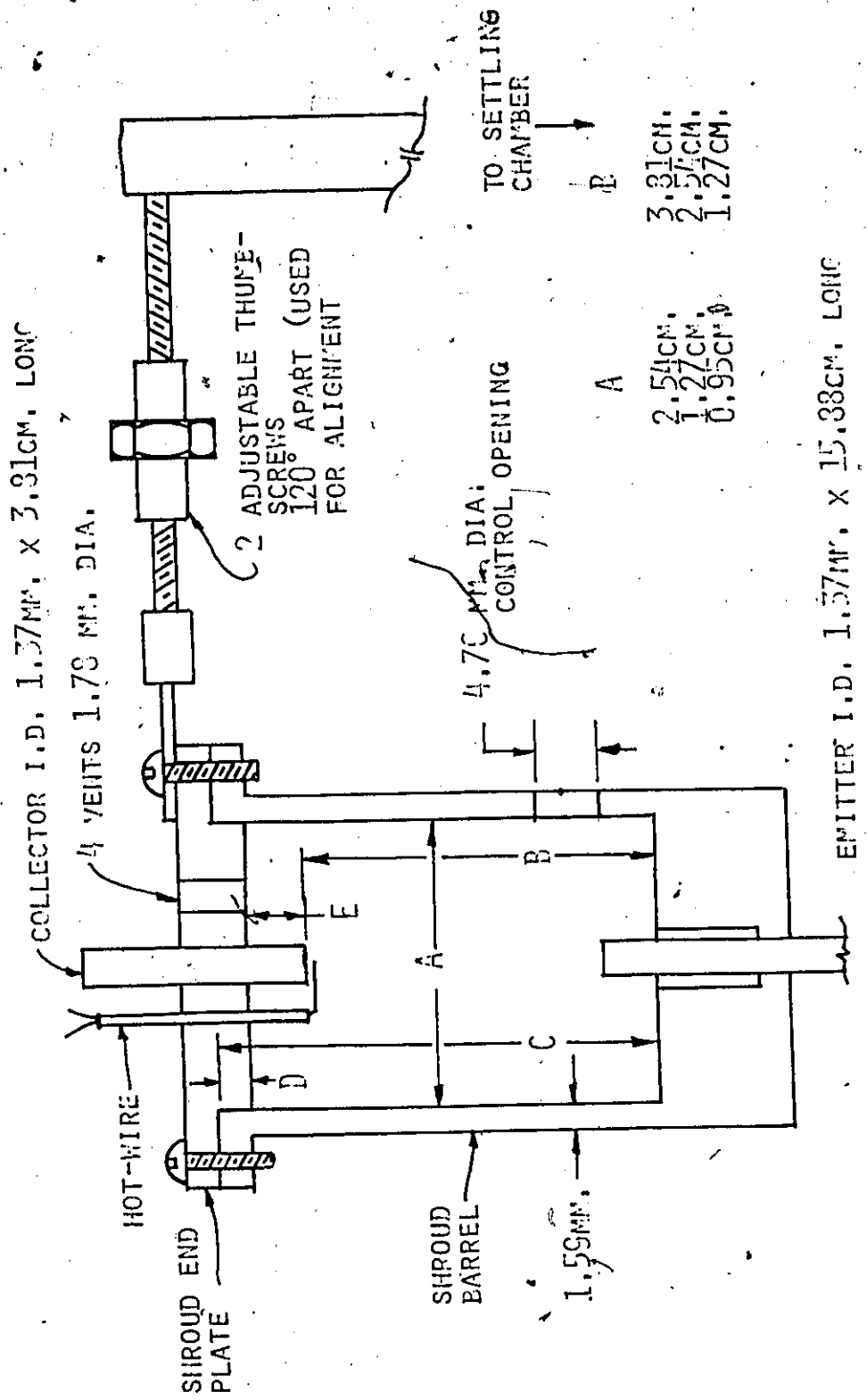


FIG. 3 EXPERIMENTAL TURBULENCE AMPLIFIER AND SUPPORT

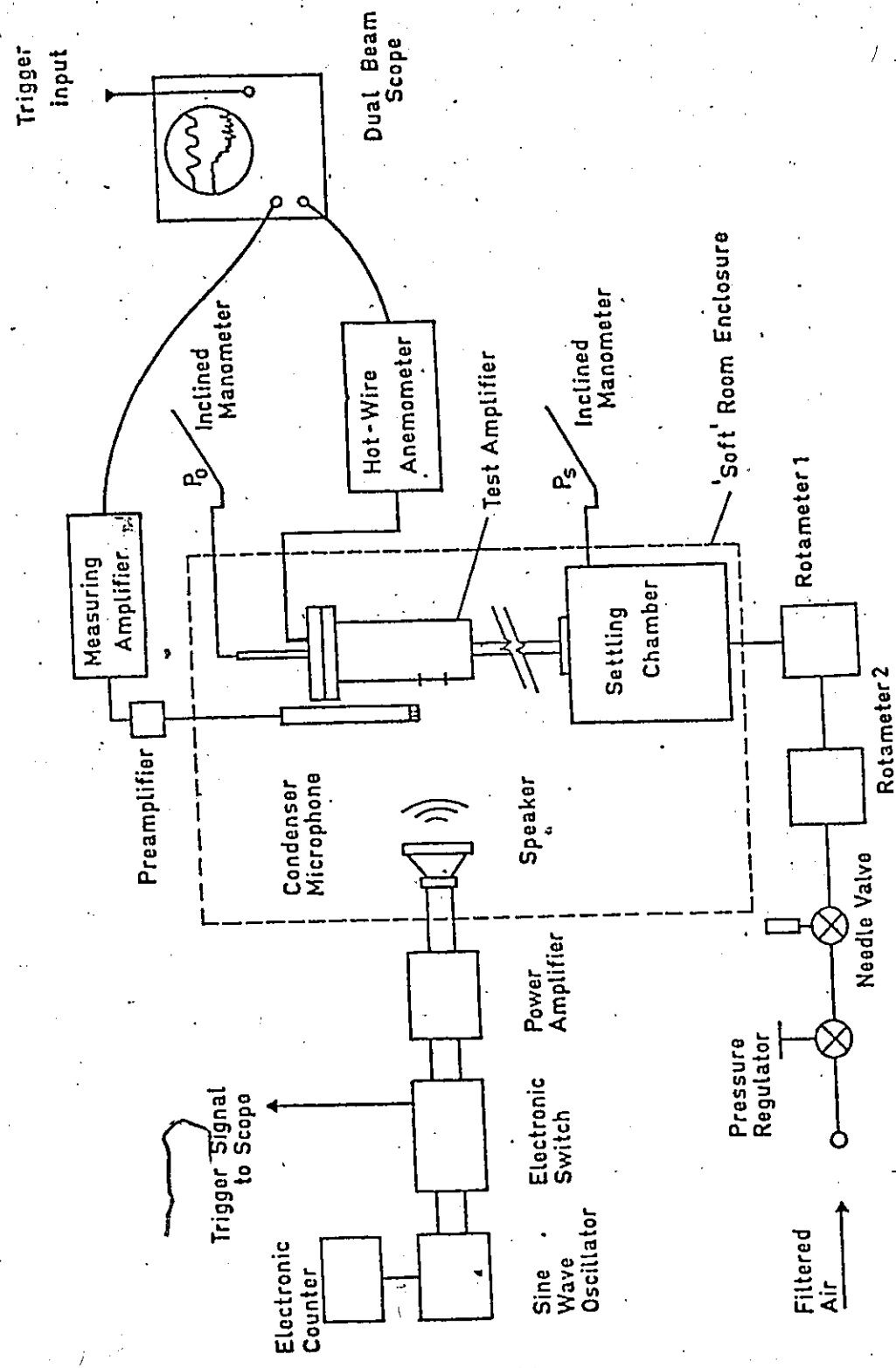


FIGURE 4 TEST FACILITY

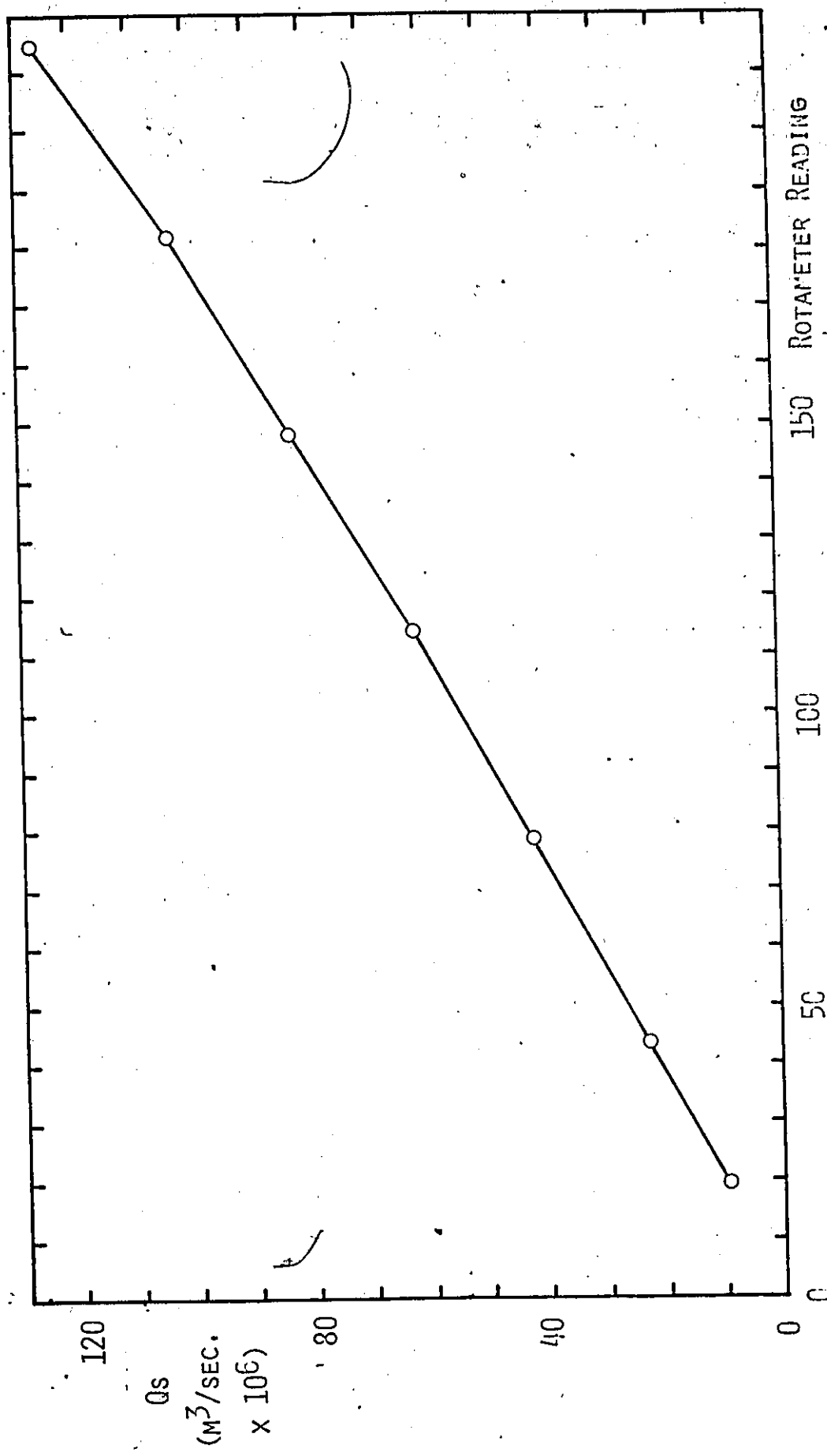


FIG. 5 CALIBRATION CURVE FOR ROTA L10/400-6135 ROTAMETER

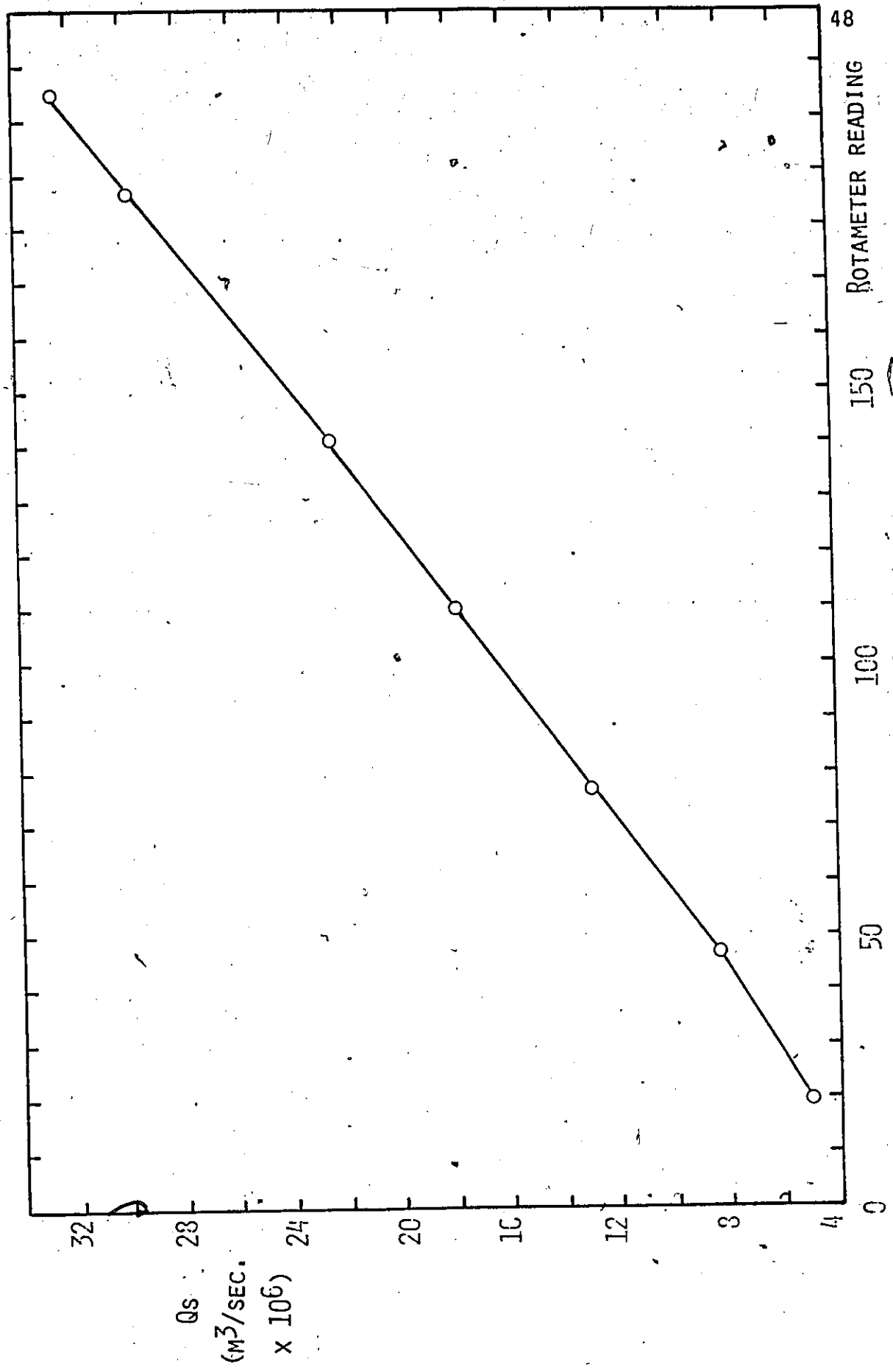


FIG. C CALIBRATION CURVE FOR ROTAMETER L2.5/100-3458.

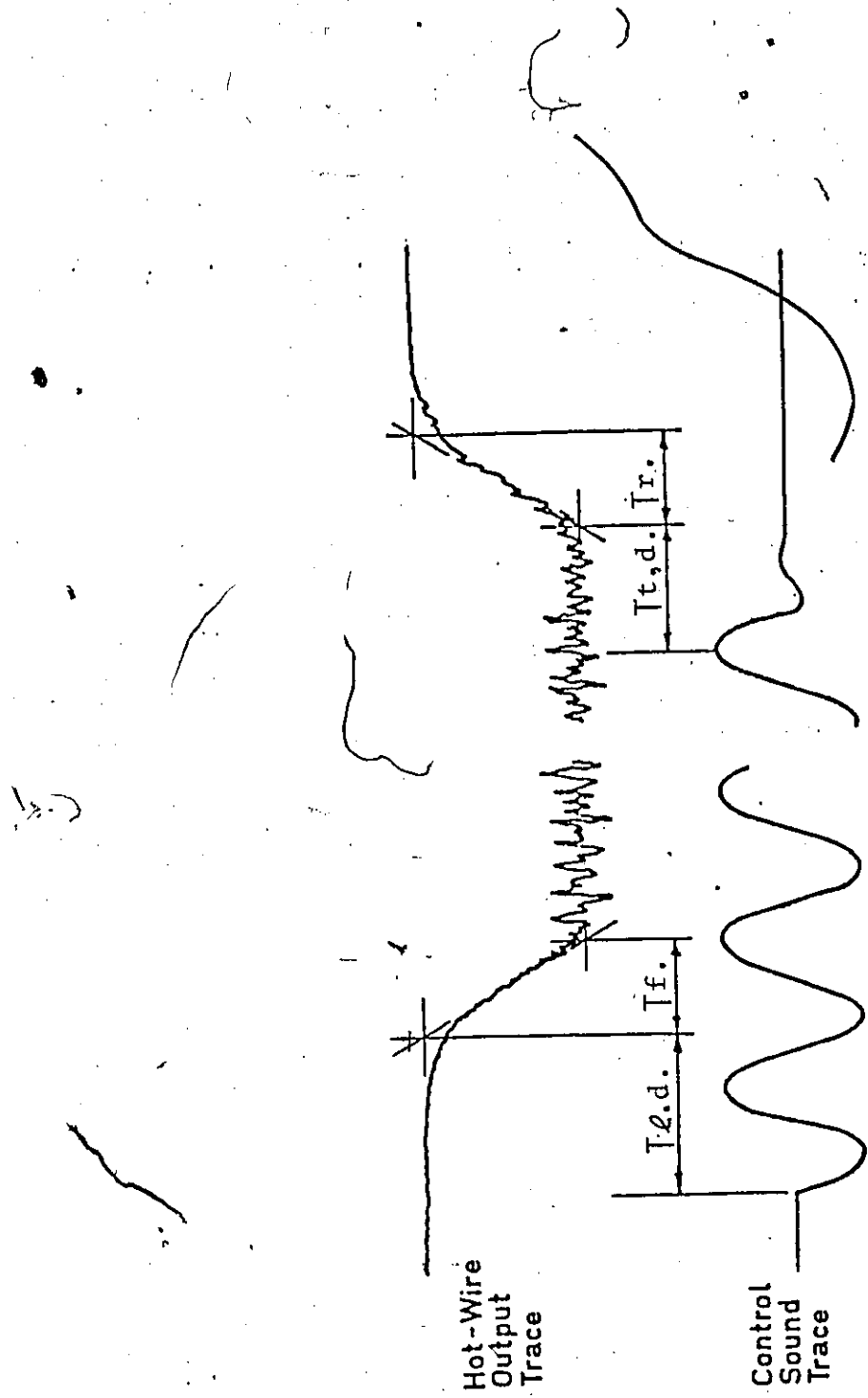


FIG. 7 RESPONSE TIME DEFINITIONS

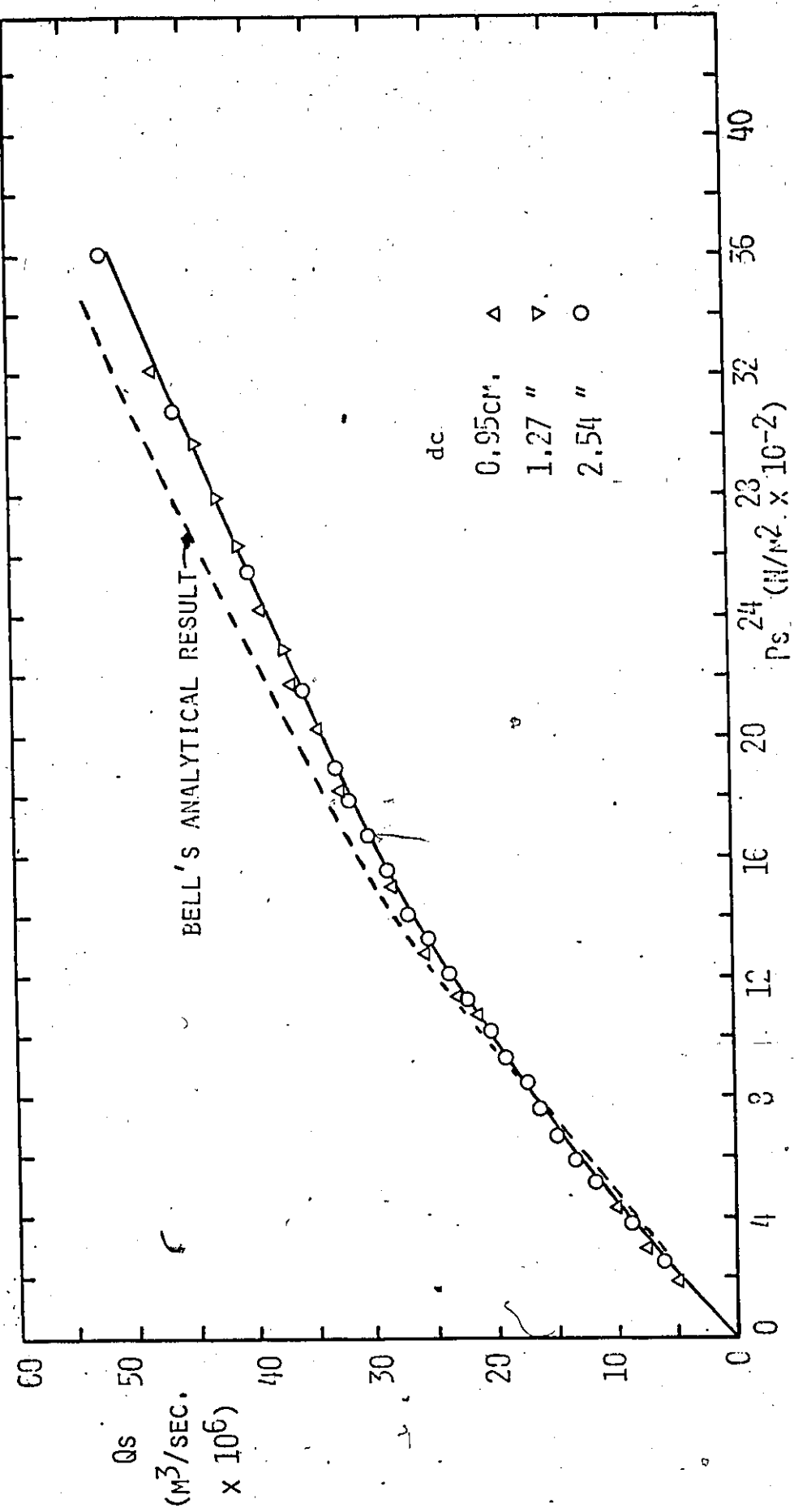


FIG. 8 SUPPLY FLOW RATE VERSUS SUPPLY PRESSURE

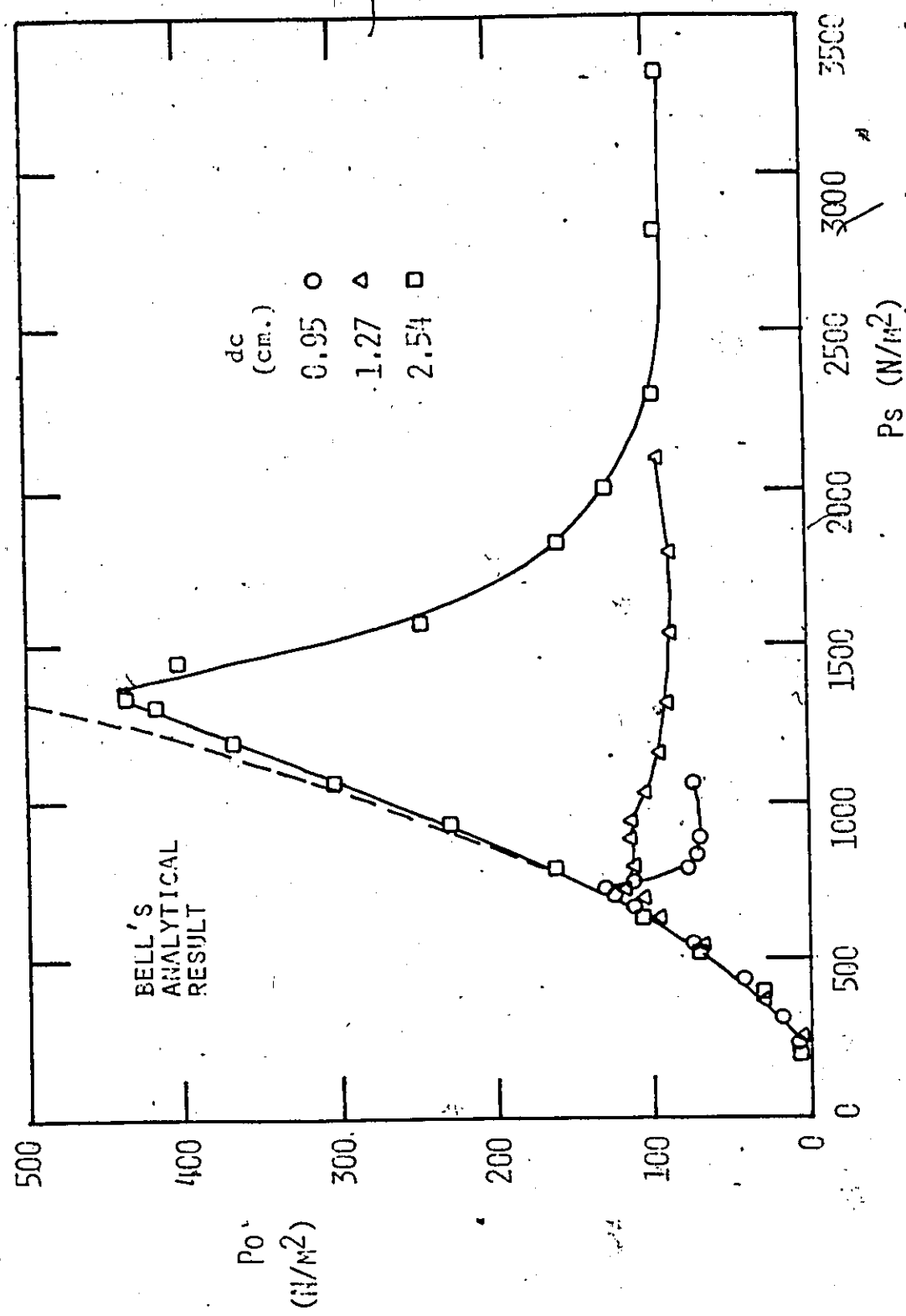


Fig. 9(A) OUTPUT PRESSURE VERSUS SUPPLY PRESSURE ($g = 3.81 \text{ cm.}$)

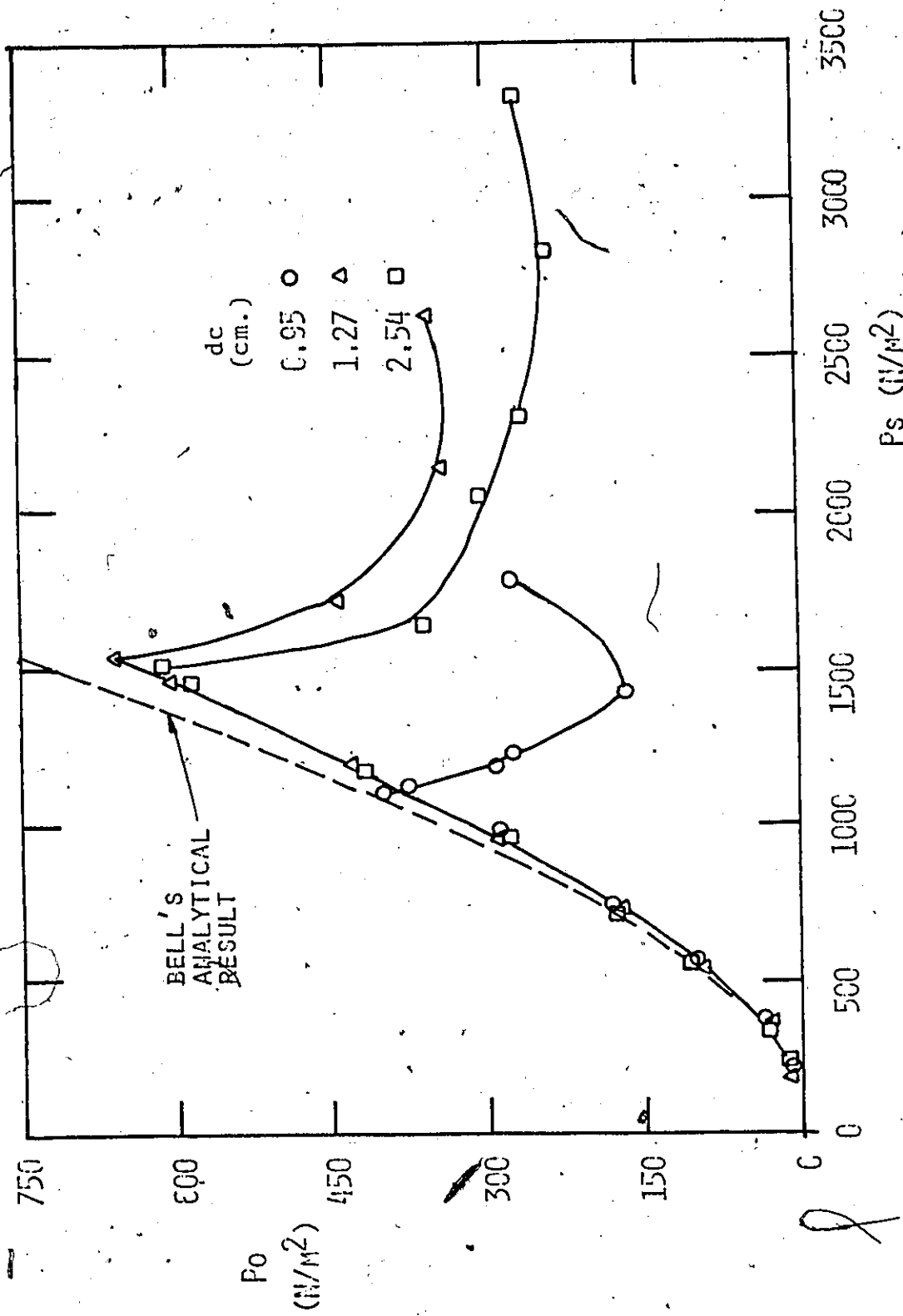


FIG. 9(B) OUTPUT PRESSURE VERSUS SUPPLY PRESSURE ($g = 2.54 \text{ cm.}$)

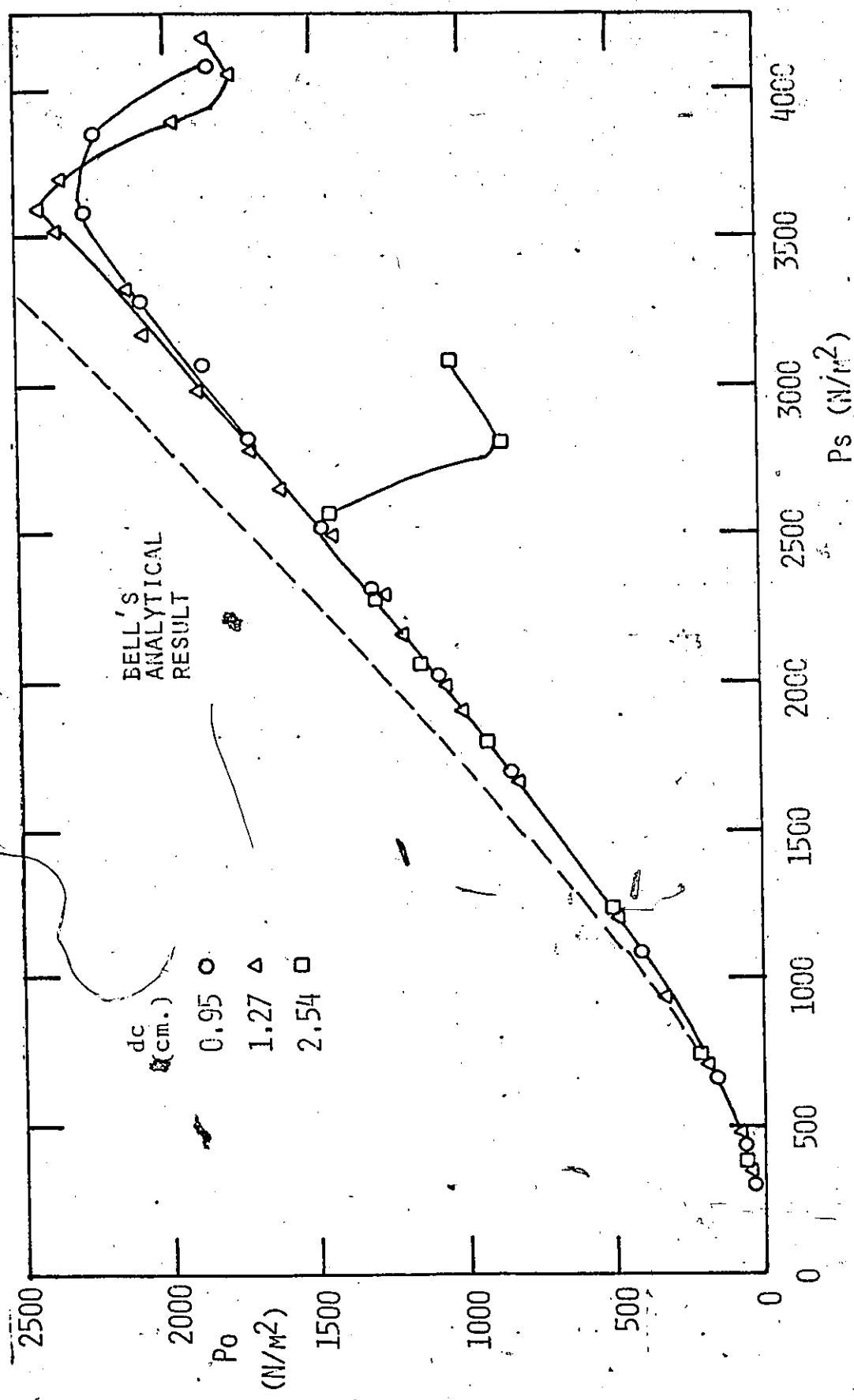


FIG. 9(c) OUTPUT PRESSURE VERSUS SUPPLY PRESSURE ($g = 1.27 \text{ cm.}$)

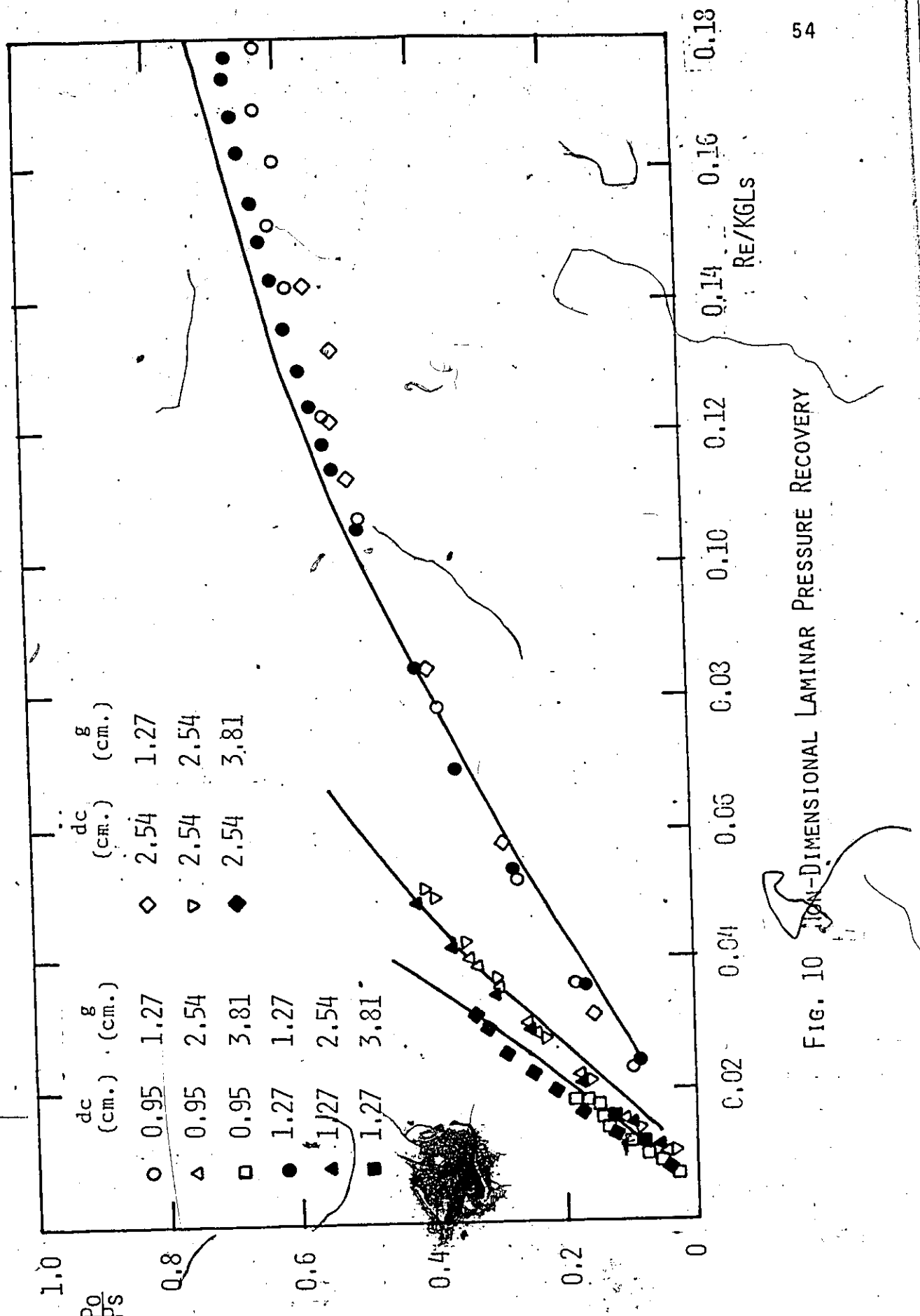


FIG. 10
ONE-DIMENSIONAL LAMINAR PRESSURE RECOVERY

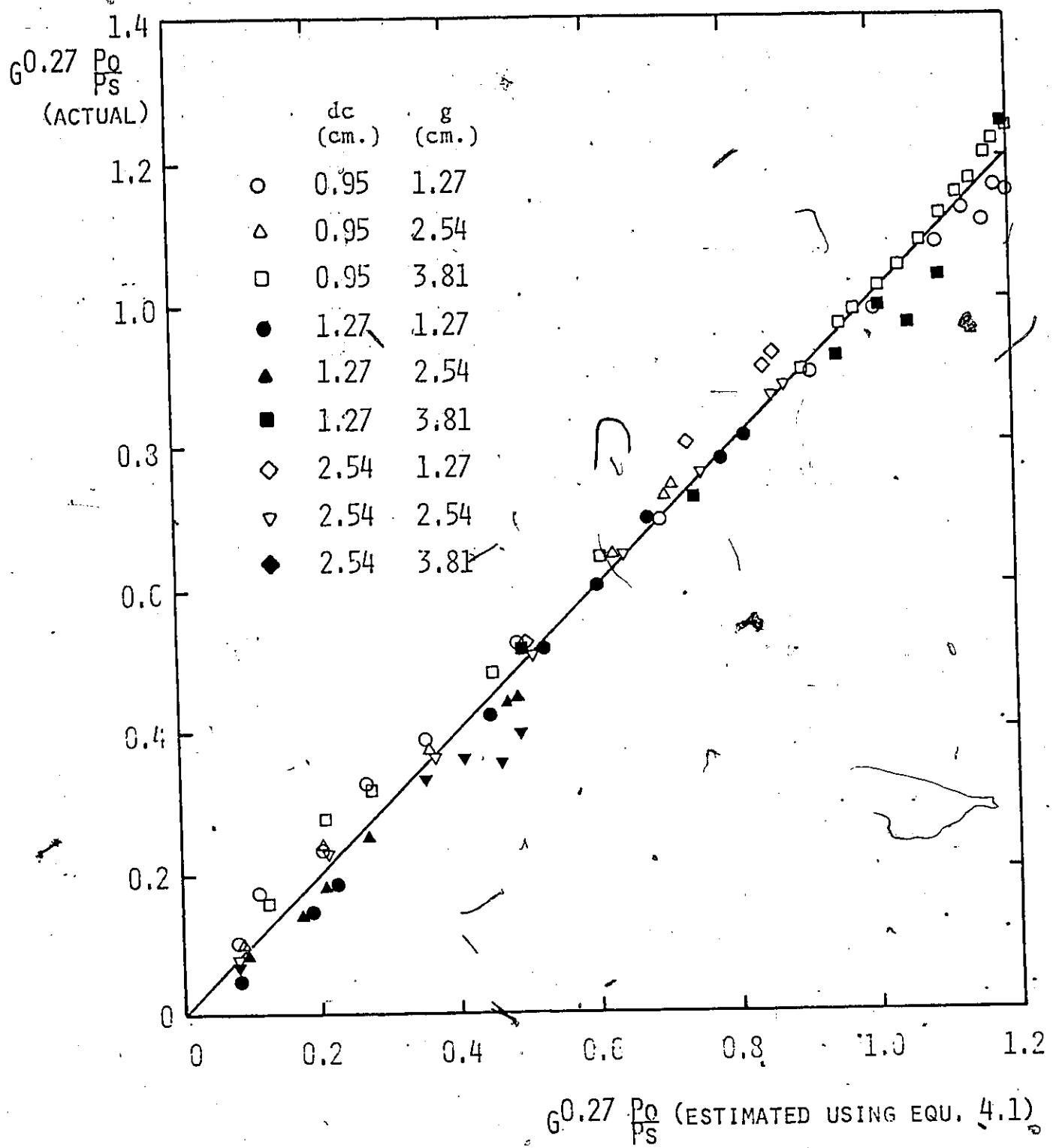


FIG. 11. TEST OF THE POLYNOMIAL FIT

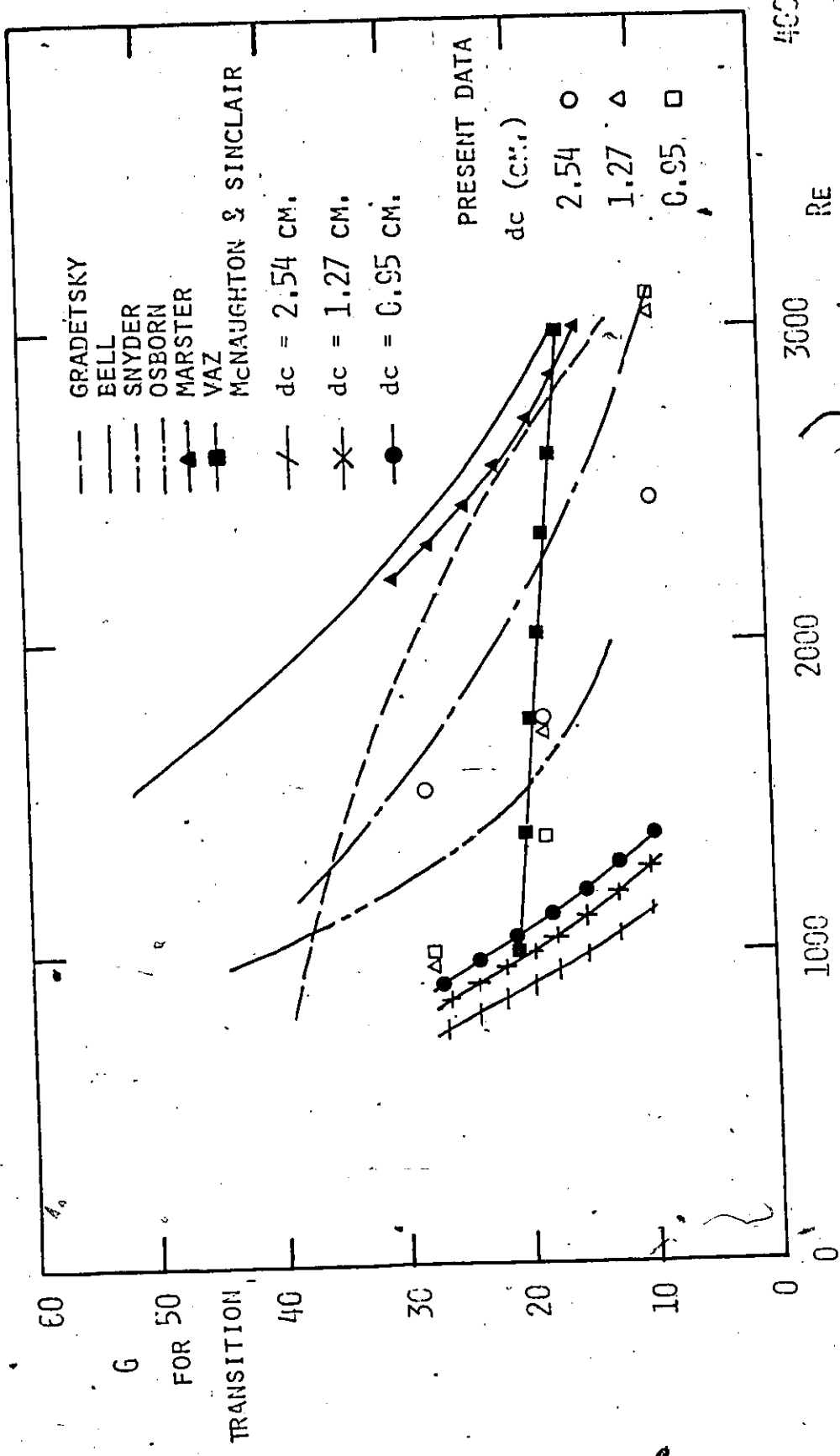
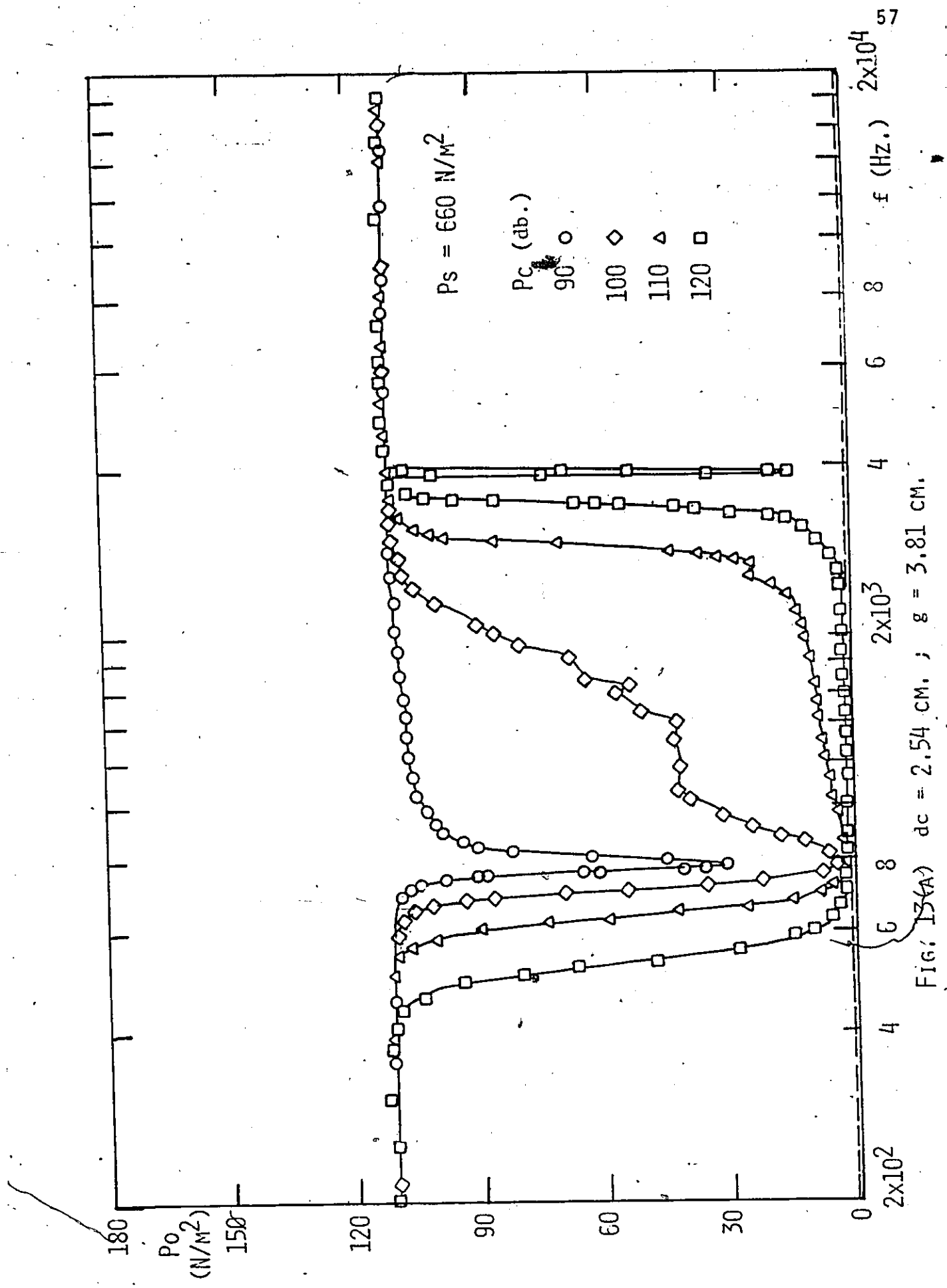


Fig. 12 Non-DIMENSIONAL GAP FOR TRANSITION VERSUS REYNOLDS NUMBER



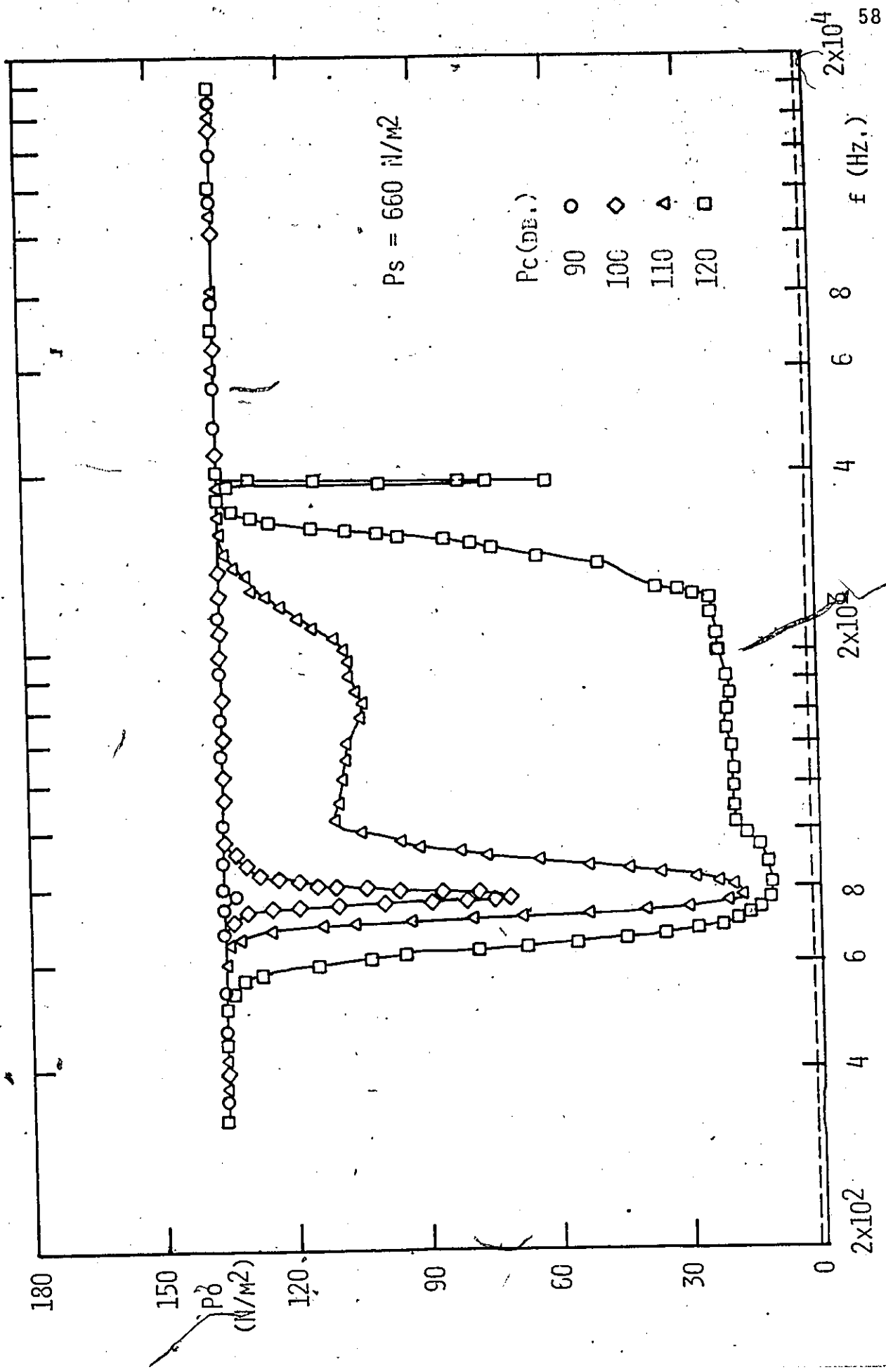
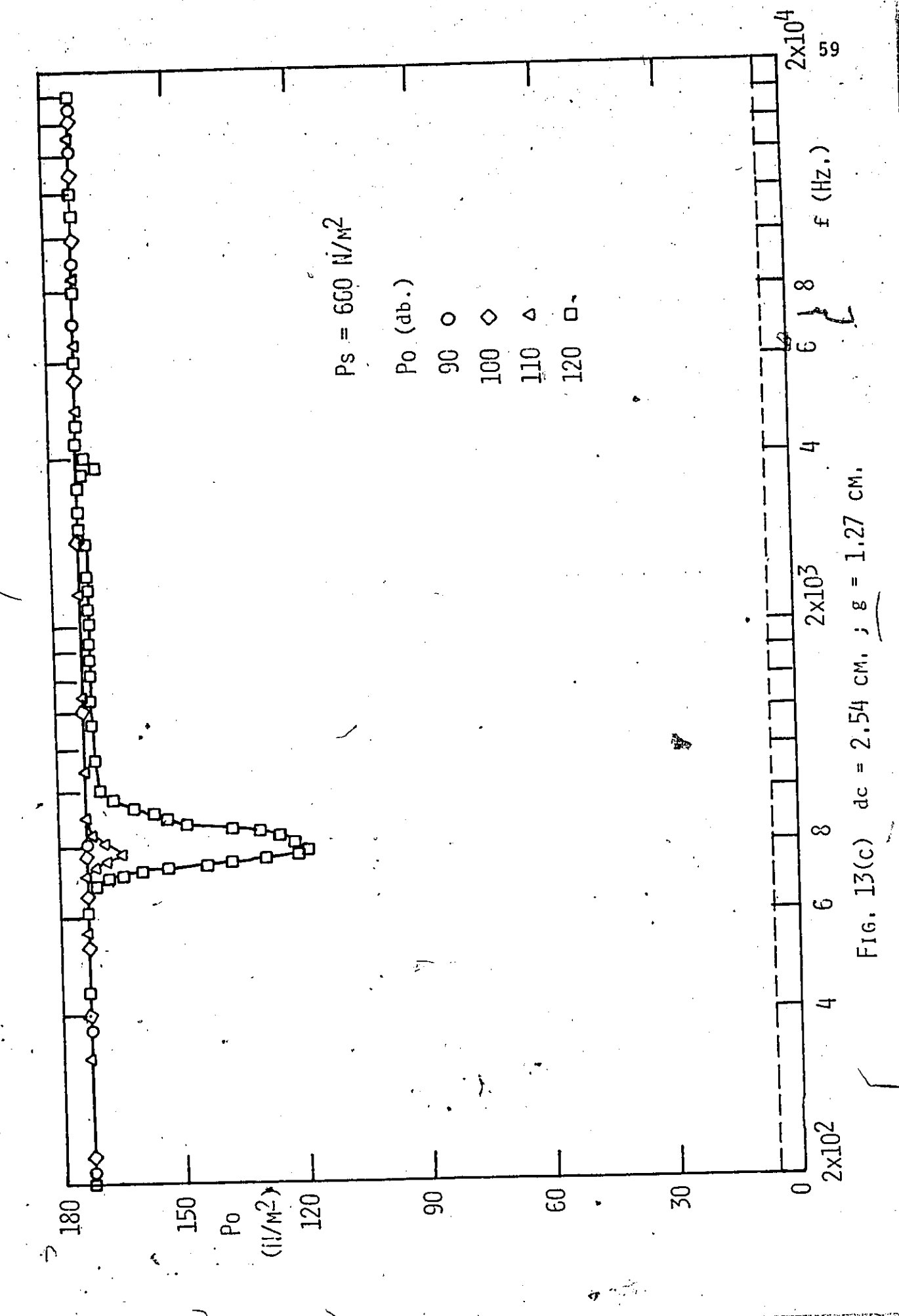


FIG. 13(B) $d_c = 2.54 \text{ cm.}$; $g = 2.54 \text{ cm.}$



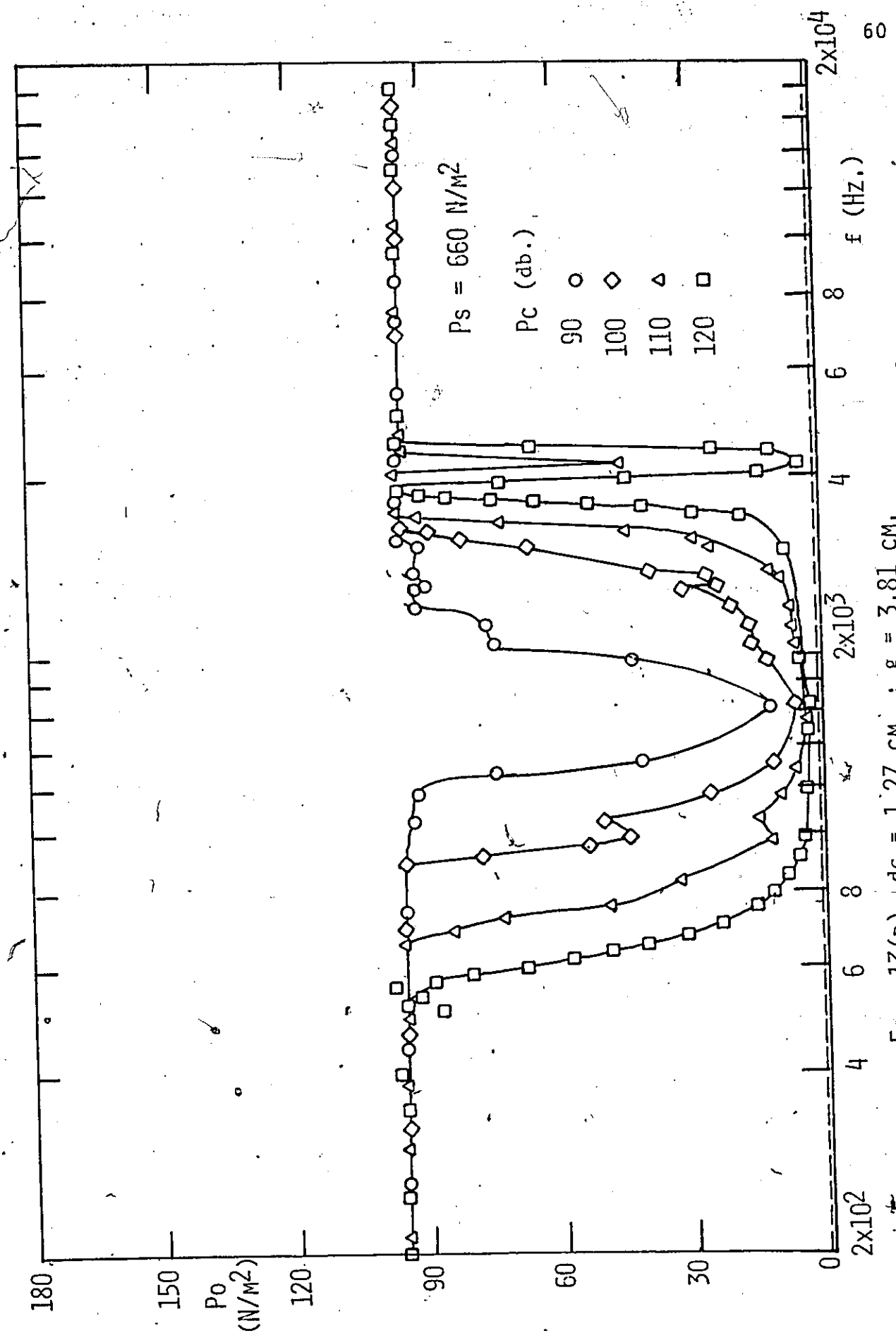


FIG. 13(D) | $a_c = 1.27$ CM; $g = 3.81$ CM,

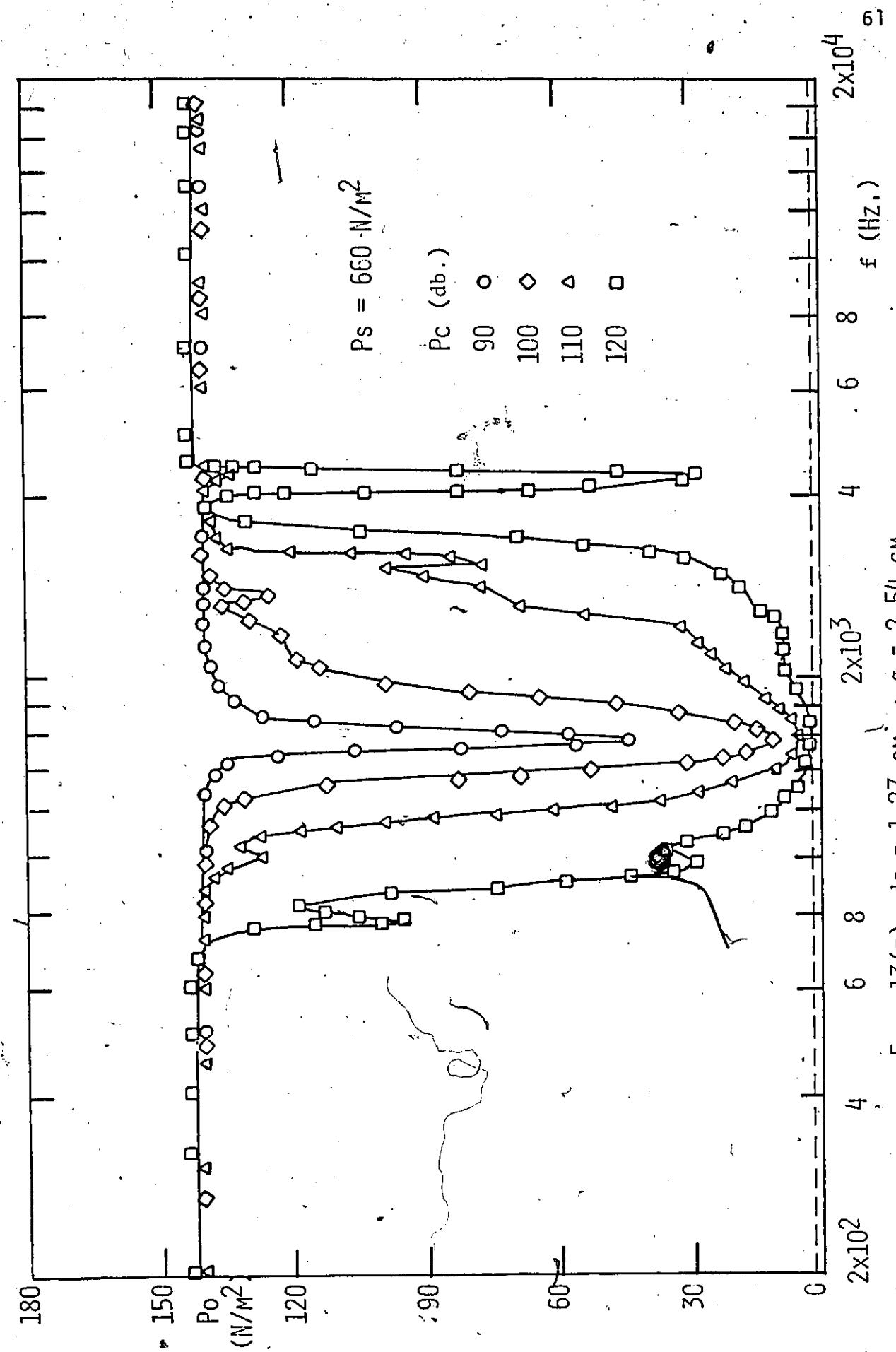


FIG. 13(E) $dc = 1.27 \text{ cm.}$; $g = 2.54 \text{ cm.}$

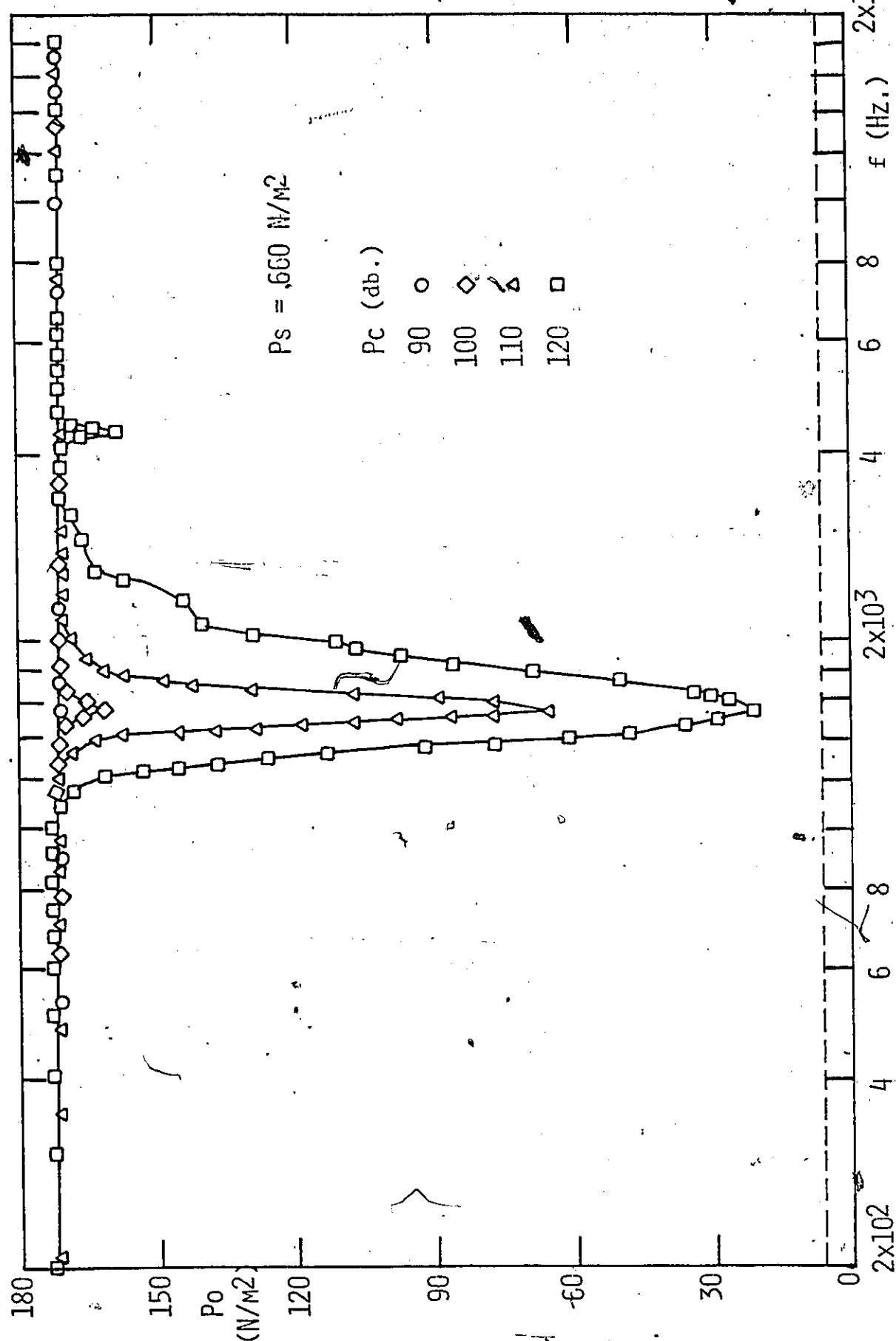


FIG. 13(F) $dc = 1.27 \text{ cm.}$; $g = 1.27 \text{ cm.}$

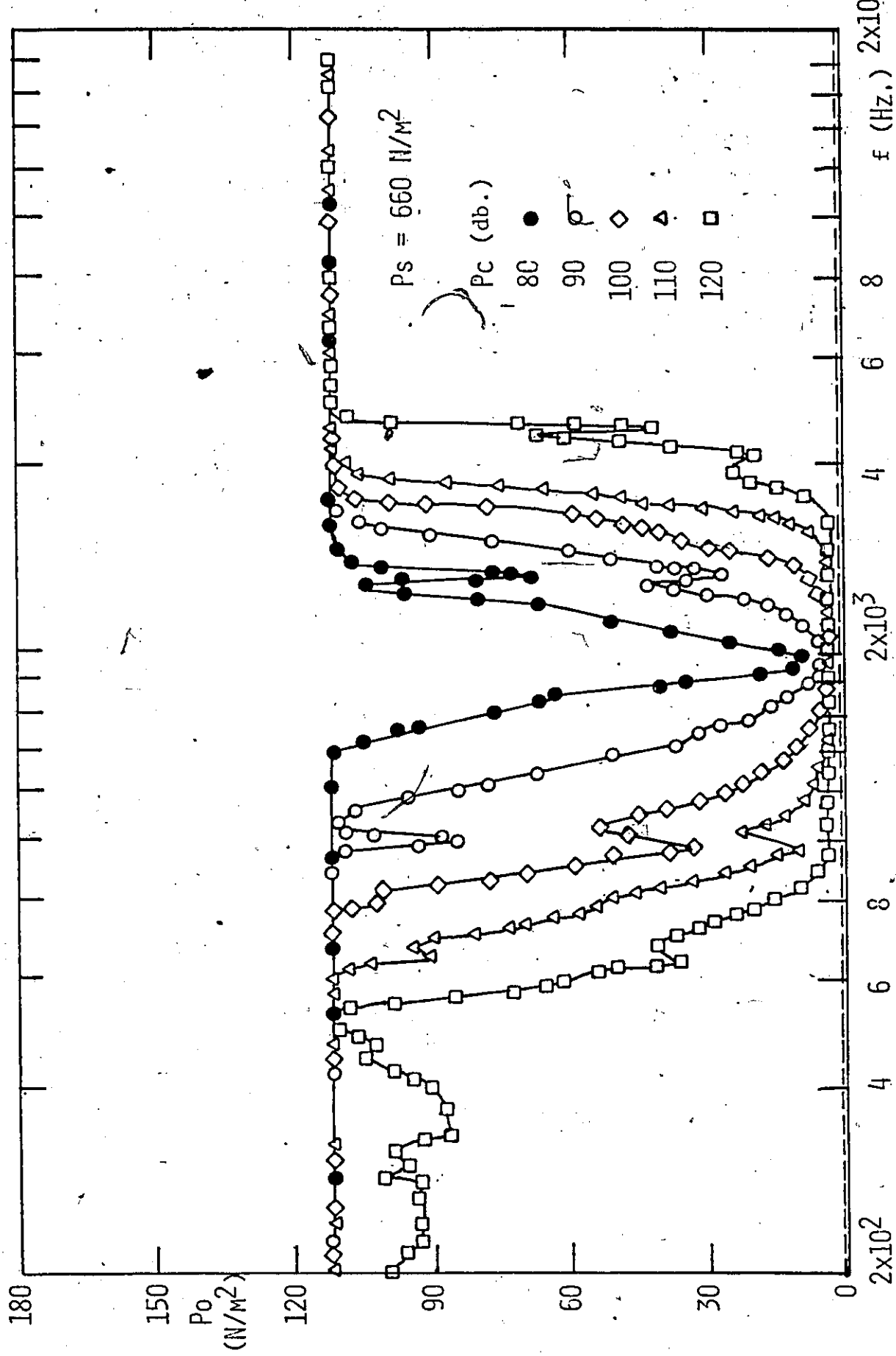


FIG. 13(6) $dc = 0.95$ cm. ; $g = 3.81$ cm.

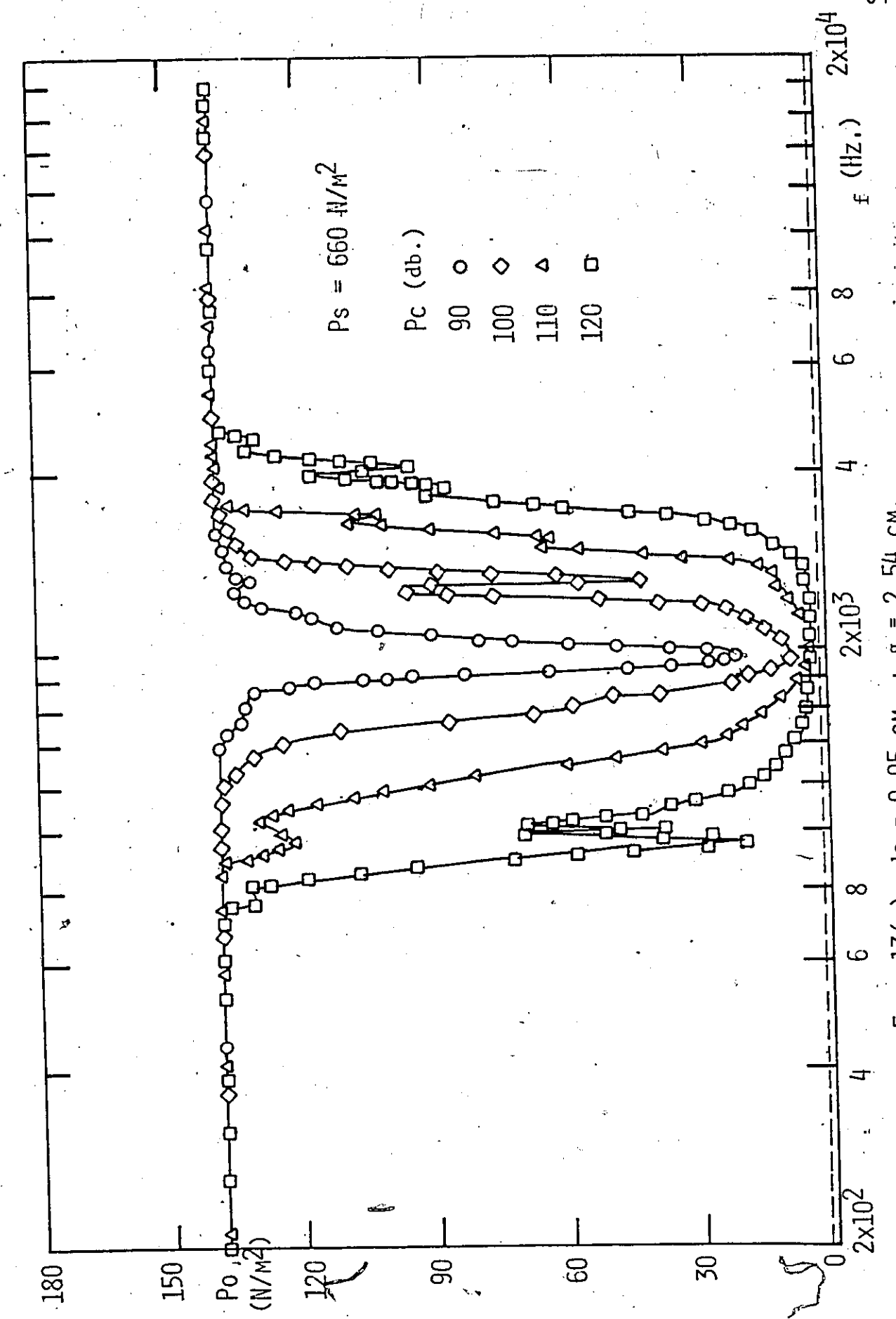


FIG. 13(H) $d_c = 0.95 \text{ cm.}$; $g = 2.54 \text{ cm.}$

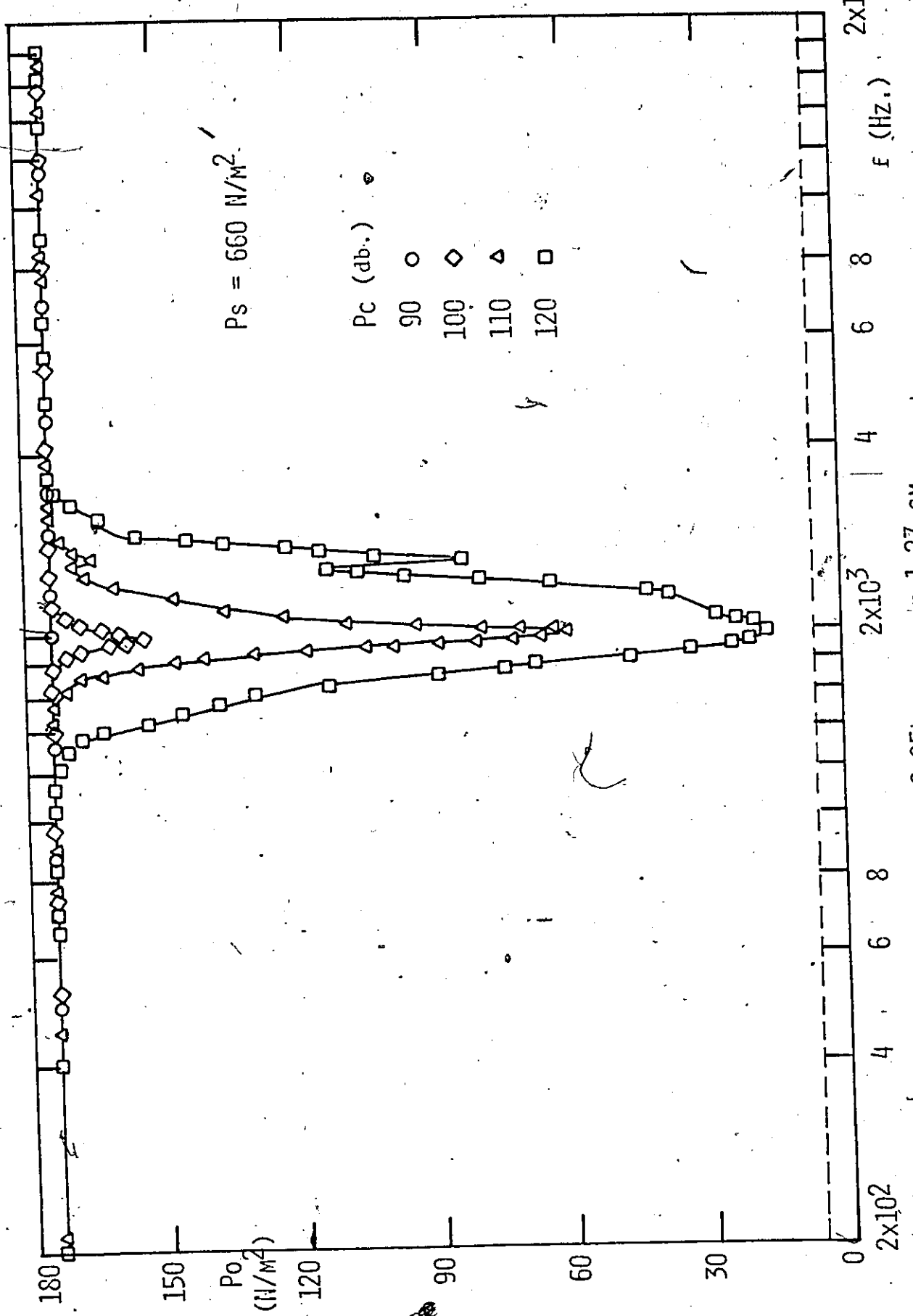


FIG. 13(1) $d_c = 0.95 \text{ cm.}$; $g = 1.27 \text{ cm.}$

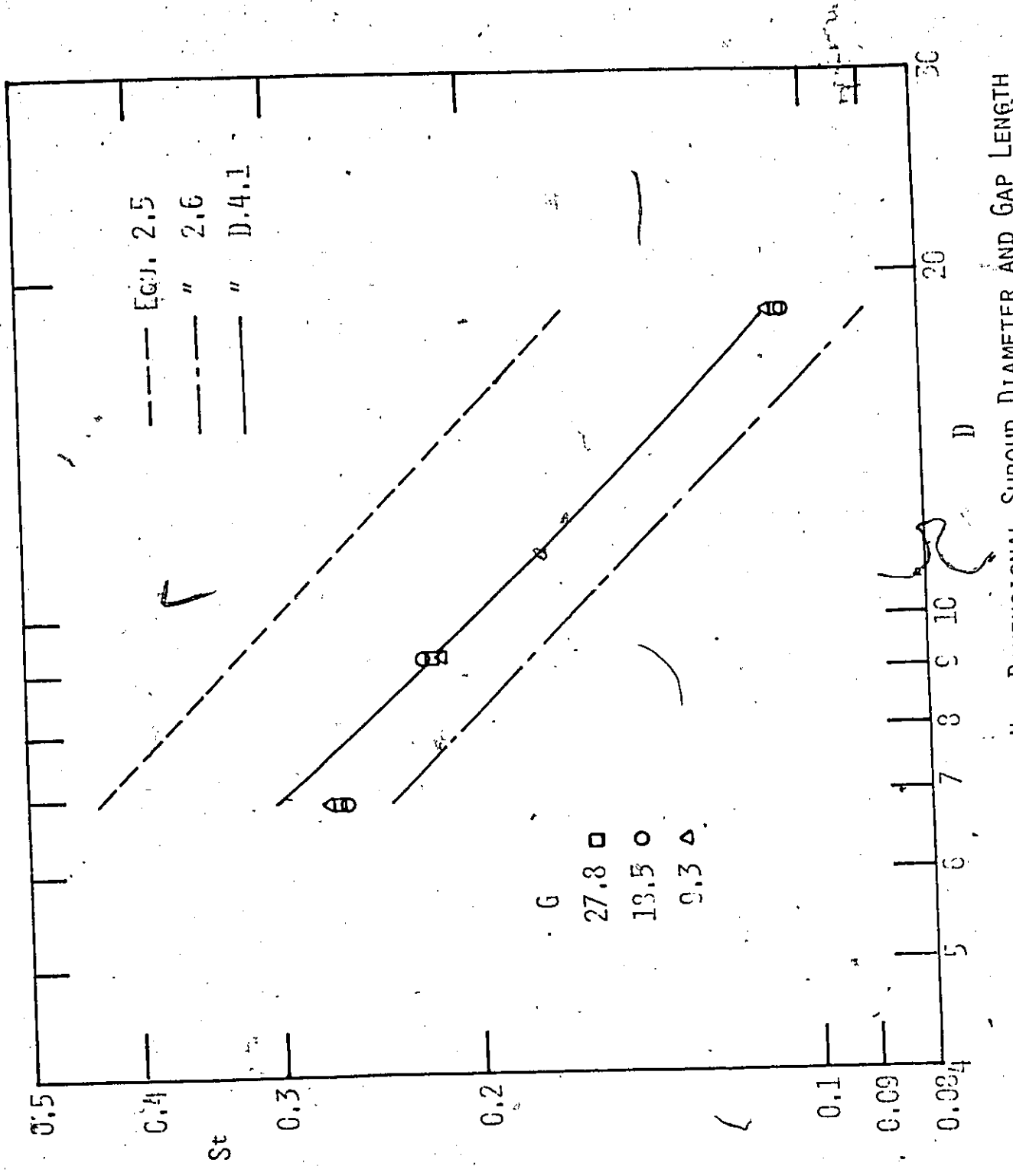


Fig. 14. STROUHAL NUMBER VERSUS NON-DIMENSIONAL SHROUD DIAMETER AND GAP LENGTH

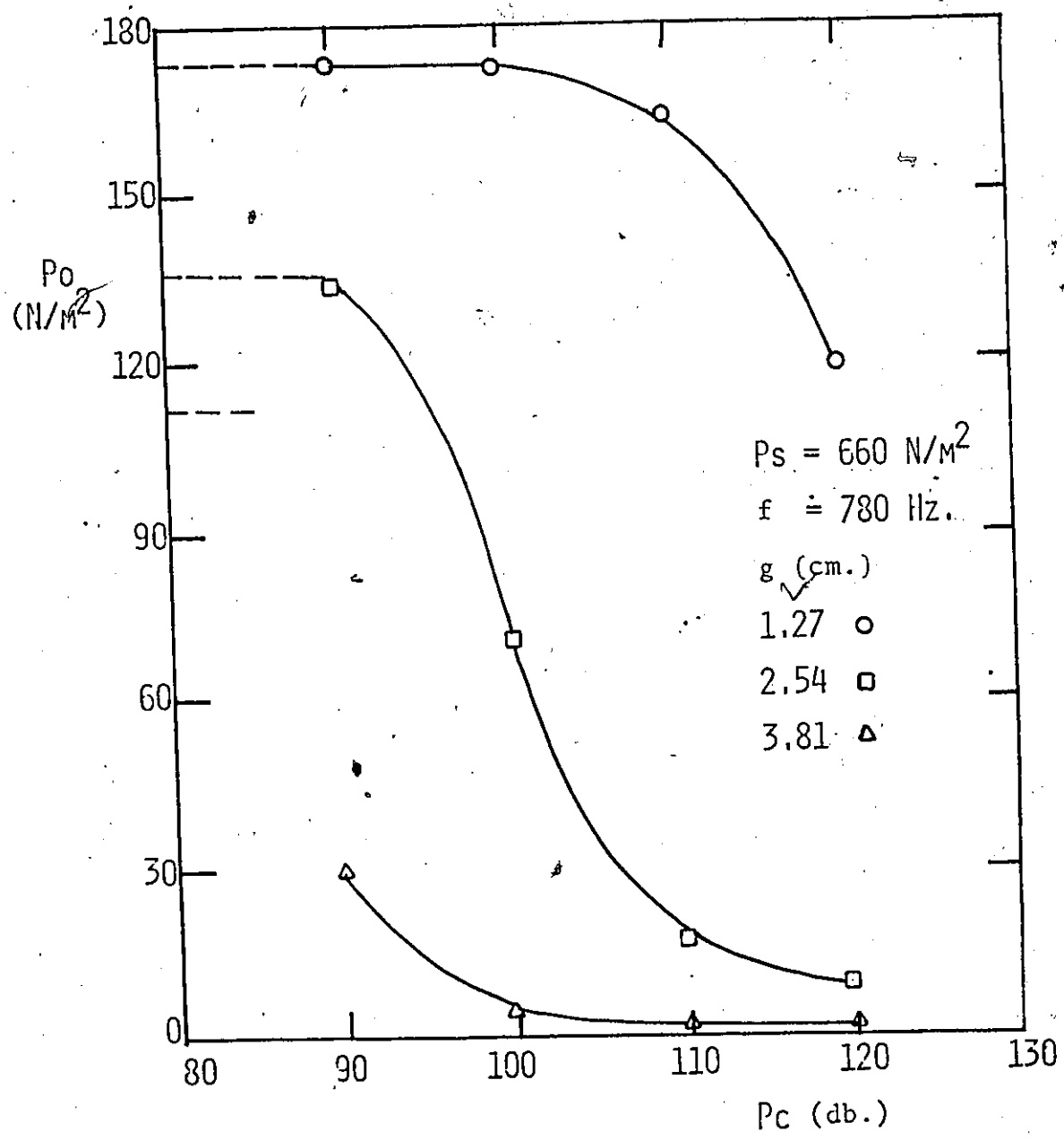


FIG. 15(A) $dc = 2.54 \text{ cm.}$

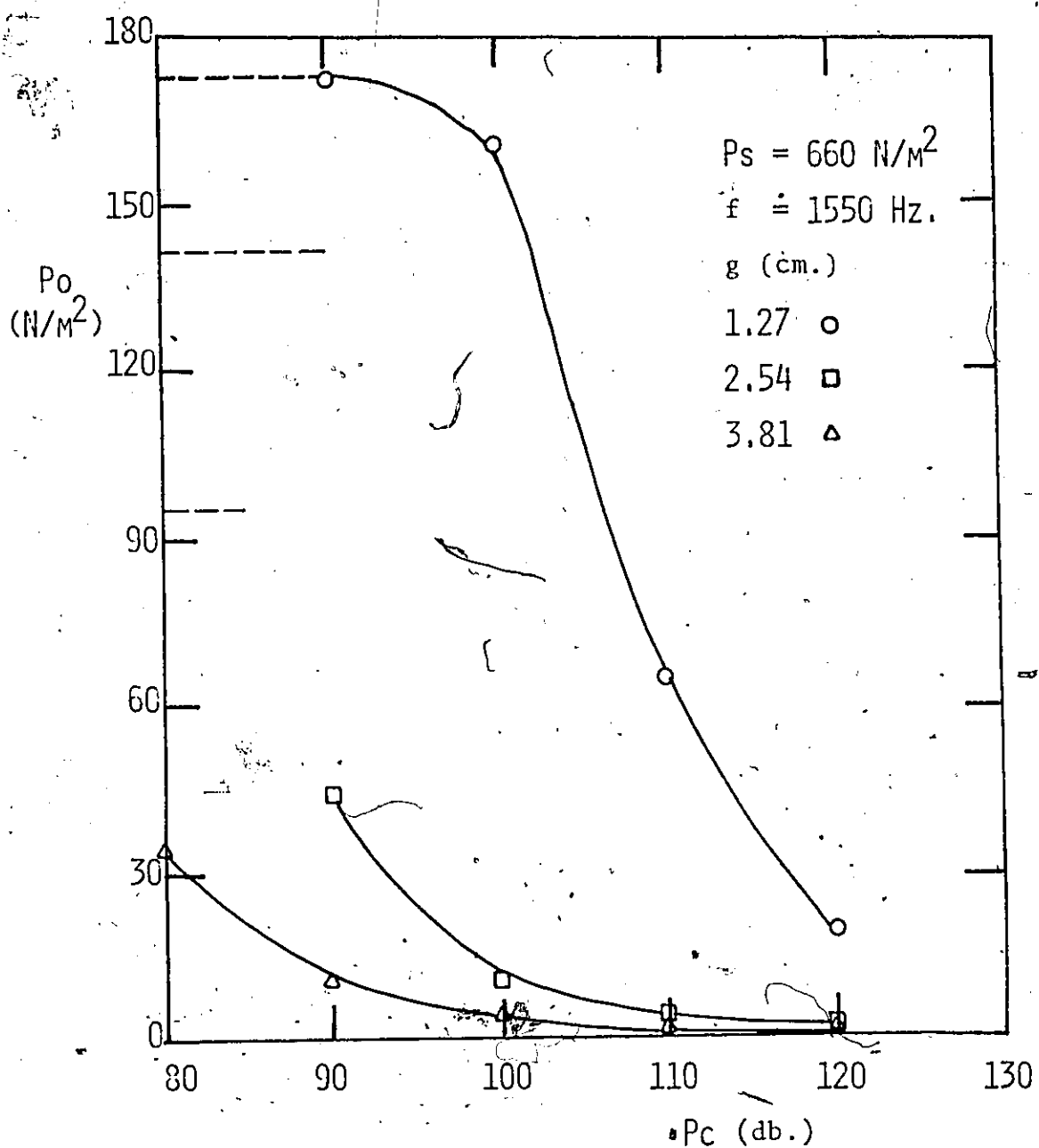


FIG. 15(B) $dc = 1.27 \text{ cm.}$

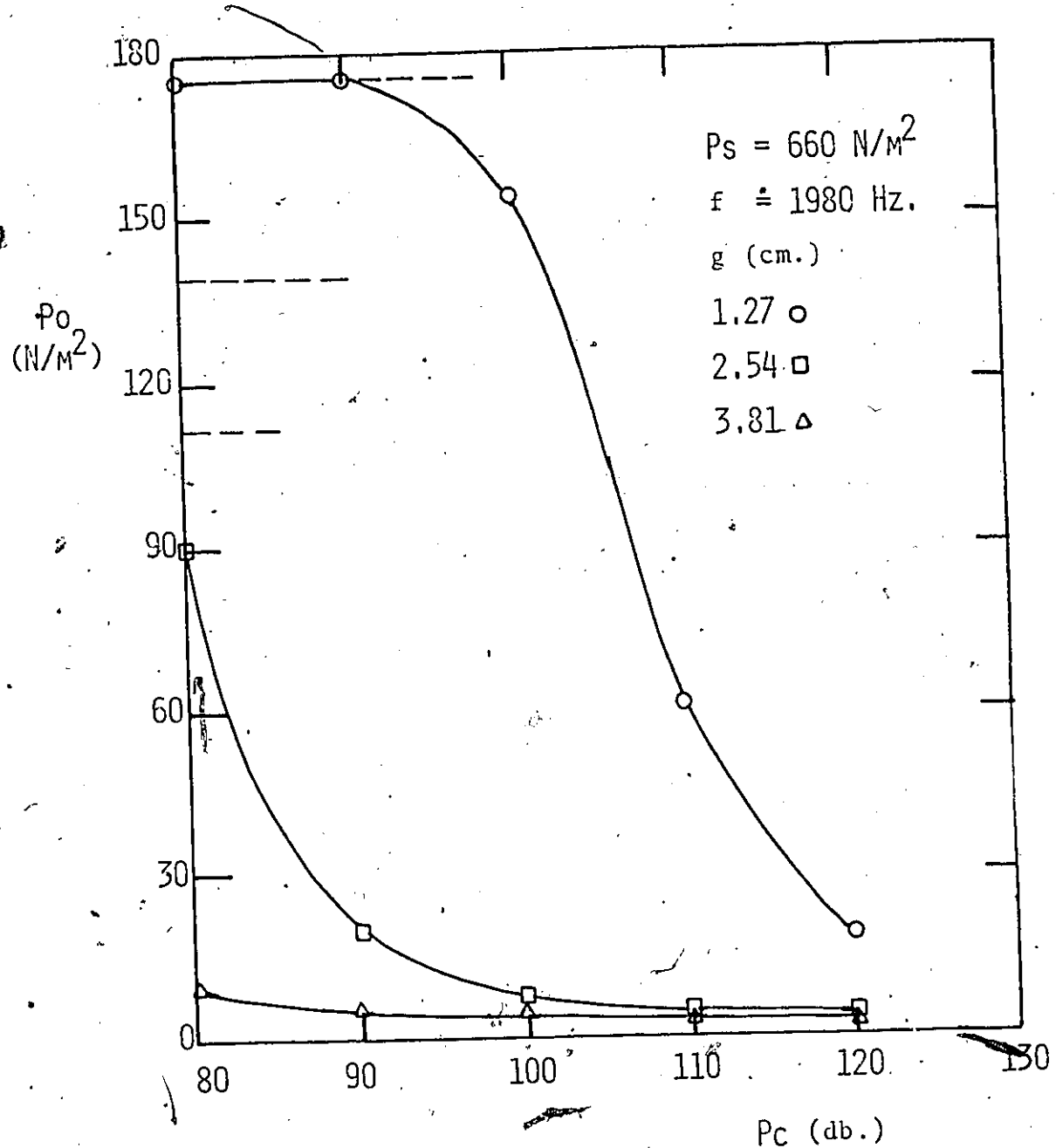


FIG. 15(c) $dc = 0.95 \text{ cm.}$

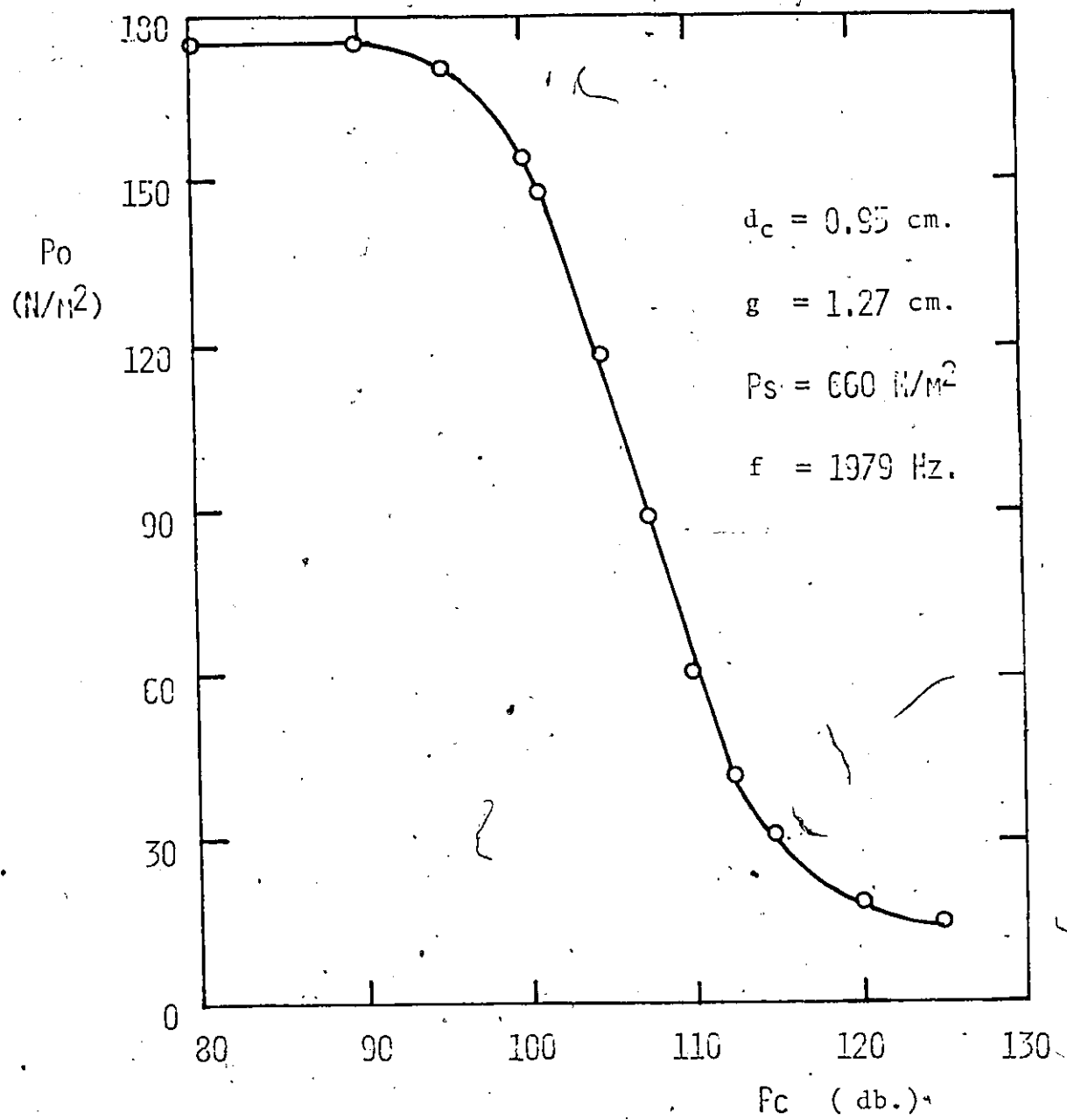


FIG. 10 PROPORTIONAL MODE OF OPERATION

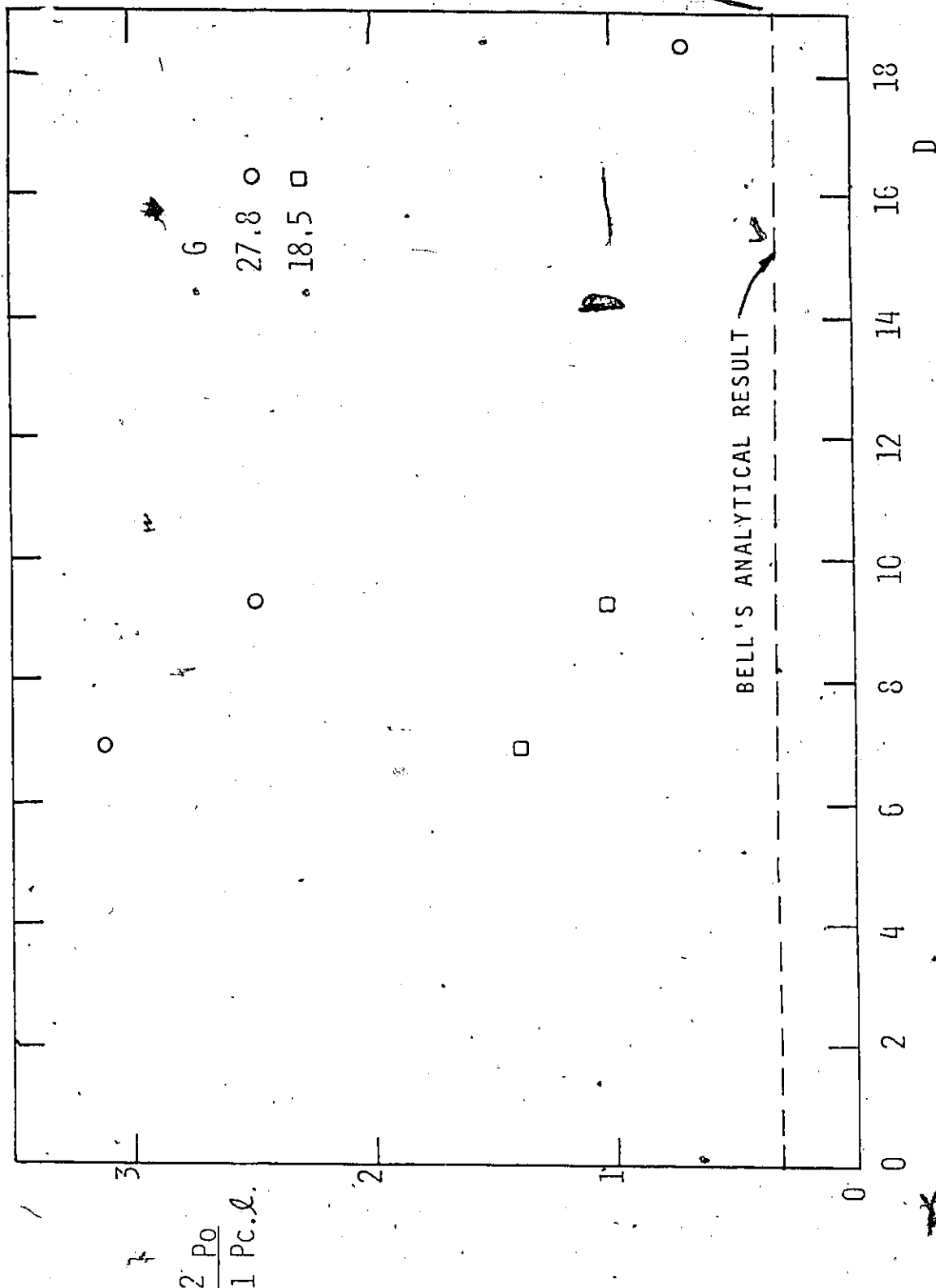


FIG. 17 NON-DIMENSIONAL TURBULENT PRESSURE RECOVERY DATA

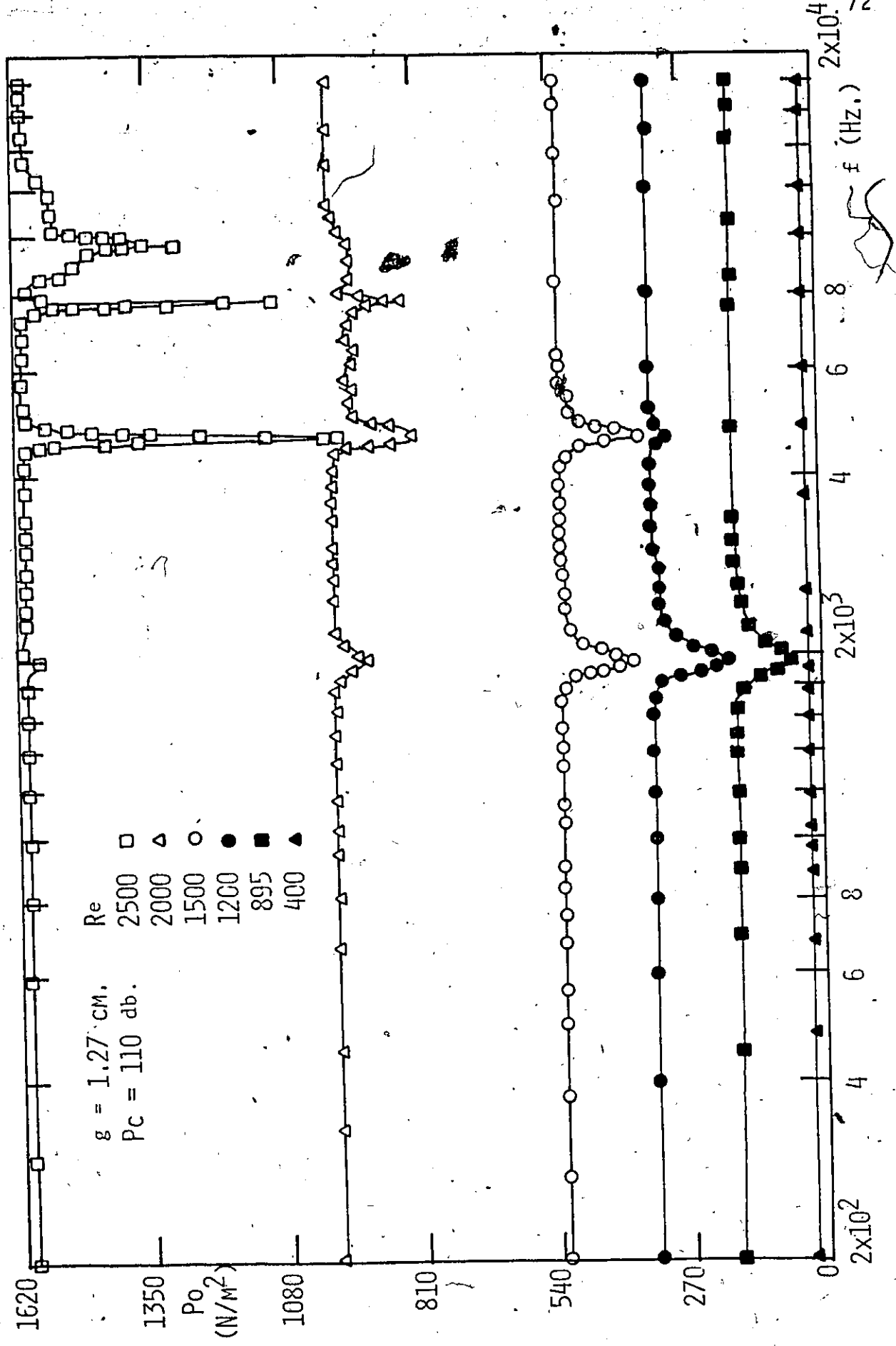


Fig. 18(A) $dc = 0.95 \text{ cm.}$

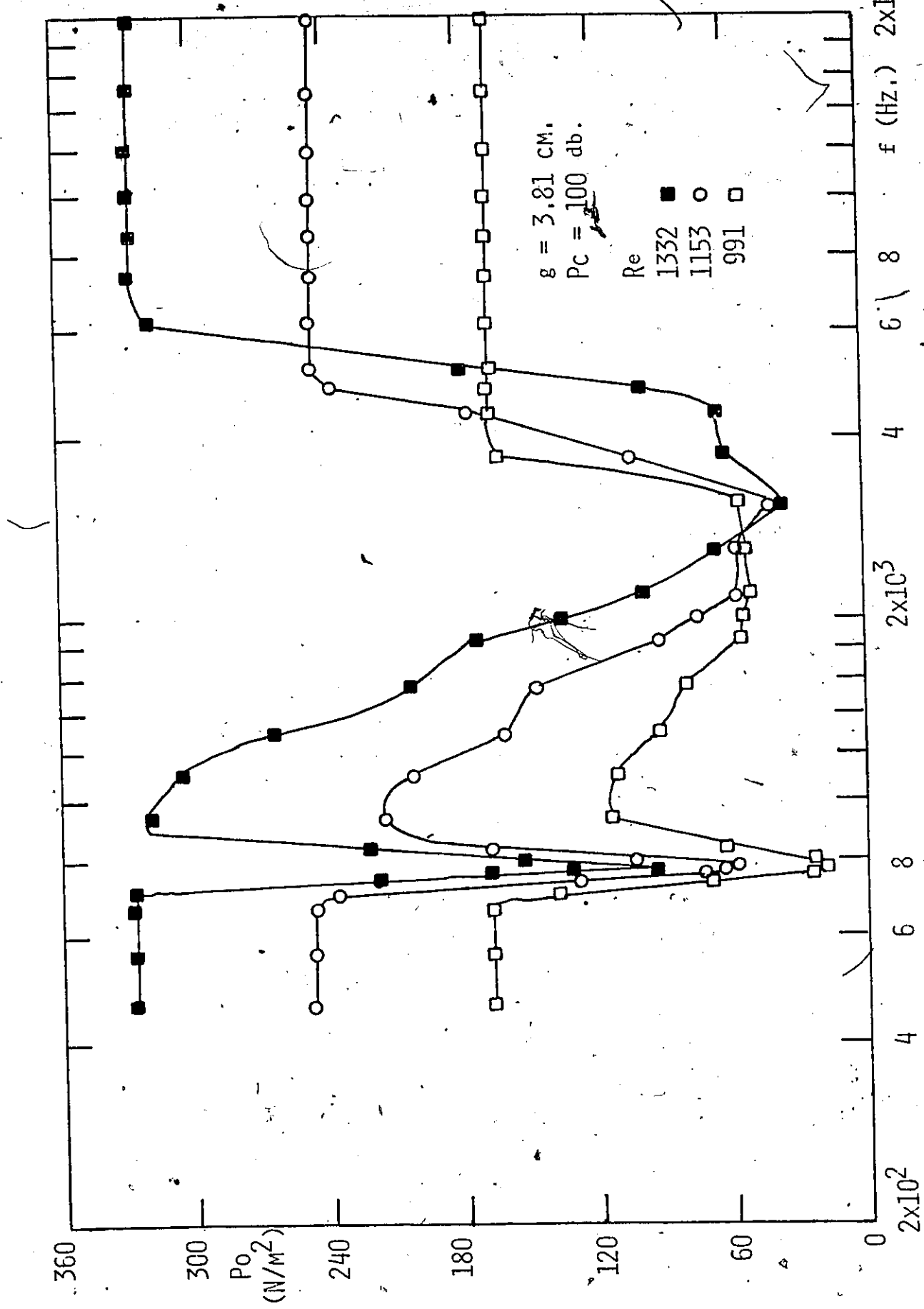


Fig. 18(B) $dc = 2.54 \text{ cm.}$

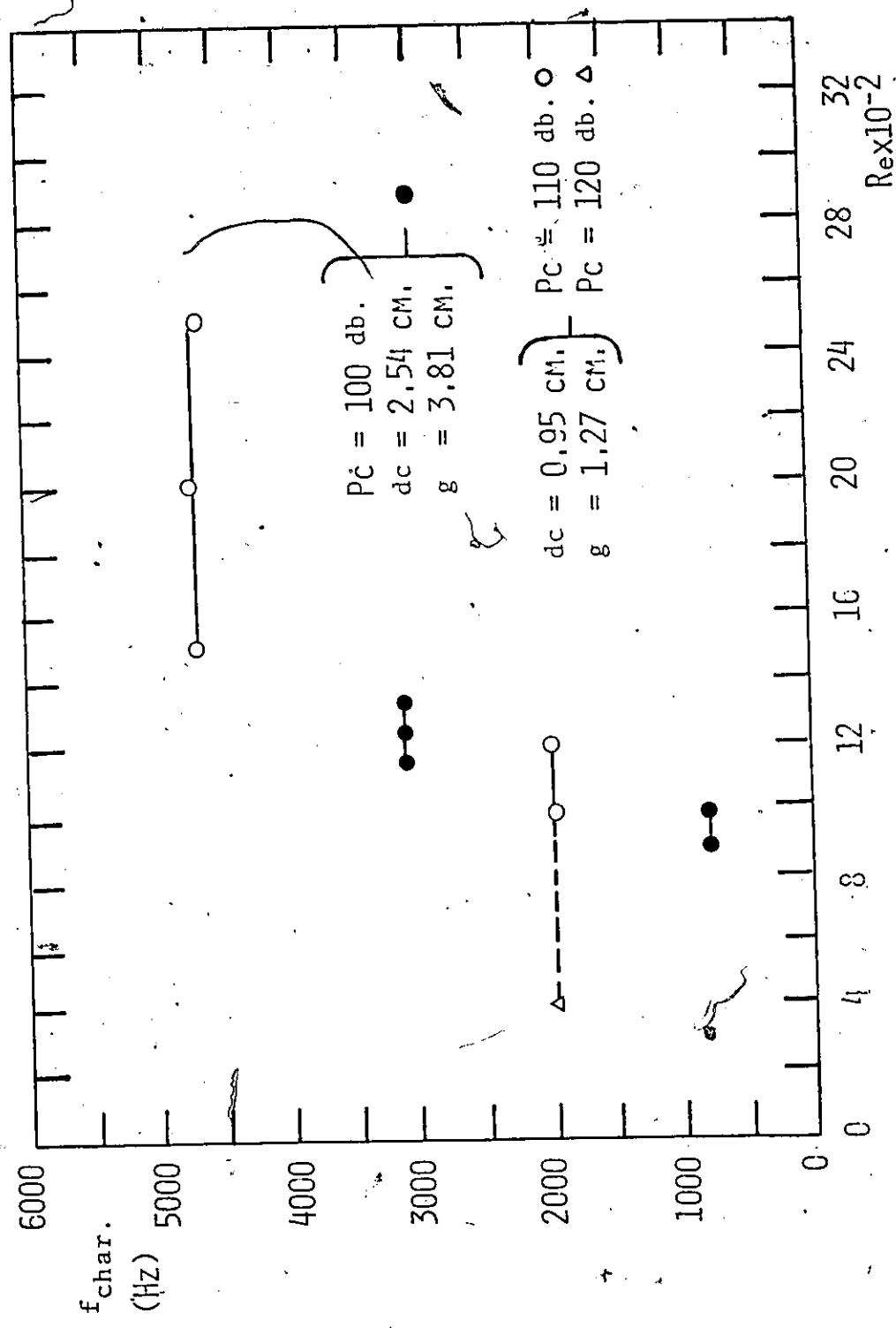


Fig. 19 | CHARACTERISTIC FREQUENCY VARIATION WITH REYNOLDS NUMBER

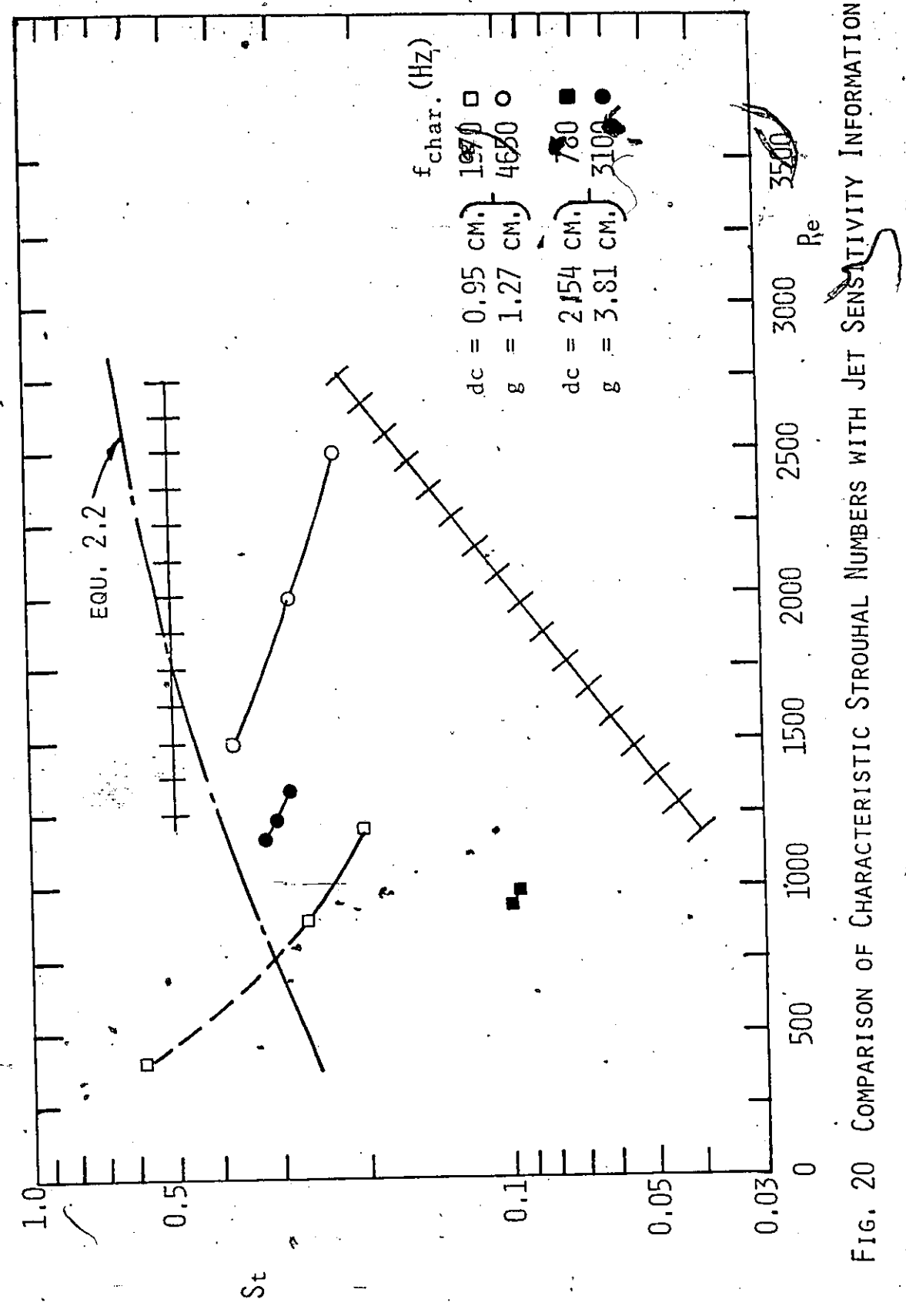


FIG. 20 COMPARISON OF CHARACTERISTIC STROUHAL NUMBERS WITH JET SENSITIVITY INFORMATION

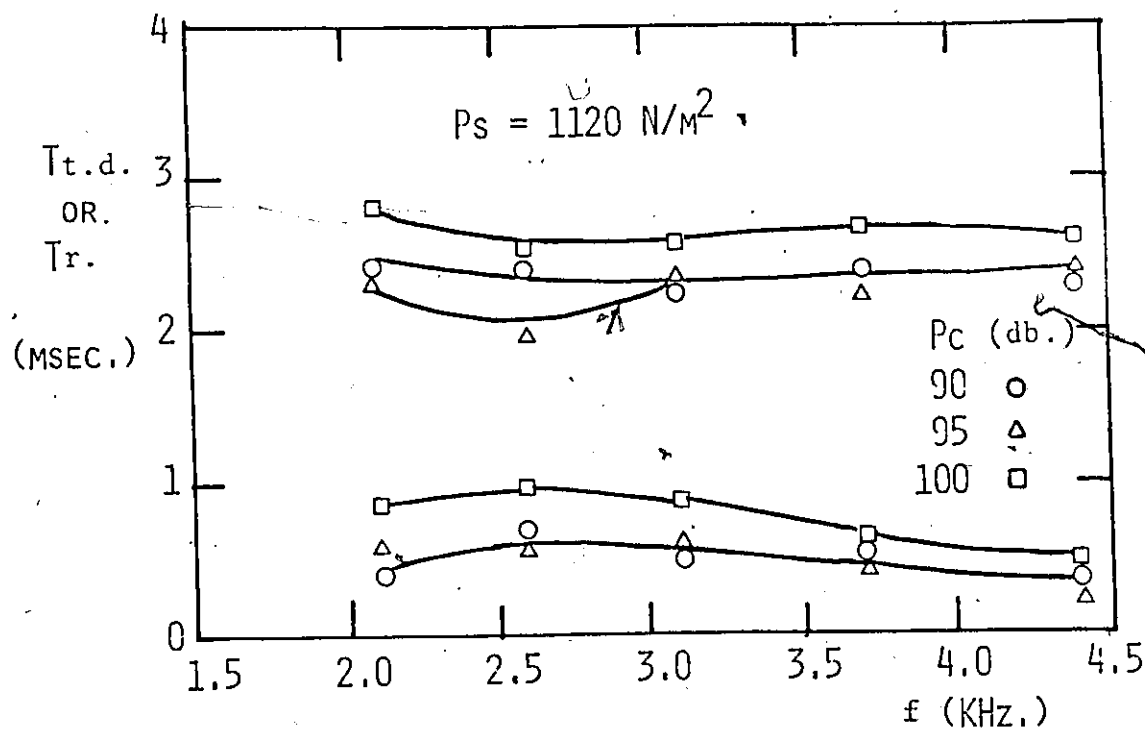
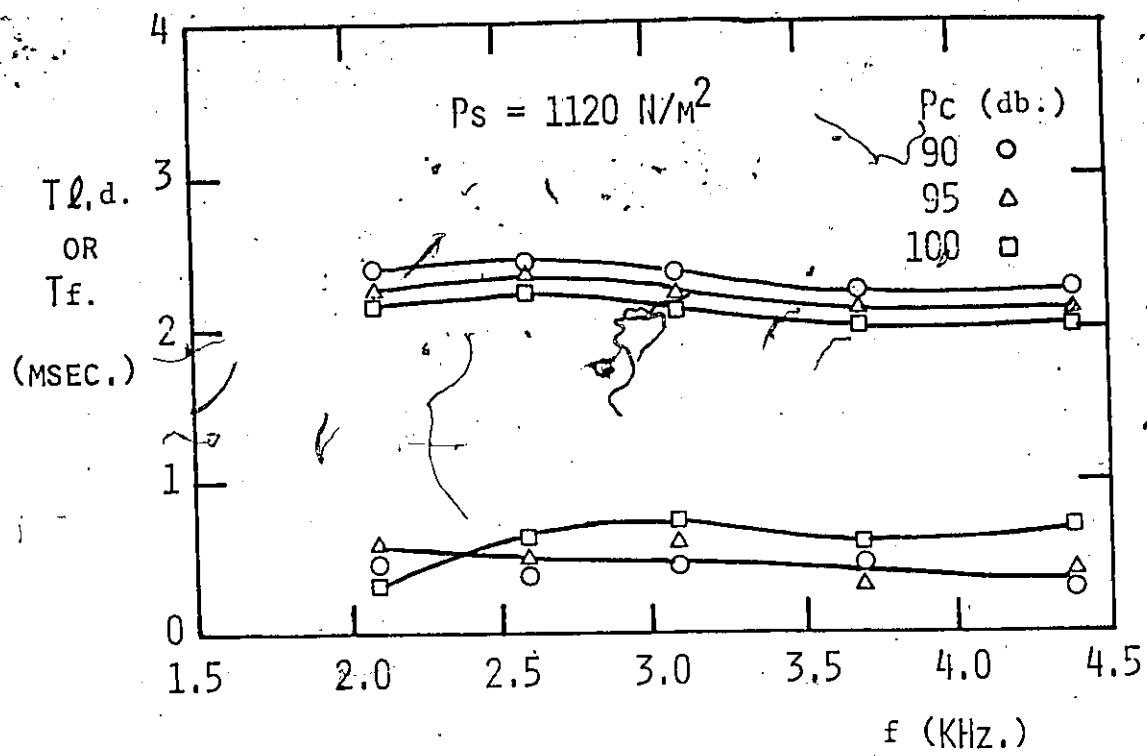
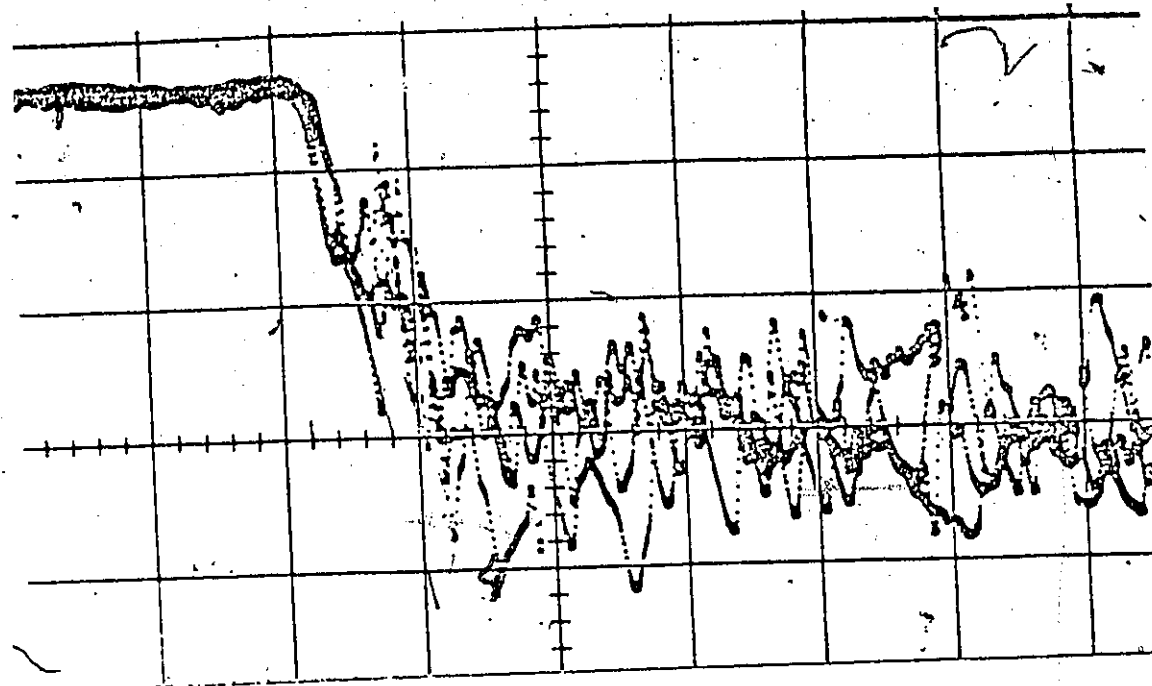
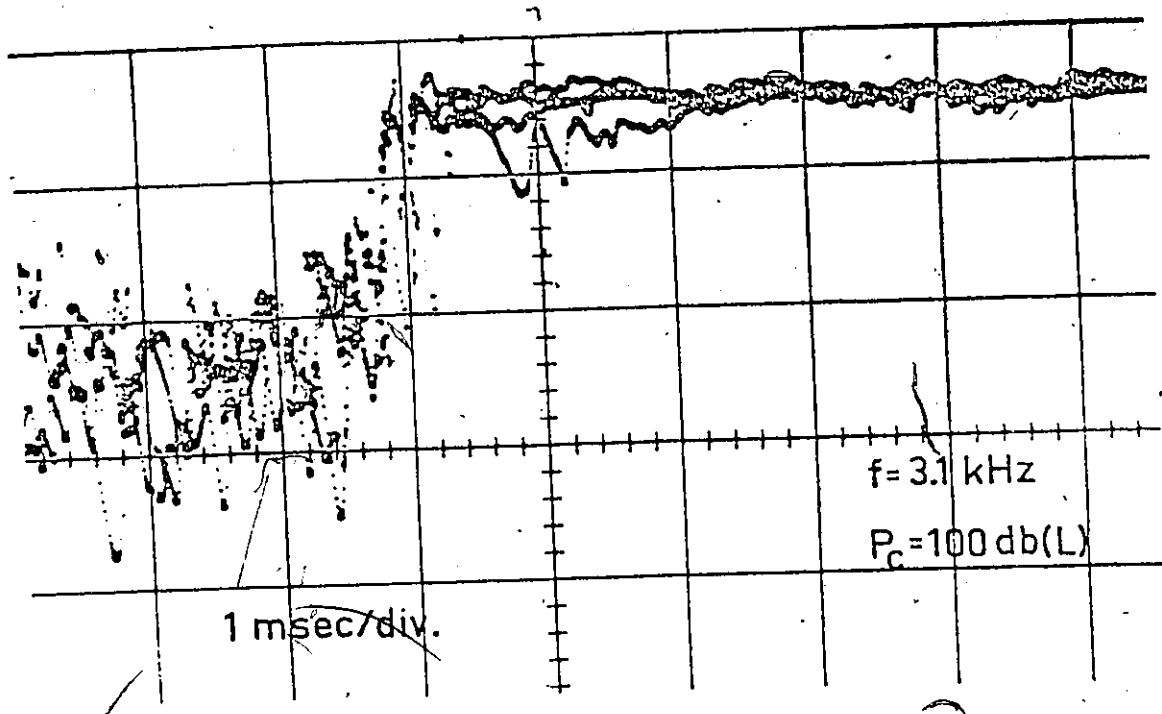


FIG. 21 EFFECT OF CONTROL SOUND VARIABLES ON RESPONSE TIME



(A) "SWITCH OFF"



(B) "SWITCH ON"

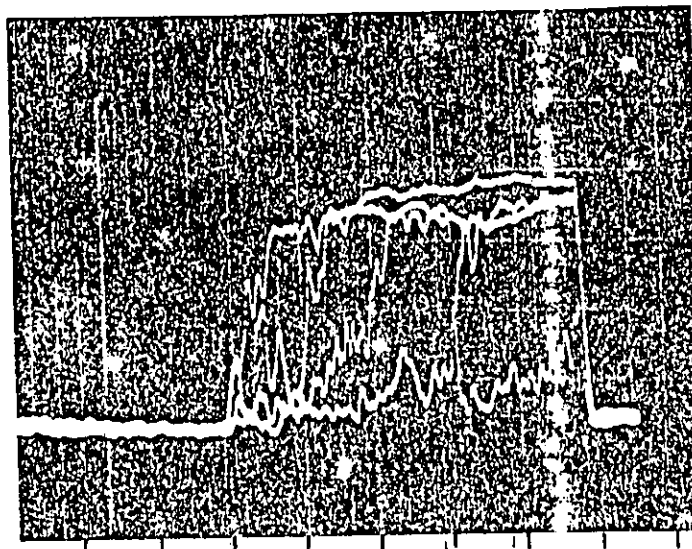
FIG. 22 MULTIPLE TRACES OF SWITCHING

$dc = 1.27 \text{ CM.}$

$Ps = 25.4 \text{ CM. OF WATER}$

$g = 2.44 \text{ CM.}$

PRESSURE



2 SEC./DIV.

FIG. 23 HAYES MULTIPLE TRACE

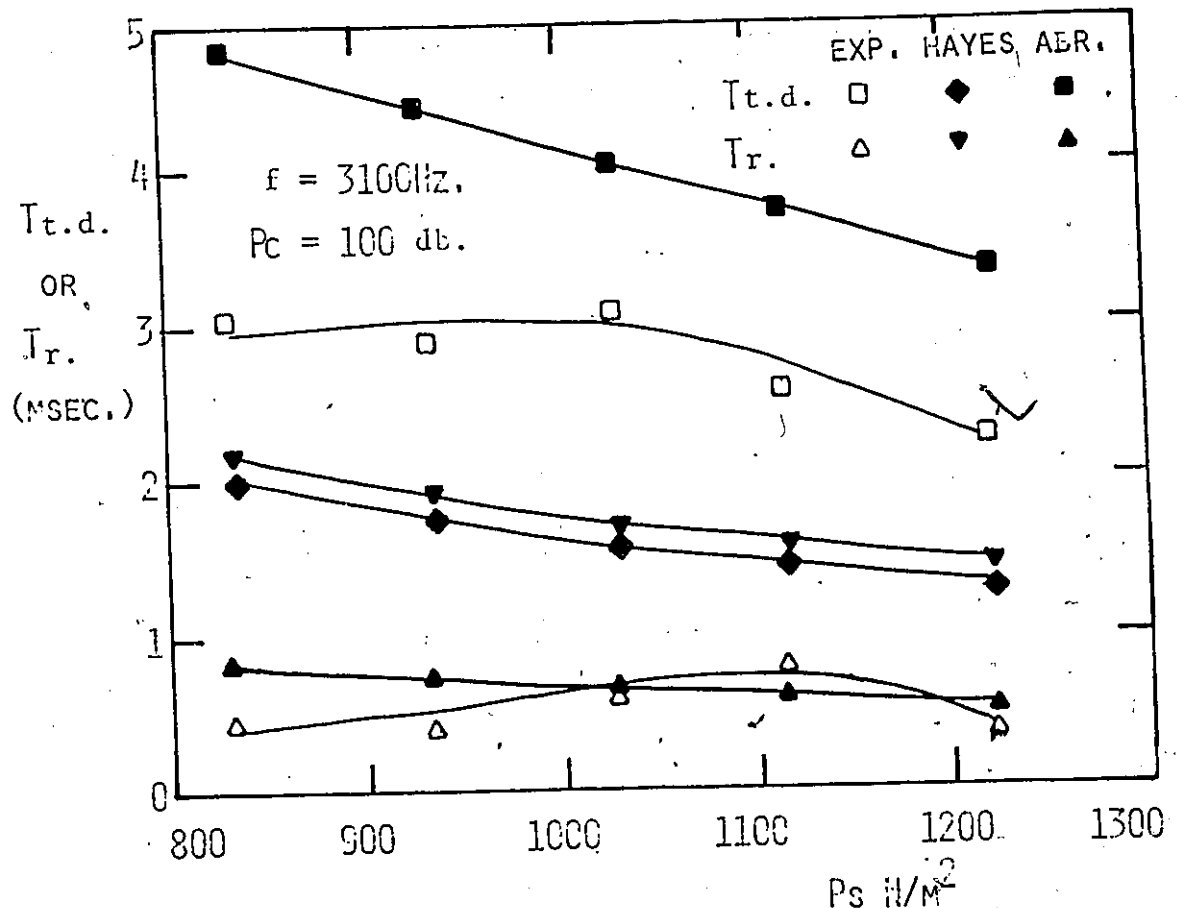
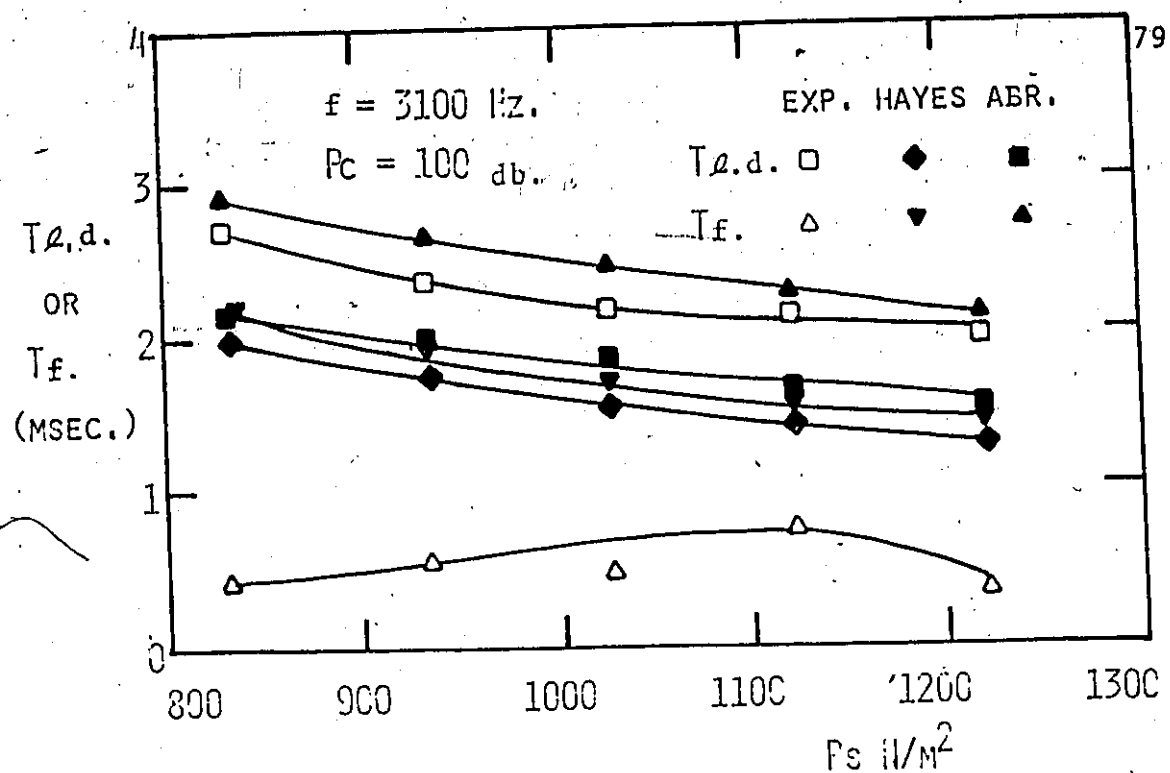


FIG. 24 RESPONSE TIME VARIATIONS WITH SUPPLY PRESSURE

dc	g	1.27 cm.	2.54 cm.	3.81 cm.
0.95 cm.		A,B,C	A,B	A,B
1.27 cm.		A,B	A,B	A,B
2.54 cm.		A,B	A,B	A,B,C,D

A Po vs P_s

B Po vs f for Different P_c

C Po vs f for Different Re , with $P_c = \text{constant}$

D Switching Time

TABLE I SUMMARY OF TEST PROGRAMME

APPENDIX A

DIMENSIONAL ANALYSIS

The quantities which are pertinent to the present study are listed below along with their symbols and dimensions according to the MLT system.

Quantity	Symbol	Dimension
supply tube diameter	d_s	L
output tube diameter	d_o	L
shroud diameter	d_c	L
control hole diameter (neck diameter)	d_n	L
vent hole diameter	d_v	L
number of vent holes	N	-
supply tube length	ℓ_s	L
output tube length	ℓ_o	L
gap length	g	L
control hole thickness (neck length)	ℓ_n	L
vent hole thickness	ℓ_v	L
supply pressure	P_s	$ML^{-1}T^{-2}$
output pressure	P_o	$ML^{-1}T^{-2}$
control sound pressure	P_c	$ML^{-1}T^{-2}$
average supply tube velocity	U_s	LT^{-1}
average output tube velocity	U_o	LT^{-1}
*frequency of sound	f	T^{-1}

*NOTE: The dimensions of f are actually cycles/sec, however this can be converted to rad/sec or T^{-1}

dynamic viscosity	μ	$ML^{-1}T^{-1}$
density	ρ	ML^{-3}
laminar-turbulent delay time	T_{ld}	T
laminar-turbulent fall time	T_f	T
turbulent-laminar delay time	T_{td}	T
turbulent-laminar rise time	T_r	T

The physical phenomenon of interest can be represented by writing the 23 quantities in the following form.

function ($ds, d_o, dc, dn, dv, N, l_s, l_o, g, l_n, l_v,$

$P_s, P_o, P_c, U_s, U_o, f, \rho, \mu, T_{ld}, T_f, T_{td}, T_r$) = 0

Choosing the repeating variables as

ds, U_s, ρ

the following non-dimensional groups can be found by inspection.

$$\frac{d_o}{ds}, \frac{dc}{ds}, \frac{dn}{ds}, \frac{dv}{ds}, N, \frac{l_s}{ds}, \frac{l_o}{ds}, \frac{g}{ds}, \frac{l_n}{ds}, \frac{l_v}{ds}$$

Using the Buckingham π method the remainder of the groups listed below can be found.

$$\frac{P_s}{\rho U_s^2}, \frac{P_o}{\rho U_s^2}, \frac{P_c}{\rho U_s^2}$$

$$\frac{T_{ld} \cdot U_s}{ds}, \frac{T_f \cdot U_s}{ds}, \frac{T_{td} \cdot U_s}{ds}, \frac{T_r \cdot U_s}{ds}$$

$$\frac{f}{ds}, \frac{U_o}{U_s} \text{ and } \frac{U_s ds}{\rho}$$

All of the quantities listed were not varied in the present experiment. Those that were varied are listed below:

$$\frac{dc}{ds}, \frac{g}{ds}, \frac{P_s}{\rho U_s^2}, \frac{P_o}{\rho U_s^2}, \frac{P_c}{\rho U_s^2}, \frac{T_{ld} \cdot U_s}{ds}$$

$$\frac{Tf \cdot Us}{ds}, \frac{Tt \cdot d \cdot Us}{ds}, \frac{Tr \cdot Us}{ds}, \frac{fds}{Us}, \frac{\mu \cdot Us \cdot ds}{\rho}$$

The non-dimensional groups that were actually used in present analysis are given below with their respective symbols.

$$D = \frac{dc}{ds}; G = \frac{g}{ds}; Re = \frac{Us \cdot ds}{\rho}$$

$$ST = \frac{fds}{Us}; Ls = \frac{ds}{ds} \cdot \frac{Po}{Ps}$$

The non-dimensional response times were not used in order to make comparisons with information in the literature.

The term P_c was not used due to the preference of expressing the sound pressure level in decibels with a standard reference pressure (P_r) of $2 \times 10^{-5} \text{ N/m}^2$ as defined below.

$$P_c = 20 \log_{10} \frac{P_c}{P_r} (\text{db})$$

APPENDIX. B
UNCERTAINTY ANALYSIS

An uncertainty analysis of the experimental quantities is given below for one complete set of experimental conditions of the amplifiers. Throughout the analysis a double apostrophe after a symbol denotes the uncertainty in the quantity (ie. R_e''). The conditions for which the uncertainty analysis is done are given below.

$$dc = 12.7 \times 10^{-3} \text{ m.}$$

$$ds' = 1.37 \times 10^{-3} \text{ m.}$$

$$g = 12.7 \times 10^{-3} \text{ m.}$$

$$P_s = 660 \text{ N/m}^2 \quad (Re = 895)$$

$$f_{\text{char.}} = 1554 \text{ Hz.}$$

$$P_0 = 21 \text{ N/m}^2$$

$$Q_s = 14.9 \times 10^{-6} \text{ m}^3/\text{sec.}$$

$$P_c = 120 \text{ db.}$$

$$\nu = 0.1547 \times 10^{-4} \text{ m}^2/\text{sec.}$$

(a) Supply Pressure

$$P_s = 9.78 R_s \sin \theta \text{ N/m}^2 \\ = 660 \text{ N/m}^2$$

where

$$R_s = \text{manometer reading} = 135 \text{ mm. H}_2\text{O}$$

$$\theta = \text{manometer slope} = 30^\circ$$

$$R_s'' = \pm 1 \text{ mm.}$$

$$\theta'' = \pm 0.25^\circ \quad (0.00436 \text{ rad.})$$

$$P_s'' = \left[\left(\frac{\delta P_s}{\delta R_s} R_s'' \right)^2 + \left(\frac{\delta P_s}{\delta \theta} \theta'' \right)^2 \right]^{1/2}$$

$$\frac{\delta P_s}{\delta R_s} = 9.78 \sin\theta = 4.89 \frac{N}{m^2 mm} H_2O$$

$$\frac{\delta P_s}{\delta \theta} = 9.78 R_s \cos\theta = 1143$$

$$P_s'' = 7.0 \frac{N}{m^2}$$

$$\frac{P_s'' \times 100}{P_s} \pm 1\%$$

(b) Output Pressure

$$P_o = 9.78 \frac{R_o}{S} (S.G.)$$

where

$$R_o = \text{Output manometer reading} = 13$$

$$S = \text{manometer slope factor} = 5$$

$$S.G. = \text{manometer fluid specific gravity} = 0.827$$

$$P_o = 21 \frac{N}{m^2}$$

$$R_o'' = \pm 0.5 \text{ mm.}$$

S'' = assumed equal to 0 due to standard slope fixtures holding the tube in place

$$(S.G.)'' = 2\% = 0.016$$

$$P_o'' = \left[\left(\frac{\delta P_o}{\delta R_o} R_o'' \right)^2 + \left(\frac{\delta P_o}{\delta (S.G.)} \right)^2 \right]^{1/2}$$

$$\frac{\delta P_o}{\delta R_o} = \frac{9.78 (S.G.)}{S} = 1.62 \frac{N}{m^2 mm} H_2O$$

$$\frac{\delta P_o}{\delta (S.G.)} = \frac{9.78 R_o}{S} = 25.4 \frac{N}{m^2}$$

$$P_o'' = 0.91 \frac{N}{m^2}$$

$$\frac{P_o'' \times 100}{P_o} = 4.3\%$$

(c) Reynolds Number

$$Re = \frac{40s}{\pi ds \nu} = 895$$

$$Qs'' = 0.1 \times 10^{-6} \text{ m}^3/\text{sec.}$$

$$ds'' = 0.03 \times 10^{-3} \text{ m.}$$

$$v'' = 0.03 \times 10^{-6} \text{ m}^2/\text{sec.}$$

$$Re'' = \left[\left(\frac{\delta Re}{\delta Qs} Qs'' \right)^2 + \left(\frac{\delta Re}{\delta ds} ds'' \right)^2 + \left(\frac{\delta Re}{\delta v} v'' \right)^2 \right]^{1/2}$$

$$\frac{\delta Re}{\delta Qs} = \frac{4}{\pi ds v} = 6.0 \times 10^7 \text{ sec. m}^3$$

$$\frac{\delta Re}{\delta ds} = \frac{-4}{\pi ds^2 v} = -6.5 \times 10^5 \text{ m}^{-3}$$

$$\frac{\delta Re}{\delta v} = \frac{-4Qs}{\pi ds v^2} = -5.8 \times 10^7 \text{ sec. m}^2$$

$$Re'' = 20.4$$

$$\frac{Re''}{Re} \times 100 = 2.3\%$$

(d) Non-Dimensional Shroud Diameter

$$D = \frac{dc}{ds} = 9.27$$

$$dc'' = \pm 0.03 \times 10^{-3} \text{ m.}$$

$$ds'' = \pm 0.03 \times 10^{-3} \text{ m.}$$

$$D'' = \left[\left(\frac{\delta D ds''}{\delta ds} \right)^2 + \left(\frac{\delta D dc''}{\delta dc} \right)^2 \right]^{1/2}$$

$$\frac{\delta D}{\delta ds} = - \frac{dc}{ds^2} = -4939 \text{ m}^{-1}$$

$$\frac{\delta D}{\delta dc} = \frac{1}{ds} = .730 \text{ m}^{-1}$$

$$D'' = 0.18$$

$$\frac{D''}{D} \times 100 = 2\%$$

(e) Non-Dimensional Gap Length

$$G = \frac{g}{ds} = 9.27$$

$$g'' = \pm 0.15 \times 10^{-3} \text{ m.}$$

$$G'' = \left[\left(\frac{\delta G}{\delta g} g'' \right)^2 + \left(\frac{\delta G}{\delta s} ds'' \right)^2 \right]^{1/2}$$

$$\frac{\delta G}{\delta g} = \frac{1}{ds} = 730 \text{ m}^{-1}$$

$$\frac{\delta G}{\delta s} = -g = 4939 \text{ m}^{-1}$$

$$G'' = 0.18$$

$$\frac{G''}{G} \times 100 = 2\%$$

(f) Non-Dimensional Output Pressure

$$\frac{P_o}{P_s} = 0.0318$$

$$\left(\frac{P_o}{P_s} \right)'' = \left[\left(\frac{\delta (P_o/P_s)}{\delta P_o} P_o'' \right)^2 + \left(\frac{\delta (P_o/P_s)}{\delta P_s} P_s'' \right)^2 \right]^{1/2}$$

$$\frac{\delta (P_o/P_s)}{\delta P_o} = \frac{1}{P_s} = 1.515 \times 10^{-3} \frac{\text{m}^2}{\text{N}}$$

$$\frac{\delta (P_o/P_s)}{\delta P_s} = -\frac{P_o}{P_s^2} = -4.82 \times 10^{-5} \frac{\text{m}^2}{\text{N}}$$

$$\left(\frac{P_o}{P_s} \right)'' = 0.00142$$

$$\left(\frac{P_o}{P_s} \right)'' \times 100 = 4.5\%$$

(g) Go. 27 $\frac{P_o}{P_s}$ (let this term be called Z in this section)

$$Z = 0.0580$$

$$Z'' = \left[\left(\frac{\delta Z}{\delta G} G'' \right)^2 + \left(\frac{\delta Z}{\delta (P_o/P_s)} \left(\frac{P_o}{P_s} \right)'' \right)^2 \right]^{1/2}$$

$$\frac{\delta Z}{\delta G} = 0.27 G^{-0.73} \quad \frac{P_o}{P_s} = 0.00169$$

$$Z'' = 0.0026 \quad \frac{\delta Z}{\delta (P_o/P_s)} = G^{0.27} = 1.82$$

$$Z'' \times 100 = 4.5\%$$

(h) Characteristic Strouhal Number

$$\text{Stchar.} = \frac{\text{fchar.} \cdot ds}{Us} = \frac{\text{fchar.} ds^3}{4Qs}$$

$$\text{fchar.} = 1554$$

$$\text{Stchar.} = 0.211$$

$$\text{fchar."} = \pm 10\text{Hz}$$

$$\text{Stchar."} = \left[\left(\frac{\delta \text{Stchar.}}{\delta \text{fchar.}} \cdot \text{fchar."} \right)^2 + \left(\frac{\delta \text{Stchar.}}{\delta ds} \cdot ds" \right)^2 + \left(\frac{\delta \text{fchar.}}{\delta Qs} \cdot Qs" \right)^2 \right]^{1/2}$$

$$\frac{\delta \text{Stchar.}}{\delta \text{fchar.}} = \frac{\pi d^3}{4Qs} = 1.36 \times 10^{-4} \text{ sec.}$$

$$\frac{\delta \text{Stchar.}}{\delta ds} = \frac{3ds^2\pi fchar.}{Qs} = 461 \text{ m}^{-1}$$

$$\frac{\delta \text{Stchar.}}{\delta Qs} = \frac{fchar.\pi dz^3}{4Qs^2} = -14136 \text{ sec.}^{-3} \text{ m}^{-3}$$

$$\text{Stchar."} = 0.0139$$

$$\frac{\text{St.char."}}{\text{St. char.}} \times 100 = 6.6\%$$

(i) Response Times

The response times could be measured with an uncertainty of ± 0.2 msec. considering the sweep time of the oscilloscope (1m.sec./cm.) and possible errors involving the attainment of a reading according to the definitions of the times.

(j) Control Sound Pressure Level

Based on the calibration procedure used to obtain these values and the position of the microphone in front of the control hole opening the uncertainty ($Pc"$) is estimated as ± 1 db.

$$(k) \frac{G^2 P_0}{41 \text{ P.c.} \ell}$$

Only certain variables were used to calculate $\frac{G^2 P_0}{41 \text{ P.c.} \ell}$.

The following data consists of the information required to obtain one of the points in Fig. 17.

$$ds = 1.37 \times 10^{-3} \text{ m.} \quad f_{\text{char.}} = 780 \text{ Hz.}$$

$$dc = 25.4 \times 10^{-3} \text{ m.} \quad R_o = 3 \text{ mm.}$$

$$g = 38.1 \times 10^{-3} \text{ m.} \quad S = 25$$

$$Q_s = 14.9 \times 10^{-6} \text{ m}^3/\text{sec.} \quad S.G. = \pm 0.016$$

$$P_s = 660 \text{ N/m}^2 \quad \rho = 1.189 \text{ Kg/m}^3$$

$$\rho'' = \pm 2.08 \times 10^{-3} \text{ Kg/m}^3$$

It can be shown using the previous methods that

$$P_0 = 0.97 \text{ N/m}^2, \quad P_0'' = 0.325 \text{ N/m}^2$$

$$G = 27.8 \quad \text{and} \quad G'' = 0.619$$

also

$$\text{P.c.} \ell. = \frac{8 \rho Q_s}{\pi ds^2} = 24.0 \text{ N/m}^2$$

$$\begin{aligned} \text{P.c.} \ell. '' &= \left[\left(\frac{\delta \text{P.c.} \ell.}{\delta \rho} \rho'' \right)^2 + \left(\frac{\delta \text{P.c.} \ell.}{\delta Q_s} Q_s'' \right)^2 \right. \\ &\quad \left. + \left(\frac{\delta \text{P.c.} \ell.}{\delta ds} ds'' \right)^2 \right]^{\frac{1}{2}} \end{aligned}$$

$$\frac{\delta \text{P.c.} \ell.}{\delta \rho} = \frac{8 Q_s}{\pi ds^2} = 20.2 \frac{\text{N.m}}{\text{Kg}}$$

$$\frac{\delta \text{P.c.} \ell.}{\delta Q_s} = \frac{8 \rho}{\pi ds^2} = 1.61 \times 10^6 \frac{\text{N.sec}}{\text{m}^5}$$

$$\frac{\delta \text{P.c.} \ell.}{\delta ds} = - \frac{16 \rho Q_s}{\pi ds^3} = - 3.51 \times 10^4 \frac{\text{N}}{\text{m}^3}$$

$$\text{P.c.} \ell. '' = 1.07 \text{ N/m}^2$$

$$\text{letting } Y = \frac{G^2 Po}{41.0 \text{ P.C. } \ell} = 0.761$$

$$Y'' = \left[\left(\frac{\delta Y}{\delta G} G'' \right)^2 + \left(\frac{\delta Y}{\delta Po} Po'' \right)^2 + \left(\frac{\delta Y}{\delta \text{P.C. } \ell} \text{P.C. } \ell'' \right)^2 \right]^{\frac{1}{2}}$$

$$\frac{\delta Y}{\delta G} = \frac{2GPo}{41.0 \text{ P.C. } \ell} = 0.055$$

$$\frac{\delta Y}{\delta Po} = \frac{G^2}{41.0 \text{ P.C. } \ell} = 0.785 \frac{\text{m}^2}{\text{N}}$$

$$\frac{\delta Y}{\delta \text{P.C. } \ell} = - \frac{G^2 Po}{41.0 (\text{P.C. } \ell)^2} = - 0.0317 \frac{\text{m}^2}{\text{N}}$$

$$\frac{Y''}{Y} \times 100 = 34\%$$

APPENDIX C
EQUIPMENT TABLE

No.	Equipment	Model/Type	Range	Accuracy	Measurement	Manufacturer/Company
1	Dual Beam Oscilloscope	564			Switching times	Tektronix, Inc. Portland, Oregon
2	Hot-Wire Anemometer	SSM			"	Disa Elektronik Herlev, Denmark
3	Measuring Amplifier	2607			Control Sound pressure level	B&K Copenhagen, Denmark
4	Preamplifier	2618			"	"
5	Condenser Microphone	4138	70-180 db	± 1 db.	"	"
6	Inclined Manometer	320111	0-807 N/m ² .	± 0.5% Full Scale	Output pressure with Lambrecht Göttingen, W. Germany	
7	Inclined Manometer	9845	0-7000 N/m ²	± 0.2% Full Scale	Supply pressure T.E.M. Instruments Ltd. Crawley; Sussex	
8	Manometer Bank	*ME C406	0-30600 N/m ²	± 0.2% Full Scale	Supply pressure U. of N.	
9	Rotameter	L10/400-6185	0-120x10 ⁻⁶ m ³ /sec	± 0.2% Full Scale	ROTA Oeflingen Baden	
10	Rotameter	L2.5/100-3458	0-33x10 ⁻⁶ m ³ /sec	± 0.2% Full Scale	"	
11	Needle Valve	1135 G2B				Hoke Inc. Cresskill, N.J.
		1° Stem				

No.	Equipment	Model/Type	Range	Accuracy	Measurement	Manufacturer/Company
12	Pressure Regulator	7266-1	0-508 cm. H ₂ O			Moore Products Spring House, Pa.
13	Filter	A-11138-8				Wilkerson Inc. Englewood, Colorado
14	8" Speaker	LS-809-14W	170-18 KHz			Marsland Eng. Ltd. Waterloo, Ont.
15	4" Dome Tweeter	AD.0160/TA	1 KHz-22 KHz			DeForéster (Phillips) Toronto, Ont.
16	5" Speaker	AD 5060/508	400-8KHz			
17	Sine Wave Oscillator	200 CP	5-600KHz	± 1 Hz	Control Sound Frequency	Hewlett Packard Loveland, Col.
18	Electronic Counter	5221B	99999 Hz			Hewlett-Packard
19	Power Amplifier	ME C515	25W			U. of W.
20	Electronic Switch					U. of W.
21	Sound Level Meter	2204	0-20K Hz 0-130 db		Background noise level	B&K
22	Sound Level Calibrator	4220	250 Hz 124 db.	± 0.2db	"	"

* NOTE: M/E. Number Correspond to the Department Stock Numbers.

APPENDIX D

ANALYTICAL METHODS	Page
D.1 Bell's Analytical Procedure	94
D.2 Haye's Theoretical Switching Times	102
D.3 Abramovich's Empirical Switching Times	103
D.4 Alster's Helmholtz Formula	104

APPENDIX D.1

BELL'S ANALYTICAL PROCEDURE

A general description of the theoretical methods that Bell used is given in Chapter II. In this section, emphasis is given to the usage of the standard mathematical relationships, given by Bell in Ref. 12 for determining the characteristics of the unshrouded turbulence amplifier.

In the following analysis it is assumed that d_s , g , P_s , and ℓ_s are known.

- (1) Estimate Q_s from

$$Q_s = \frac{\pi d_s^4 P_s}{128 \ell_s} \quad D.1.1$$

- (2) Calculate Re from

$$Re = \frac{4 Q_s}{L_s \pi d_s v} \quad D.1.2$$

- (3) Find $\frac{P_{cl}}{P_s}$ using Table D.1.1 (Ref. 12) shown on the next page.

$\frac{P_s}{P_{cl}}$ can be found by adding 1 to ΔP to include the $\frac{172}{L_s^2}$.

non-dimensional Bernouli pressure drop incurred by the fluid passing from the settling chamber into the tube through a bellmouth entrance. $\frac{P_{cl}}{P_s}$ is then found by inverting these values and interpolating for the particular Re found from step 2.

- (4) λ_0 is found by interpolating the $R=0$ column of Table D.1.1 for the particular value of Re mentioned previously.

- (5) Calculate P_{cl} from

$$P_{cl} = 0.5 g \left(\frac{4 \lambda_0 Q_s}{\pi d_s} \right)^2 \quad D.1.3$$

$R = \frac{r}{(ds/2)}$	$\lambda = \frac{U(R)}{(4Q_s/\pi ds^2)}$	$\frac{\Delta P}{2\rho U_s^2}$
0	0	0
0.1	0.0000	0.0000
0.2	1.1503	1.1503
0.3	1.2269	1.2269
0.4	1.3125	1.3125
0.5	1.3779	1.3779
0.6	1.4324	1.4324
0.7	1.4799	1.4799
0.8	1.5120	1.5120
0.9	1.5252	1.5252
1.0	1.5460	1.5460
1.1	1.5727	1.5727
1.2	1.6148	1.6148
1.3	1.6562	1.6562
1.4	1.7000	1.7000
1.5	1.7448	1.7448
1.6	1.7820	1.7820
1.7	1.8122	1.8122
1.8	1.8366	1.8366
1.9	1.8563	1.8563
2.0	1.8763	1.8763
2.1	1.8969	1.8969
2.2	1.9177	1.9177
2.3	1.9382	1.9382
2.4	1.9583	1.9583
2.5	1.9780	1.9780
2.6	1.9975	1.9975
2.7	2.0160	2.0160

NOTE: The value of $\frac{\Delta P}{2\rho U_s^2}$ given by Bell for $\frac{Re}{L_s} = 0$ is shown in brackets. This value must be infinity as can be easily seen by considering the cases of L_s and Re approaching infinity and zero respectively.

r is the radial distance from the centre of the tube

TABLE D.1.1 Hornbeck's Solution for Pressure Drops in Developing Flow Through Tubes

(6) Calculate P_s estimate from

$$P_s \text{ estimate} = \frac{\text{step 6}}{\text{step 4}} \quad D.I.4$$

(7) Compare P_s estimate to P_s . If they are not equal within certain error bounds guess a new value of Q_s and return to Step 3. If they are equal the values of Q_s , $\frac{Re}{L_s}$, $\frac{P_{c,l}}{P_s}$, λ_0 are determined.

This portion of Bell's procedure was used to determine the theoretical line shown in Fig. 8.

(8) Calculate β from Table D.I.1 by interpolating λ 's for $0 < R < 1.0$ at $\frac{Re}{L_s}$ from step 7 and numerically integrating these λ 's over $0 < R < 1.0$.

(9) Calculate K from

$$K = \frac{32\lambda_0}{3\beta} \quad D.I.5$$

(10) Calculate G from

$$G = \frac{g}{ds} \quad D.I.6$$

(11) Calculate P_o from

$$\frac{P_o}{P_{c,l}} = \frac{1}{\left(\frac{KG}{Re} + 1\right)^2} \quad D.I.7$$

(12) Calculate P_o from

$$P_o = (\text{step 11}) \times (\text{Step 7}) \quad D.I.8$$

This value of P_o with the value of P_s in step 7 were used to plot the theoretical lines in Fig. 9.

(13) Calculate Re from

$\frac{KGL_s}{P_o}$

$$\frac{Re}{NGLs} = \frac{(step\ 7)}{(step\ 10)\ (step\ 9)}$$

D.1.9

This value along with P_0 from Step 7 were used to plot P_s

the theoretical lines in Fig. 10.

(14) Calculate P_{oturb} from

$$P_{oturb} = \frac{41.0 \beta P c \ell}{G^2 \lambda o^2}$$

D.1.10

This value was used to plot the theoretical lines in Fig. 13.

(15) Calculate $\frac{G^2 P_0}{41. P c \ell}$ from

$$\frac{G^2 P_0}{41. P c \ell} = \frac{\beta}{(step\ 14) \lambda o^2}$$

D.1.11

This value was used to plot the theoretical line in Fig. 17.

The program that is used to perform the previous computations is given in the remainder of this section.

```

C **** RFLL'S ANALYTICAL PROCEDURE (MAIN PROGRAM)
C ****
C ****
C ****
C ****
C ****
C ****
1   REAL K, LAMDA
2   DIMENSION RF(16)
3   EXTERNAL LAMDA, PES1,BF1A
4   COMMON RF1
5   READ J , FL , G , D
6   1 FORMAT ( 3F10.5 )
7   G = G / 12.
8   D = D / 12.0
9   EL = FL / 32.0
10  GG=6*2.54
11  DD=0*2.54
12  EELL=EL*2.54
13  GE = G / D
14  ELL = EL / D
15  PRINT 100,DD,GG,EELL
16  100 FORMAT('1', 'DIAMETER = ', F10.3, 'X', 'GAP = ', F10.3, 'X', 'L/D = ', 
1    F10.2)
17  PRINT 200
18  200 FORMAT('0', 'X', ' 0  ', '3X,' KEY, '3X,' REL, '3X,' LAMDA, ' 
1.3X,' K '3X,' POPS '3X,' PS '3X,' REOKGL '10', 
2 'PUTURB' '2X,' TURB')
19  10 READ 2, PS
20  2 FORMAT ( F10.5 )
21  IF(PS.EQ.0.0) GO TO 999
22  PS=PS/248.142
23  PS= PS / 12.0
24  CALL PSTHER( B , FL , PS , '0 , REL , AMDA , PCLPS , PCL )
25  REY = RFL * FL / D
26  B = BETAL ( LAMDA )
27  K = 32.0 * AMDA / ( 3.0 * B )
28  REOKG = REY / ( K * GE ) *
29  POPCL = 1.0 / ( ( 1.0 / REOKG ) + B.0 ) **
30  PU = POPCL * PCL
31  PS = PS * 12.0
32  PCL = PCL * 12.
33  PD = PU * 12.
34  C PD , PS , PCL IN INCHES OF WATER
35  Q = Q * 28316.8 * 60.
36  C Q IN CC / MIN
37  PU=PU*248.142
38  PS=PS*248.142
39  PCL=PCL*248.142
40  REOKGL=REOKG/Ell
41  POPS=PU/PS
42  YYY=GE**0.27*POPS
43  PUTURB=(B*41.0*PCL)/(GE*AMDA)**2.0
44  TURB=B/AMDA**2.0
45  Q=Q/60.
46  C Q IN CC/SEC
47  PRINT 4,0,REY,RFL,AMDA,K,POPS,YYY,PS,REOKGL,POPCL,PD
48  4 FORMAT( 11 1 2X , F8.3 ) )
49  PRINT 5,PUTURB,TURB,B
50  5 FORMAT( ' ',3F10.3)
51  GO TO 10
52  999 STOP
53  END

```

```

51      FUNCTION BETAL LAMBDA )
52      COMMON REL
53      DIMENSION RF(16)
54      REAL LAMBDA
55      A=0.0
56      B=1.0
57      N=10
58      H = 0.1
59      SUM = 0.0
60      K = N - 1
61      DO 61 I = 1,K
62      61 SUM = SUM + LAMBDA(      A + I * H )
63      BETA = ( LAMBDA( A ) + LAMBDA( B ) + 2.0 * SUM ) * T^H / 2.0
64      RETURN
65      END

```

```

66      SUBROUTINE PSTHEO( D , EL , PS , Q , A , ALMDA , PCLPS , PCL )
67      COMMON REL
68      DIMENSION RF(16)
69      REAL LAMBDA
70      N = 0
71      Q = 3.14159 * L**4 * PS * 0.4335 * 144. * 32.2 / ( 128. *
72      * 0.1468E-04 * EL )
73      C 0.1N FEET**2 / SEC
74      20 CONTINUE
75      REL = 4.0 * Q / ( 3.14159 * EL * 1.55E-04 )
76      PCLPS = PFST(REL)
77      PCL = ( 8.0 * 0.0750 * ( LAMBDA(0.0) * Q / ( 3.14159 * Q**2 ) )
78      * 1.0E-2 ) * 0.192227 / ( 12. * 32.2 )
79      P1 = PCL / PCLPS
80      C PCL + P1 , PS IN FEET OF WATER
81      IF ( PS - P1 .GT..0001 .AND. N .EQ. 0 ) GO TO 25
82      IF( P1 - PS .GT..0001 .AND. N .EQ. 0 ) GO TO 26
83      IF ( N .NE. 0 ) GO TO 99
84      IF ( PS - P1 .GT..0001 .AND. N .NE. 0 ) GO TO 27
85      IF( P1 - PS .GT..0001 .AND. N .NE. 0 ) GO TO 28
86      GO TO 99
87      25 ORIT = 2.0 * 0
88      OLFET = 0
89      GO TO 30
90      26 ORIT = 0
91      OLFET = 0.0
92      GO TO 30
93      27 OLFET = 0
94      GO TO 30
95      28 ORIT = 0
96      GO TO 30
97      30 Q = ( OLFET + ORIT ) / 2.0
98      N = N + 1
99      GO TO 20
100     99 CONTINUE
101     A = REL
102     ALMDA = LAMBDA( 0.0 )
103     RETURN
104     END

```

```

101      REAL FUNCTION LAMDA ( R )
102      REAL/RE(16), M(16,11), RR(11)
103      COMMON KFL
104      DATA RF/0.0,16.0,20.0,25.0,33.3,44.4,57.1,80.0,100.0,133.0,
105      1,200.0,267.0,400.0,800.0,2000.0,9999.9/
106      DATA PR/0.0,0.1,0.2,0.3,0.4,0.5,0.6,0.7,0.8,0.9,1.0/
107      DATA M(1,1),M(2,1),M(3,1),M(4,1),M(5,1),M(6,1),M(7,1),M(8,1),
108      1,M(9,1),M(10,1),M(11,1),M(12,1),M(13,1),M(14,1),M(15,1),M(16,1)/
109      2,2.0000,1.9863,1.9698,1.9431,1.9202,
110      3,1.8724,1.7555,1.6595,1.5977,1.5239,1.4332,1.3782,1.3126,1.2264,
111      4,1.1503,1.0000/
112      DATA M(1,2),M(2,2),M(3,2),M(4,2),M(5,2),M(6,2),M(7,2),M(8,2),
113      1,M(9,2),M(10,2),M(11,2),M(12,2),M(13,2),M(14,2),M(15,2),M(16,2)/
114      2,1.9800,1.9672,1.9517,1.9266,1.8785,
115      3,1.8142,1.7488,1.6562,1.5960,1.5232,1.4331,1.3781,1.3126,1.2264,
116      4,1.1503,1.0000/
117      DATA M(1,3),M(2,3),M(3,3),M(4,3),M(5,3),M(6,3),M(7,3),M(8,3),
118      1,M(9,3),M(10,3),M(11,3),M(12,3),M(13,3),M(14,3),M(15,3),M(16,3)/
119      2,1.9200,1.9095,1.8969,1.8763,1.8366,
120      3,1.7824,1.7269,1.6448,1.5893,1.5204,1.4324,1.3779,1.3125,
121      4,1.2269,1.1503,1.0000/
122      DATA M(1,4),M(2,4),M(3,4),M(4,4),M(5,4),M(6,4),M(7,4),M(8,4),
123      1,M(9,4),M(10,4),M(11,4),M(12,4),M(13,4),M(14,4),M(15,4),M(16,4)/
124      2,1.8200,1.8128,1.8042,1.7901,1.7626,
125      3,1.7244,1.6821,1.6188,1.5727,1.5120,1.4299,1.3770,1.3124,1.2264,
126      4,1.1503,1.0000/
127      DATA M(1,5),M(2,5),M(3,5),M(4,5),M(5,5),M(6,5),M(7,5),M(8,5),
128      1,M(9,5),M(10,5),M(11,5),M(12,5),M(13,5),M(14,5),M(15,5),M(16,5)/
129      2,1.6800,1.6764,1.6721,1.6650,1.6509,
130      3,1.6306,1.6073,1.5675,1.5358,1.4902,1.4214,1.3733,1.3115,1.2268,
131      4,1.1503,1.0000/
132      DATA M(1,6),M(2,6),M(3,6),M(4,6),M(5,6),M(6,6),M(7,6),M(8,6),
133      1,M(9,6),M(10,6),M(11,6),M(12,6),M(13,6),M(14,6),M(15,6),M(16,6)/
134      2,1.5000,1.4990,1.4990,1.4981,1.4962,
135      3,1.4927,1.4874,1.4751,1.4623,1.4395,1.3959,1.3596,1.3068,1.2264,
136      4,1.1503,1.0000/
137      DATA M(1,7),M(2,7),M(3,7),M(4,7),M(5,7),M(6,7),M(7,7),M(8,7),
138      1,M(9,7),M(10,7),M(11,7),M(12,7),M(13,7),M(14,7),M(15,7),M(16,7)/
139      2,1.2800,1.2818,1.2840,1.2875,1.2913,
140      3,1.3034,1.3125,1.3245,1.3308,1.3369,1.3292,1.3160,1.2867,1.2230,
141      4,1.1502,1.0000/
142      DATA M(1,8),M(2,8),M(3,8),M(4,8),M(5,8),M(6,8),M(7,8),M(8,8),
143      1,M(9,8),M(10,8),M(11,8),M(12,8),M(13,8),M(14,8),M(15,8),M(16,8)/
144      2,1.0200,1.0229,1.0264,1.0321,1.0333,
145      3,1.0588,1.0757,1.1023,1.1218,1.1476,1.1814,1.2000,1.2144,1.2016,
146      4,1.1485,1.0000/
147      DATA M(1,9),M(2,9),M(3,9),M(4,9),M(5,9),M(6,9),M(7,9),M(8,9),
148      1,M(9,9),M(10,9),M(11,9),M(12,9),M(13,9),M(14,9),M(15,9),M(16,9)/
149      2,0.7200,0.7229,0.7263,0.7314,0.7429,
150      3,0.7584,0.7756,0.8040,0.8261,0.8585,0.9107,0.9511,1.0098,1.0950,
151      4,1.1293,1.0000/
152      DATA M(1,10),M(2,10),M(3,10),M(4,10),M(5,10),M(6,10),M(7,10),
153      1,M(8,10),M(9,10),M(10,10),M(11,10),M(12,10),M(13,10),M(14,10),
154      2,M(15,10),M(16,10)/
155      3,0.3800,0.3818,0.3840,0.3877,0.3947,
156      4,0.4047,0.4159,0.4346,0.4496,0.4720,0.5100,0.5417,0.5908,0.6893,
157      5,0.8436,1.0000/
158      DATA M(1,11),M(2,11),M(3,11),M(4,11),M(5,11),M(6,11),M(7,11),
159      1,M(8,11),M(9,11),M(10,11),M(11,11),M(12,11),M(13,11),M(14,11),
160      2,M(15,11),M(16,11)/

```

```

3 .0000,0.0000,0.0000,0.0000,0.0000,0.0000,
40.0000,0.0000,0.0000,0.0000,0.0000,0.0000,0.0000,
5 0.0000,0.0000/
117 NDIM = 15
118 NDIM = 10
119 DO 1 I = 1 : NDIM
120 IF( RFL .LT. REL(I+1) ) OR. I .EQ. NDIM ) GO TO 2
121 1 CONTINUE
122 2 DO 3 J = 1 : NDIM
123 IF( R .LT. RR(J+1) ) OR. J .EQ. NDIM ) GO TO 4
124 3 CONTINUE
125 4 ALPHA = ( REL - RR(I) ) / ( RR(I+1) - RR(I) )
126 BETA = ( R - RR(J) ) / ( RR(J+1) - RR(J) )
127 LAMBDA = ( 1.0 - ALPHA ) * ( 1.0 - BETA ) *
128 1 BETA * ( 1.0 - ALPHA ) * M(I,J+1) + ALPHA * ( 1.0 -
2 * M(I+1,J) + ALPHA * BETA * M(I+1,J+1)
129 RETURN
END

```

```

130 FUNCTION PEST ( REL )
131 DIMENSION P(19),RR(19)
132 DATA RR/0.0,5.5,10.0,12.5,16.0,20.0,25.0,33.3,44.4,57.1,80.0,
1 100.0,133.0,200.0,267.0,400.0,800.0,2000.0,1E11/
133 DATA P/0.100,0.244,0.420,0.511,0.629,0.712,0.788,0.872,0.932,
1 0.966,0.990,0.997,1.000,1.002,1.002,1.001,1.001,1.00,1.00/
134 NDIM = 18
135 DO 1 I = 1 : NDIM
136 IF( RFL .LT. RE(I+1) ) OR. I .EQ. NDIM ) GO TO 2
137 1 CONTINUE
138 2 PEST = P(I) + ( REL - RE(I) ) * ( P(I+1) - P(I) ) / ( RE(I+1)
1 - P(I) )
139 RETURN
END

```

APPENDIX D.2

HAYES' THEORETICAL SWITCHING TIMES

Hayes (Ref. 13) derived theoretical relationships to describe the various switching times associated with the turbulence amplifier. He assumed that the velocity profile at the emitter exit was parabolic. Schlichting's point source model (Ref. 34) was used with centerline velocity matching, to model the laminar jet. To obtain an estimate of the "so called" inviscid core length $\ell_{i.c.}$, he assumed similarity between planar and axisymmetric free laminar jet spreading and "so called" inviscid core length. He also assumed that the control action was concentrated at the point where the control jet hit the supply jet. Such an assumption is not realized in the present case and therefore the control action was assumed to occur at the jet exit. The equations obtained are shown below converted to the terms used in the present investigation.

$$X_0 = 0.0624 ds Re \quad \text{---D.2.1.}$$

$$\ell_{i.c.} = 0.00762 ds Re \quad \text{---D.2.2}$$

$$T\ell.d. = Tt.d. = \frac{\ell_{i.c.}}{2U_s} + \frac{g - \ell_{i.c.}}{2X_0 U_s} \left[X_0 + \frac{g - \ell_{i.c.}}{2} \right] \quad \text{---D.2.3.}$$

$$Tr. = Tf. = \frac{1.10g}{2U_s} \quad \text{---D.2.4.}$$

APPENDIX D.3

ABRAMOVICH'S EMPIRICAL SWITCHING TIMES

Abramovich (Ref. 1) found experimental correlations for the switching times of the laminar jet. The definitions for $T_{\ell.d.}$, $T_f.$ and $T_{t.d.}$ are similar to those of the present study. The rise time is based on 70% of the particular velocity rise. Since the velocity versus the time in this region was approximated by a straight line the time corresponds to 70% of the T_r . definition used in the present study. The empirical equations for the switching times converted to account for the present definition are given below.

$$T = \left[A \frac{G^2}{Re} + B \frac{G^2}{Re} \right] \frac{ds^2}{2v\sqrt{Re}} \quad \text{---D.3.1.}$$

	A	B
$T_{t.d.}$	1.58	1.48
T_r	0.39	0.17
$T_{\ell.d.}$	0.60	0.76
$T_f.$	0.60	1.20

APPENDIX D.4
ALSTER'S HELMHOLTZ FORMULA

The equations that were given by Alster (Ref. 2) to predict the resonant frequency of a circular cylinder with a centered lateral hole are given on the next page and the computer program used to calculate the resonant frequency follows in the remainder of this section.

$$f = \frac{c}{2h} \sqrt{\frac{An}{1.21(V_c + V_n) \left\{ \left(\frac{V_c}{V_c + V_n + V_{o1}} \right) \left(\frac{h}{h + l_n + l_{o1}} \right) \right\} \left[l_n + (l_n + l_{o1}) (1 + 1/2 \left[\frac{(V_n + V_{o1})}{V_c} + \frac{l_n + l_{o1}}{h} \right]) \right. \\ \left. + 1/3 \frac{V_n + V_{o1}}{V_c} \frac{l_n + l_{o1}}{h} + l_{o2} \right]}}$$

D.41

where:

v = form factor

$$= \frac{\pi d n^2}{8 h V_c} \left[\frac{h^3}{3} - \frac{d c^2 h}{8} \right] \frac{\pi d c^2}{4} \left(\sqrt{d c h - h^2} + \frac{h^{1.5}}{3 \sqrt{d c / 2}} \right) + \frac{d c^3}{8} \left(4.88 + \sin^{-1} \left(\frac{2 h - d c}{d c} \right) \right)$$

h = effective depth of the chamber

$$= 1/2(d c + \sqrt{d c^2 - d n^2})$$

V_c = effective volume of the chamber

$$= \frac{\pi c}{2} \left[d n \sqrt{d c^2 - d n^2} + \frac{d n^2}{2} \sin^{-1} \sqrt{\frac{1}{2} \left(\frac{d c^2 + d n^2}{d c} \right)} + \frac{d c^2}{8 \pi} \right]$$

l_{o1}, l_{o2} = two parts of the total end correction

factor due to the motion of the gas

outside the resonator empirically

determined to be $l_{o1} = l_{o2} = 0.24$

$$V_{o1} = An l_{o1}$$

```

1      DIMENSION FF(10)
2      CONTINUE
3      READ 100,RC,EEL,RH,FLN
4      FORMAT(6F10.5)
5      NNN=1
6      IF(RC.GT.2.0)GO TO 999
7      CONTINUE
8      IF(RH<.E0.3) GO TO 10
9      IF(RH>E1.3) GO TO 20
10     RC=RC*2.54/2.0
11     RH=RH*2.54/2.0
12     EL=EEL*2.54
13     FLN=FLN*2.54
14     C=344.0*02
15     H=RC*SORT(RC**2.0-RH**2.0)
16     V1=RC**2.0*3.14159/2.0
17     V2=RC**2.0*ARSIN((SQR1(RC**2.0-RH**2.0))/RC).
18     V3=RH*SORT(RC**2.0-RH**2.0)
19     V=EL*(V1+V2+V3)
20     ELV1=RC**3.0*(4.8E+3.14159*ARSIN((H-RC)/RC))
21     ELV2=3.14159*(C**2.0*(B0)(1(2.0*RC*H-RH**2.0)+0.04*1.5/3.0/SORT(RC)))
22     ELV3=RC**2.0*H/2.0
23     ELV4=1.0*2.0/3.0
24     ELV=3.14159*RH**2.0*(ELV1-ELV2-ELV3+ELV4)/2.0/H/V
25     IF(RH.E0.2) ELV=1.08*RH**2.0/EL
26     GO TO 20
27     CONTINUE
28     RH=0.070*2.54
29     H=EL
30     FLN=0.1875*2.54
31     ELW=(RH/RC)**2.0*H/3.0
32     CONTINUE
33     EL01=0.24*RH
34     EL02=0.24*RH
35     FN=3.14159*RH**2.0
36     VH=FN*EL01
37     VN=FN*ELN
38     F1=(VN+VH)/V
39     F2=(ELN+EL01)/H
40     F3=(1.0+0.5*(F1+F2)+F1*F2/3.0)*(ELN+EL01)
41     F4=ELV+F3
42     F5=V/(L+VN+VH)
43     F6=H/(H+FLN+EL01)
44     F7=F5*F6*F4+EL02
45     FH=1.21*(V+VN)*F7
46     FF=FN*SORT(FM/FK)/2.0/3.14159
47     FF(NNN)=F
48     NNN=NNN+1
49     GO TO 6
50     CONTINUE
51     PRINT 200,RC,EEL,RH,FLN,FF(1),FF(2),FF(3)
52     FORMAT(1X,7F11.5)
53     GO TO 5
54     999 CONTINUE
55     STOP
56     END

```

APPENDIX E
EXPERIMENTAL DATA

In general the significant figures shown in the following tables are more than those claimed on the basis of the Uncertainty Analysis (Appendix B).

	Page
E.1 Output Pressure vs Supply Pressure	108
E.2 Output Pressure vs Sound Variables	111
E.3 Switching Times	137

APPENDIX E.1
OUTPUT PRESSURE VS. SUPPLY PRESSURE

$d_c = 0.95 \text{ cm.}$

	P_s (N/m ²)	P_o (N/m ²)	Q_s (m ³ /sec. x 10 ⁶)
$g = 1.27 \text{ cm.}$	248.1 440.5 633.8 1098.0	23.4 78.3 174.3 415.6	6.7 10.3 14.9 22.3
$T_a = 23.9^{\circ}\text{C}$	1693.6 2024.4 2528.2 2813.3 3079.4 3288.5 3592.7 3847.4 4080.6	821.3 1093.0 1492.7 1729.8 1862.9 2081.5 2262.0 2250.2 1865.4	30.5 35.0 40.6 43.3 46.1 48.3 51.1 53.3 55.6
$P_a = 748.28$ mm. Hg.			
$B.N.L. = 66 \text{ db.}$			
$g = 2.54 \text{ cm.}$	217.1 378.4 558.3 744.4 986.4	9.7 41.2 94.4 175.9 288.9	6.0 8.8 12.6 16.4 20.2
$T_a = 23.90^{\circ}\text{C}$	1116.6 1129.0 1172.5 1246.9 1420.6 1780.4	371.2 374.3 282.4 262.3 161.4 181.6	22.5 22.7 23.3 24.7 27.4 31.8
$P_a = 749.3$ mm. Hg.			
$B.N.L. = 660$ db.			
$g = 3.81 \text{ cm.}$	223.3 304.0 440.5 545.9 663.8 707.2 719.6 750.6 787.8 837.5 893.3 980.2 1073.2	7.3 16.9 44.4 75.1 113.0 125.9 128.2 113.0 76.7 70.2 70.2 71.8	6.0 8.0 10.3 12.6 14.9 15.6 15.9 16.4 17.2 17.9 18.7 20.2 21.7
$T_a = 23.9^{\circ}\text{C}$			
$P_a = 75.84$ mm. Hg.			
$B.N.L. = 68$ db.			

$dc = 1.27 \text{ cm.}$

	P_s (N/m ²)	F_0 (N/m ⁴)	Q_s (m ³ /sec. x 10 ⁶)
$g = 1.27 \text{ cm.}$	246.1 441.3 666.2 942.1 1200.9 1684.2 1910.7 1985.1 2158.8 2289.1 2444.2 2632.7 2704.8 2955.9 3165.0 3326.5 3509.3 3602.6 3707.5 3905.7 4094.3 4181.2	21.2 76.4 174.0 331.0 492.2 825.1 1005.0 1067.0 1203.5 1308.9 1449.4 1619.7 1748.8 1803.4 2081.5 2224.0 2378.4 2425.0 2355.1 1970.3 1774.2 1885.9	6.4 10.5 15.0 19.7 24.1 30.2 32.8 33.9 35.6 37.2 38.9 41.1 42.8 44.4 46.7 48.3 50.0 50.8 51.7 53.3 55.0 56.1
$T_a = 24.4^\circ\text{C}$			
$P_a = 745.45$ mm. Hg.			
$B.N.L. = 68$ db.			
$g = 2.54 \text{ cm.}$	210.9 372.2 545.9 732.0 967.8 1203.5 1464.0 1532.3 1772.1 2168.5 2658.2	19.7 38.7 95.2 172.7 290.5 425.8 605.2 645.6 443.8 334.9 351.0	6.0 8.8 12.6 16.2 20.2 24.0 27.9 28.4 31.8 30.1 41.7
$T_a = 25.6^\circ\text{C}$			
$P_a = 751.08$ mm. Hg.			
$B.N.L. = 65 \text{ db.}$			
$g = 3.81 \text{ cm.}$	210.9 372.2 545.9 632.8 707.2 744.4 794.1 893.3 930.5 1029.8 1166.3 1215.2 1538.5 1799.0 2098.6	5.6 27.4 73.4 92.8 101.7 119.4 113.8 117.0 111.4 103.2 95.2 87.2 79.9 76.7 82.3	6.4 8.8 12.6 14.1 15.6 16.4 17.2 18.7 19.4 20.9 23.2 25.5 28.7 31.8 35.0
$T_a = 26.7^\circ\text{C}$			
$P_a = 749.55$ mm. Hg.			
$B.N.L. = 66$ db.			

dc = 2.54 cm.

	P_s (N/m ²)	B_o (N/m ²)	Q_s (m ³ /sec. x 10 ⁶)
g = 1.27 cm.	372.2 744.4 1203.5	45.8 210.4 477.7	18.8 16.4 24.0
Ta = 23.9°C	1799.0 2052.9	905.7 1112.0	32.2 35.0
Pa = 751.84 mm. Hg.	2290.6 2556.7 2813.3 3069.9	1207.1 1444.7 893.4 1045.5	37.8 40.6 43.3 46.1
B.N.L.=68 db.			
g = 2.54cm.	217.1 366.0 545.9	8.1 37.1 90.4	6.0 8.8 12.6
Ta = 21.7°C	744.4 967.8	171.1 282.4	16.4 20.2
Pa = 749.81 mm. Hg.	1197.3 1488.9	411.6 585.1	24.0 27.9
B.N.L.= 67 db.	1526.1 1650.1 2053.4 2338.1 2841.8 3346.1	609.3 363.1 306.7 262.3 238.1 262.3	28.5 30.2 35.0 37.8 43.3 48.9
g = 3.81cm.	217.1 372.2 539.7	4.0 26.6 72.6	6.0 8.8 12.6
Ta = 24.4°C	663.8 787.8	113.0 164.6	14.9 17.2
Pa = 748.54 mm. Hg.	936.7 1073.2 1209.7 1308.9 1333.8 1470.2 1581.9 1823.8 2009.9 2300.1 2822.8 3326.5	227.6 302.6 367.2 411.6 435.8 403.5 246.1 157.4 125.1 88.8 80.7 76.7	19.4 21.8 24.1 25.5 26.8 27.6 29.0 32.3 34.4 37.8 43.3 48.9
B.N.L.=67 db.			

APPENDIX E:2
OUTPUT PRESSURE VS. SOUND VARIABLES

$d_c = 0.95 \text{ cm.}$

$g = 1.27 \text{ cm.}$

$$P_s = 660 \text{ N/m}^2$$

$$Q_s = 14.9 \times 10^{-6} \text{ m}^3/\text{sec.}$$

P_c (db)	f (Hz)	P_o (N/m ²)	f (Hz)	P_o (N/m ²)	f (Hz)	P_o (N/m ²)
90	180.000	174.300	2300.000	174.300	8200.000	174.300
	500.000	174.300	2900.000	174.300	11400.000	174.300
	900.000	174.300	3700.000	174.300	14750.000	174.300
	1200.000	174.300	4500.000	174.300	16650.000	174.300
	1500.000	174.300	6900.000	174.300	18000.000	174.300
100	170.000	174.300	1947.000	158.200	2500.000	174.300
	520.000	174.300	1958.000	158.600	2800.000	174.300
	770.000	174.300	1970.000	154.400	4850.000	174.300
	990.000	174.300	1982.000	153.300	5700.000	174.300
	1150.000	174.300	1997.000	156.600	8200.000	174.300
	1450.000	174.300	2010.000	159.800	9400.000	174.300
	1550.000	174.300	2035.000	163.000	11900.000	174.300
	1770.000	174.300	2070.000	167.900	14600.000	174.300
	1860.000	172.700	2096.000	169.500	16000.000	174.300
	1848.000	171.100	2122.000	171.100	18000.000	174.300
	1888.000	167.900	2172.000	172.700		
	1928.000	161.400	2234.000	174.300		
	180.000	174.300	1909.000	88.800	2668.000	164.600
	450.000	174.300	1924.000	80.700	2734.000	169.500
	700.000	174.300	1938.000	72.600	2771.000	171.100
110	900.000	174.300	1958.000	66.200	2817.000	171.100
	1000.000	174.300	1960.000	64.600	2849.000	171.100
	1200.000	174.300	1979.000	59.700	2878.000	172.700
	1400.000	174.300	1989.000	62.900	2912.000	172.700
	1500.000	174.300	2004.000	71.000	2961.000	172.700
	1591.000	172.700	2021.000	79.100	3113.000	174.300
	1625.000	171.100	2053.000	93.600	3245.000	174.300
	1682.000	169.500	2077.000	108.100	3352.000	174.300
	1720.000	163.000	2126.000	122.700	3500.000	174.300
	1749.000	154.900	2182.000	135.600	4800.000	174.300
	1780.000	154.900	2222.000	145.300	7600.000	174.300
	1806.000	146.900	2301.000	146.900	8500.000	174.300
	1828.000	140.400	2393.000	159.800	10500.000	174.300
	1857.000	129.100	2448.000	164.600	14300.000	174.300
	1873.000	117.800	2521.000	167.900	16200.000	174.300
	1888.000	104.900	2644.000	169.500	17000.000	174.300
	1898.000	98.500	2625.000	164.600	18000.000	174.300

$d_c = 0.95 \text{ cm.}$ $g = 1.27 \text{ cm.}$

$$P_s = 660 \text{ N/m}^2$$

$$Q_s = 14.9 \times 10^{-6} \text{ m}^3/\text{sec.}$$

Pc (db)	f (Hz)	Po (N/m ²)	f (Hz)	Po (N/m ²)	f (Hz)	Po (N/m ²)
120	175.000	174.300	1890.000	24.200	2910.000	154.900
	400.000	174.300	1918.000	20.200	2967.000	163.000
	658.000	174.300	1939.000	19.400	3009.000	164.600
	825.000	174.300	1947.000	16.900	3062.000	163.000
	1030.000	174.300	1993.000	16.900	3100.000	163.000
	1126.000	174.300	2021.000	19.400	3145.000	163.000
	1178.000	174.300	2061.000	23.400	3207.000	167.900
	1213.000	172.700	2106.000	27.400	3267.000	169.500
	1299.000	171.100	2270.000	37.900	3333.000	171.100
	1350.000	167.900	2313.000	42.800	3418.000	173.000
	1391.000	163.000	2393.000	63.800	3469.000	173.000
	1429.000	153.300	2439.000	79.100	3529.000	173.000
	1488.000	145.300	2479.000	96.000	3601.000	174.300
	1547.000	137.200	2514.000	106.500	4800.000	174.300
	1597.000	129.100	2535.000	113.000	5700.000	174.300
	1646.000	113.000	2627.000	83.100	6500.000	174.300
	1710.000	88.800	2670.000	102.500	7800.000	174.300
	1738.000	74.200	2717.000	114.600	8900.000	174.300
	1775.000	67.800	2764.000	121.900	13500.000	174.300
	1812.000	46.800	2813.000	135.600	15700.000	174.300
	1859.000	33.100	2860.000	143.600	18000.000	174.300

dc = 0.95 cm.

$$P_s = 660 \text{ N/m}^2$$

g = 2.54 cm.

$$Q_s = 14.9 \times 10^{-6} \text{ m}^3/\text{sec.}$$

Pc (db)	f (Hz)	Po (N/m ²)	f (Hz)	Po (N/m ²)	f (Hz)	Po (N/m ²)
90	175.000	138.800	1880.000	35.500	2349.000	121.100
	425.000	138.800	1892.000	29.900	2401.000	128.300
	625.000	138.800	1904.000	27.400	2469.000	133.200
	1025.000	138.800	1925.000	23.400	2563.000	134.800
	1114.000	138.800	1937.000	21.800	2646.000	130.700
	1400.000	138.800	1945.000	20.200	2684.000	134.000
	1473.000	137.200	1959.000	20.200	2732.000	135.600
	1534.000	134.000	1969.000	21.000	2833.000	136.400
	1602.000	132.300	1983.000	22.000	2934.000	137.200
	1675.000	133.200	2001.000	27.400	3050.000	137.200
	1729.000	129.400	2011.000	35.500	3155.000	138.000
	1755.000	128.700	2027.000	47.600	3200.000	138.800
	1796.000	116.200	2053.000	58.900	4625.000	138.800
	1808.000	105.700	2073.000	71.800	5825.000	138.800
	1814.000	100.100	2097.000	79.100	8375.000	138.800
	1821.000	94.400	2153.000	90.400	11465.000	138.800
	1831.000	82.300	2180.000	101.700	14566.000	138.800
	1847.000	62.900	2210.000	111.400	18000.000	138.800
	1864.000	45.200	2206.000	117.000		
100	175.000	138.800	1905.000	8.100	2756.000	99.200
	420.000	138.800	1937.000	7.300	2803.000	108.900
	720.000	138.800	1980.000	8.100	2839.000	116.200
	800.000	138.800	2042.000	9.700	2873.000	122.700
	872.000	138.800	2088.000	11.200	2897.000	128.300
	950.000	138.800	2130.000	12.900	2954.000	133.200
	1018.000	138.800	2186.000	16.100	3033.000	134.000
	1126.000	138.800	2235.000	18.600	3135.000	134.800
	1203.000	138.000	2277.000	18.600	3186.000	135.600
	1254.000	135.600	2340.000	22.600	3224.000	136.400
	1301.000	133.200	2375.000	28.200	3279.000	136.400
	1354.000	130.700	2402.000	37.900	3320.000	137.200
	1413.000	124.300	2445.000	51.600	3404.000	137.200
	1492.000	111.400	2481.000	75.900	3477.000	138.000
	1524.000	86.300	2508.000	86.300	3568.000	138.800
	1565.000	67.000	2540.000	96.000	4500.000	138.800
	1627.000	58.100	2592.000	89.600	4850.000	138.800
	1683.000	49.200	2615.000	56.500	7850.000	138.800
	1702.000	37.900	2632.000	42.000	13850.000	138.800
	1755.000	21.800	2682.000	61.300	15850.000	138.800
	1800.000	18.600	2702.000	75.900	18000.000	138.800
	1846.000	12.900	2724.000	88.000		

dc = 0.95 cm.

g = 2.54 cm.

$$p_s = 660 \text{ N/m}^2$$

$$q_s = 14.9 \times 10^{-6} \text{ m}^3/\text{sec.}$$

Pc (db)	f (Hz)	Po (N/m ²)	f (Hz)	Po (N/m ²)	f (Hz)	Po (N/m ²)
110	175.000	138.800	1480.000	20.200	3087.000	62.000
	400.000	138.800	1527.000	17.800	3143.000	65.400
	750.000	138.800	1568.000	15.200	3177.000	75.100
	898.000	138.800	1602.000	13.700	3224.000	89.600
	907.000	133.200	1657.000	10.500	3295.000	100.900
	920.000	129.100	1706.000	8.900	3322.000	108.900
	940.000	125.900	1758.000	7.300	3389.000	106.500
	954.000	125.900	1822.000	6.500	3423.000	101.700
	960.000	125.100	1917.000	6.800	3465.000	124.300
	972.000	121.900	1979.000	6.800	3493.000	132.300
	983.000	124.300	2062.000	5.600	3513.000	124.800
	994.000	125.100	2119.000	5.600	3583.000	136.400
	1026.000	128.300	2225.000	6.500	3697.000	137.200
	1054.000	129.900	2303.000	6.500	3769.000	138.000
	1077.000	126.700	2378.000	8.100	3814.000	128.000
	1100.000	123.500	2452.000	8.900	3917.000	138.000
	1124.000	117.000	2511.000	11.300	4065.000	138.000
	1152.000	108.100	2575.000	12.900	4104.000	138.000
	1177.000	101.700	2598.000	11.300	4200.000	138.800
	1208.000	91.200	2718.000	12.100	4800.000	138.800
	1248.000	80.700	2765.000	15.300	5500.000	129.800
	1294.000	79.700	2825.000	21.800	7300.000	138.800
	1325.000	48.600	2869.000	32.300	8500.000	138.800
	1363.000	37.900	2920.000	41.200	10300.000	138.800
	1393.000	29.100	2957.000	55.700	16300.000	138.800
	1440.000	23.400	3012.000	64.600	18000.000	138.800
120	175.000	138.800	1019.000	69.400	859.000	107.300
	263.000	138.800	1028.000	63.800	877.000	94.400
	315.000	138.800	1040.000	58.900	898.000	72.600
	389.000	138.800	1048.000	51.600	910.000	58.100
	529.000	138.800	1059.000	42.800	917.000	45.200
	611.000	138.800	1073.000	40.400	923.000	30.700
	706.000	138.800	1098.000	36.300	931.000	28.200
	740.000	138.800	1121.000	30.700	948.000	19.400
	753.000	137.200	1158.000	23.400	956.000	27.400
	762.000	131.500	1191.000	18.600	972.000	38.700
	788.000	129.900	1224.000	15.300	985.000	51.600
	806.000	132.300	1280.000	12.900	988.000	70.200
	822.000	128.300	1321.000	10.500	995.000	37.900
	862.000	119.400	1409.000	8.100	1000.000	48.400

$d_c = 0.95 \text{ cm.}$

$g = 2.54 \text{ cm.}$

$$P_s = 660 \text{ N/m}^2$$

$$Q_s = 14.9 \times 10^{-6} \text{ m}^3/\text{sec.}$$

Pc (db)	f (Hz)	Po (N/m ²)	f (Hz)	Po (N/m ²)	f (Hz)	Po (N/m ²)
120	1482.000	6.500	3094.000	12.900	4129.000	93.600
	1515.000	6.500	3174.000	16.900	4167.000	102.500
	1592.000	5.600	3257.000	21.800	4214.000	109.800
	1704.000	4.800	3323.000	27.400	4261.000	117.000
	1807.000	4.000	3389.000	36.300	4304.000	124.300
	1913.000	4.000	3421.000	44.400	4377.000	129.900
	1992.000	4.000	3484.000	59.700	4454.000	131.500
	2094.000	4.000	3530.000	66.200	4495.000	131.500
	2165.000	4.000	3583.000	76.100	4556.000	130.700
	2259.000	4.000	3635.000	75.100	4586.000	129.100
	2368.000	4.000	3693.000	90.400	4626.000	128.300
	2425.000	4.000	3791.000	86.300	4679.000	124.000
	2469.000	4.000	3831.000	90.400	4728.000	137.200
	2518.000	4.800	3862.000	93.600	4747.000	138.000
	2547.000	5.600	3883.000	97.600	4790.000	138.800
	2772.000	5.600	3909.000	101.700	5000.000	138.800
	2818.000	6.500	3934.000	108.900	7500.000	138.800
	2844.000	8.100	4000.000	117.000	9600.000	138.800
	2889.000	8.100	4020.000	114.600	14750.000	138.800
	2927.000	9.700	4062.000	104.100	16750.000	138.800
	2991.000	12.100	4092.000	95.200	18000.000	138.800

$d_c = 0.95 \text{ cm.}$ $g = 3.81 \text{ cm.}$

$$P_s = 660 \text{ N/m}^2$$

$$Q_s = 14.9 \times 10^{-6} \text{ m}^3/\text{sec.}$$

P_c (db)	f (Hz)	P_o (N/m ²)	f (Hz)	P_o (N/m ²)	f (Hz)	P_o (N/m ²)
80	170.000	112.200	1850.000	18.600	2648.000	67.800
	200.000	112.200	1900.000	11.300	2675.000	73.400
	500.000	112.200	1929.000	8.900	2692.000	76.700
	700.000	112.200	1947.000	9.700	2727.000	96.800
	900.000	112.200	1967.000	9.700	2753.000	101.700
	1227.000	112.200	2020.000	14.500	2791.000	108.100
	1385.000	111.400	2087.000	25.000	2876.000	109.800
	1429.000	104.900	2166.000	37.900	2919.000	110.600
	1444.000	103.300	2241.000	50.800	3046.000	111.400
	1457.000	100.100	2297.000	66.900	3199.000	112.200
	1479.000	101.700	2443.000	79.900	4200.000	112.200
	1497.000	97.600	2487.000	96.000	6000.000	112.200
	1509.000	92.800	2538.000	105.700	8000.000	112.200
	1604.000	76.700	2570.000	105.700	12000.000	112.200
	1664.000	66.200	2598.000	104.900	16000.000	112.200
	1698.000	63.800	2601.000	103.300	18000.000	112.200
	1766.000	40.400	2612.000	96.800		
	1801.000	34.700	2628.000	79.100		
90	170.000	112.200	1370.000	50.800	2527.000	37.100
	656.000	112.200	1415.000	37.100	2558.000	42.800
	885.000	112.200	1481.000	32.300	2578.000	42.800
	908.000	112.200	1536.000	27.400	2608.000	54.700
	935.000	112.200	1568.000	20.900	2625.000	29.100
	960.000	108.900	1583.000	18.600	2637.000	25.800
	979.000	93.600	1645.000	16.100	2668.000	25.800
	989.000	84.700	1705.000	12.900	2678.000	27.400
	1001.000	87.900	1776.000	8.100	2700.000	30.700
	1017.000	102.500	1853.000	6.500	2730.000	36.300
	1028.000	108.900	1913.000	5.600	2751.000	40.400
	1044.000	110.600	1977.000	4.800	2827.000	50.800
	1062.000	110.600	2032.000	5.600	2916.000	60.500
	1088.000	108.900	2110.000	6.500	3015.000	76.700
	1117.000	106.500	2175.000	8.900	3096.000	90.400
	1166.000	95.200	2243.000	10.500	3150.000	100.900
	1196.000	84.700	2317.000	12.900	3232.000	105.700
	1221.000	78.300	2387.000	16.900	3316.000	108.900
	1276.000	66.900	2430.000	21.800	3370.000	110.600
	1317.000	65.400	2479.000	29.900	3412.000	111.400

$d_c = 0.95 \text{ cm.}$ $g = 3.81 \text{ cm.}$

$P_s = 660 \text{ N/m}^2$

$Q_s = 14.9 \times 10^{-6} \text{ m}^3/\text{sec.}$

P_c (db)	f (Hz)	P_Q (N/m ²)	f (Hz)	P_Q (N/m ²)	f (Hz)	P_Q (N/m ²)
90	3525.000	111.400	7600.000	112.200	15000.000	112.200
	3600.000	112.200	8500.000	112.200	18000.000	112.200
	5400.000	112.200	10000.000	112.200		
100	170.000	112.200	1154.000	31.500	2843.000	16.400
	250.000	112.200	1193.000	26.600	2911.000	25.000
	337.000	112.200	1221.000	22.600	2953.000	24.400
	460.000	112.200	1279.000	18.600	2998.000	34.700
	557.000	112.200	1314.000	15.300	3047.000	36.300
	626.000	112.200	1346.000	13.700	3124.000	41.200
	708.000	112.200	1409.000	11.300	3175.000	45.200
	767.000	112.200	1453.000	9.700	3228.000	48.400
	775.000	108.100	1498.000	8.400	3299.000	54.100
	788.000	102.500	1526.000	8.100	3345.000	58.900
	794.000	100.900	1547.000	7.300	3415.000	77.500
	814.000	103.300	1579.000	7.300	3461.000	91.200
	832.000	100.100	1606.000	6.500	3483.000	99.300
	848.000	88.800	1695.000	5.600	3508.000	104.900
	864.000	77.500	1754.000	5.600	3548.000	108.100
	882.000	69.400	1788.000	4.800	3583.000	109.800
	914.000	58.900	1840.000	4.800	3624.000	110.600
	943.000	50.800	1906.000	4.800	3756.000	111.400
	958.000	38.700	1993.000	4.800	3826.000	111.400
	967.000	34.700	2050.000	4.800	3900.000	112.200
	976.000	33.100	2141.000	4.800	4700.000	112.200
	990.000	35.500	2251.000	4.800	6400.000	112.200
	1001.000	41.900	2342.000	4.800	7800.000	112.200
	1017.000	47.600	2400.000	5.600	8600.000	112.200
	1030.000	52.500	2495.000	7.300	9800.000	112.200
	1053.000	54.100	2539.000	9.700	11000.000	112.200
	1063.000	52.500	2621.000	7.300	14500.000	112.200
	1074.000	50.800	2713.000	8.100	16500.000	112.200
	1096.000	45.200	2759.000	10.500	18000.000	112.200
	1117.000	39.500	2794.000	13.700		
110	175.000	111.400	617.000	108.400	680.000	92.800
	238.000	111.400	631.000	103.400	695.000	89.600
	322.000	111.400	648.000	90.400	706.000	80.700
	473.000	111.400	662.000	90.400	719.000	73.400
	564.000	111.400	665.000	93.600	728.000	70.200
	600.000	111.400	672.000	94.400	749.000	63.800

$d_c = 0.95 \text{ cm.}$ $g = 3.81 \text{ cm.}$

$P_s = 660 \text{ N/m}^2$

$Q_s = 14.9 \times 10^{-6} \text{ m}^3/\text{sec.}$

P_c (db)	f (Hz)	P_o (N/m ²)	f (Hz)	P_o (N/m ²)	f (Hz)	P_o (N/m ²)
110	763.000	58.100	1510.000	6.800	3448.000	37.900
	782.000	54.100	1638.000	6.800	3673.000	43.600
	809.000	50.800	1730.000	6.800	3531.000	48.400
	821.000	45.900	1789.000	6.000	3606.000	54.900
	840.000	40.400	1836.000	6.000	3665.000	65.400
	861.000	33.100	1901.000	6.000	3700.000	75.100
	887.000	26.600	2013.000	6.000	3743.000	86.300
	911.000	20.900	2139.000	6.000	3792.000	98.500
	945.000	15.300	2221.000	6.000	3838.000	106.500
	965.000	10.500	2322.000	6.000	3884.000	108.100
	986.000	12.900	2428.000	6.000	3935.000	108.100
	993.000	15.300	2501.000	6.000	3988.000	108.900
	1009.000	18.600	2612.000	6.000	4052.000	108.900
	1030.000	23.400	2756.000	6.000	4093.000	109.800
	1049.000	20.900	2818.000	6.800	4111.000	108.900
	1060.000	17.800	2916.000	6.600	4221.000	110.600
	1086.000	14.500	2986.000	7.300	4246.000	111.400
	1108.000	12.100	3038.000	7.300	4417.000	111.400
	1164.000	8.900	3133.000	8.000	4528.000	111.400
	1194.000	8.100	3184.000	10.500	4620.000	111.400
	1222.000	7.300	3234.000	12.100	4750.000	111.400
	1263.000	6.500	3299.000	16.100	7000.000	111.400
	1215.000	6.500	3330.000	18.600	11000.000	111.400
	1348.000	5.600	3286.000	24.200	17000.000	111.400
	1415.000	4.800	3421.000	30.700	14000.000	111.400
120	183.000	105.700	348.000	87.900	535.000	108.100
	192.000	103.300	368.000	87.200	544.000	98.500
	202.000	99.300	384.000	88.800	558.000	85.500
	216.000	96.000	401.000	90.400	569.000	72.600
	226.000	92.800	412.000	94.400	582.000	65.400
	239.000	92.800	424.000	98.400	592.000	62.100
	250.000	91.200	432.000	100.400	616.000	54.100
	264.000	93.600	445.000	104.400	623.000	50.000
	281.000	92.800	452.000	107.300	629.000	41.400
	284.000	100.900	464.000	102.500	639.000	36.300
	295.000	97.600	480.000	106.500	652.000	39.500
	300.000	95.200	488.000	108.900	661.000	41.400
	314.000	98.500	493.000	111.400	677.000	41.200
	329.000	91.900	512.000	112.200	682.000	41.200
	334.000	86.300	529.000	111.400	703.000	37.100

$d_c = 0.95 \text{ cm.}$ $g = 3.81 \text{ cm.}$

$$P_s = 660 \text{ N/m}^2$$

$$Q_s = 14.9 \times 10^{-6} \text{ m}^3/\text{sec.}$$

Pc (db)	f (Hz)	Po (N/m ²)	f (Hz)	Po (N/m ²)	f (Hz)	Po (N/m ²)
120	721.000	32.300	2154.000	4.000	4410.000	61.300
	740.000	29.100	2224.000	4.000	4486.000	66.400
	763.000	24.200	2376.000	4.000	4516.000	62.900
	777.000	20.200	2464.000	4.000	4587.000	50.000
	804.000	16.100	2518.000	4.000	4607.000	41.900
	842.000	9.700	2700.000	4.000	4658.000	48.400
	900.000	6.500	2948.000	4.000	4675.000	58.400
	925.000	4.800	3106.000	4.000	4687.000	71.000
	950.000	4.000	3261.000	4.000	4699.000	98.500
	985.000	5.600	3250.000	4.000	4757.000	108.100
	1011.000	5.600	3411.000	4.800	4776.000	104.800
	1056.000	4.800	3526.000	8.100	4805.000	110.600
	1103.000	4.000	3574.000	8.900	4858.000	111.400
	1155.000	4.000	3665.000	14.500	5012.000	111.400
	1284.000	4.000	3755.000	20.900	5346.000	111.400
	1379.000	4.000	3848.000	25.000	5710.000	111.400
	1495.000	4.000	3938.000	24.200	6610.000	111.400
	1565.000	4.000	4017.000	22.600	8000.000	111.400
	1675.000	4.000	4119.000	19.400	12000.000	111.400
	1798.000	4.000	4192.000	23.400	16000.000	111.400
	1907.000	4.000	4307.000	37.000	18000.000	111.400
	2022.000	4.000	4360.000	44.200		

dc = 1.27 cm.

$$P_s = 660 \text{ N/m}^2$$

g = 1.27 cm.

$$Q_s = 14.9 \times 10^{-6} \text{ m}^3/\text{sec.}$$

Pc (db)	f (Hz)	Po (N/m ²)	f (Hz)	Po (N/m ²)	f (Hz)	Po (N/m ²)
90	200.000	171.000	1120.000	171.000	6200.000	171.000
	520.000	171.000	1552.000	171.000	9900.000	171.000
	870.000	171.000	2600.000	171.000	15000.000	171.000
	950.000	171.000	4310.000	171.000	18000.000	171.000
100	190.000	171.000	1504.000	166.000	1625.000	168.000
	700.000	171.000	1521.000	165.000	1660.000	170.000
	1200.000	171.000	1543.000	163.000	1702.000	171.000
	1252.000	171.000	1552.000	161.000	1818.000	171.000
	1345.000	171.000	1564.000	163.000	3000.000	171.000
	1408.000	171.000	1575.000	165.000	8000.000	171.000
	1463.000	170.000	1586.000	165.000	14000.000	171.000
	1485.000	168.000	1600.000	166.000	18000.000	171.000
110	180.000	171.000	1462.000	118.000	2152.000	170.000
	350.000	171.000	1482.000	107.000	2253.000	170.000
	480.000	171.000	1500.000	98.000	2360.000	170.000
	700.000	171.000	1514.000	86.000	2550.000	170.000
	840.000	171.000	1524.000	77.000	2750.000	170.000
	971.000	171.000	1551.000	65.000	2916.000	170.000
	1009.000	171.000	1587.000	77.000	3112.000	170.000
	1105.000	171.000	1614.000	89.000	3368.000	171.000
	1203.000	171.000	1641.000	107.000	3580.000	170.000
	1256.000	171.000	1666.000	129.000	3789.000	170.000
	1282.000	170.000	1695.000	142.000	4033.000	170.000
	1323.000	168.000	1727.000	148.000	4217.000	170.000
	1387.000	163.000	1757.000	157.000	4330.000	171.000
	1409.000	157.000	1784.000	161.000	5600.000	171.000
	1424.000	145.000	1855.000	165.000	8000.000	171.000
	1436.000	137.000	1941.000	168.000	12000.000	171.000
	1446.000	128.000	2050.000	168.000	18000.000	171.000

dc = 1.27 cm.

$$P_s = 660 \text{ N/m}^2$$

g = 1.27 cm.

$$Q_s = 14.9 \times 10^{-6} \text{ m}^3/\text{sec.}$$

Pc (db)	f (Hz)	Po (N/m ²)	f (Hz)	Po (N/m ²)	f (Hz)	Po (N/m ²)
120	175.000	173.000	1502.000	29.000	3781.000	171.000
	300.000	173.000	1554.000	21.000	3888.000	171.000
	400.000	173.000	1625.000	27.000	4033.000	171.000
	500.000	173.000	1644.000	31.000	4108.000	171.000
	600.000	173.000	1663.000	34.000	4156.000	170.000
	667.000	173.000	1741.000	50.000	4193.000	168.000
	736.000	173.000	1793.000	69.000	4230.000	166.000
	818.000	173.000	1830.000	86.000	4290.000	158.000
	912.000	173.000	1893.000	97.000	4322.000	160.000
	950.000	171.000	1944.000	107.000	4335.000	163.000
	997.000	173.000	1985.000	111.000	4374.000	168.000
	1049.000	173.000	2032.000	129.000	4446.000	171.000
	1081.000	171.000	2109.000	140.000	4513.000	171.000
	1109.000	170.000	2153.000	140.000	4613.000	171.000
	1148.000	168.000	2316.000	144.000	4761.000	171.000
	1183.000	166.000	2492.000	157.000	4855.000	171.000
	1215.000	161.000	2529.000	161.000	5041.000	171.000
	1235.000	153.000	2569.000	163.000	5376.000	171.000
	1251.000	145.000	2818.000	165.000	5704.000	171.000
	1267.000	137.000	2897.000	166.000	6159.000	171.000
	1295.000	126.000	2946.000	168.000	6463.000	171.000
	1325.000	113.000	3044.000	168.000	8000.000	171.000
	1355.000	92.000	3147.000	168.000	11000.000	171.000
	1375.000	77.000	3239.000	170.000	14000.000	171.000
	1404.000	61.000	3361.000	171.000	16000.000	171.000
	1427.000	48.000	3434.000	171.000	18000.000	171.000
	1472.000	36.000	3590.000	171.000		

$d_c = 1.27 \text{ cm.}$ $g = 2.54 \text{ cm.}$

$$P_s = 660 \text{ N/m}^2$$

$$Q_s = 14.9 \times 10^{-6} \text{ m}^3/\text{sec.}$$

P_c (db)	f (Hz)	P_o (N/m ²)	f (Hz)	P_o (N/m ²)	f (Hz)	P_o (N/m ²)
90	180.000	140.000	1537.000	44.000	2334.000	140.000
	500.000	140.000	1559.000	44.000	2401.000	140.000
	800.000	140.000	1583.000	58.000	2505.000	140.000
	1010.000	140.000	1602.000	73.000	2603.000	140.000
	1104.000	140.000	1628.000	96.000	2696.000	140.000
	1250.000	140.000	1662.000	115.000	2772.000	140.000
	1295.000	139.000	1694.000	127.000	2964.000	140.000
	1349.000	138.000	1793.000	133.000	3245.000	140.000
	1406.000	135.000	1873.000	136.000	7000.000	140.000
	1448.000	123.000	1943.000	137.000	13000.000	140.000
	1486.000	106.000	2010.000	138.000	17000.000	140.000
	1504.000	82.000	2100.000	139.000		
	1522.000	56.000	2202.000	140.000		
100	175.000	140.00	1512.000	15.00	2694.000	125.00
	269.000	140.00	1552.000	11.00	2754.000	136.00
	476.000	140.00	1613.000	15.00	2818.000	138.00
	634.000	140.00	1657.000	20.00	2929.000	139.00
	700.000	140.00	1732.000	33.00	3115.000	140.00
	953.000	140.00	1789.000	47.00	3371.000	140.00
	1008.000	139.00	1832.000	64.00	3583.000	140.00
	122.000	139.00	1862.000	80.00	3800.000	140.00
	1200.000	136.00	1938.000	99.00	4054.000	140.00
	1234.000	132.00	2047.000	114.00	4168.000	140.00
	1305.000	112.00	2115.000	119.00	4252.000	139.00
	1338.000	83.00	2269.000	123.00	4309.000	139.00
	1355.000	69.00	2330.000	122.00	6100.000	140.00
	1384.000	53.00	2464.000	130.00	9000.000	140.00
	1421.000	31.00	2552.000	135.00	11000.000	140.00
	1449.000	23.00	2605.000	136.00	18000.000	140.00
	1479.000	18.00	2614.000	132.00		
110	175.000	140.00	1014.000	129.00	1412.000	10.00
	300.000	140.00	1032.000	132.00	1460.000	7.00
	450.000	140.00	1057.000	129.00	1499.000	6.00
	600.000	140.00	1073.000	127.00	1572.000	5.00
	758.000	140.00	1095.000	118.00	1601.000	5.00
	774.000	138.00	1112.000	110.00	1654.000	6.00
	790.000	140.00	1135.000	99.00	1700.000	8.00
	802.000	140.00	1152.000	88.00	1754.000	10.00
	828.000	140.00	1173.000	74.00	1821.000	13.00
	872.000	140.00	1190.000	61.00	1944.000	18.00
	914.000	138.00	1210.000	48.00	2045.000	22.00
	945.000	135.00	1238.000	37.00	2152.000	25.00
	973.000	132.00	1278.000	28.00	2262.000	28.00
	983.000	127.00	1317.000	21.00	2298.000	25.00
	993.000	126.00	1364.000	14.00	2408.000	32.00

$dc = 1.27 \text{ cm.}$ $g = 2.54 \text{ cm.}$

$$P_s = 660 \text{ N/m}^2$$

$$Q_s = 14.9 \times 10^{-6} \text{ m}^3/\text{sec.}$$

Pc (db)	f (Hz)	Po (N/m ²)	f (Hz)	Po (N/m ²)	f (Hz)	Po (N/m ²)
110	2517.000	54.00	3206.000	120.00	4386.000	137.00
	2594.000	68.00	3232.000	134.00	4415.000	139.00
	2800.000	77.00	3385.000	137.00	4514.000	139.00
	2837.000	87.00	3589.000	138.00	6000.000	139.00
	2919.000	90.00	3889.000	139.00	8000.000	139.00
	3010.000	98.00	4070.000	139.00	12000.000	139.00
	3048.000	77.00	4122.000	138.00	15000.000	139.00
	3143.000	84.00	4230.000	136.00	17000.000	139.00
	3172.000	94.00	4313.000	131.00		
	3189.000	106.00	4346.000	133.00		
120	175.000	143.60	1246.000	9.00	3916.000	139.00
	319.000	143.60	1300.000	6.00	3963.000	134.00
	400.000	143.60	1347.000	5.00	3996.000	128.00
	500.000	143.60	1423.000	4.00	4013.000	121.00
	600.000	143.60	1536.000	3.00	4022.000	103.00
	667.000	142.00	1664.000	3.00	4039.000	82.00
	718.000	140.00	1788.000	5.00	4056.000	66.00
	752.000	129.00	1884.000	6.00	4107.000	52.00
	761.000	115.00	2031.000	8.00	4137.000	44.00
	769.000	100.00	2127.000	9.00	4253.000	31.00
	775.000	95.00	2212.000	9.00	4300.000	28.00
	789.000	105.00	2341.000	9.00	4344.000	46.00
	803.000	113.00	2495.000	11.00	4361.000	82.00
	819.000	119.00	2549.000	14.00	4377.000	115.00
	863.000	98.00	2796.000	19.00	4399.000	128.00
	879.000	74.00	2946.000	23.00	4416.000	133.00
	903.000	58.00	3126.000	31.00	4489.000	143.60
	923.000	44.00	3202.000	39.00	4576.000	143.60
	942.000	34.00	3296.000	54.00	5000.000	143.60
	977.000	29.00	3388.000	69.00	7000.000	143.60
	1021.000	36.00	3459.000	104.00	10000.000	143.60
	1051.000	31.00	3610.000	130.00	13000.000	143.60
	1085.000	23.00	3687.000	139.00	16000.000	143.60
	1120.000	18.00	3784.000	142.00	18000.000	143.60
	1183.000	12.00	3889.000	142.00		

$dc = 1.27 \text{ cm.}$ $g = 3.81 \text{ cm.}$

$P_s = 660 \text{ N/m}^2$

$Q_s = 14.9 \times 10^{-6} \text{ m}^3/\text{sec.}$

P_c (db)	f (Hz)	P_o (N/m ²)	f (Hz)	P_o (N/m ²)	f (Hz)	P_o (N/m ²)
90	400.000	95.20	2608.000	89.60	3664.000	95.20
	500.000	95.20	2702.000	92.00	3694.000	96.80
	1058.000	92.80	2765.000	92.80	3732.000	95.20
	1177.000	92.00	3045.000	91.20	3800.000	96.00
	1281.000	74.20	3122.000	96.00	3937.000	96.00
	1325.000	41.20	3242.000	95.20	3961.000	96.80
	1636.000	11.30	3362.000	96.80	4036.000	96.00
	1973.000	42.80	3426.000	95.20	4200.000	97.60
	2100.000	74.20	3472.000	96.00	4400.000	96.80
	2256.000	75.90	3542.000	96.80	4434.000	95.20
	2423.000	92.00	3589.000	95.20	4485.000	95.20
	2590.000	92.00	3622.000	95.20	4600.000	92.80
100	400.000	95.20	2423.000	20.20	3664.000	96.80
	500.000	95.20	2590.000	31.50	3694.000	96.00
	900.000	95.20	2608.000	23.40	3732.000	96.80
	927.000	77.50	2702.000	25.80	3800.000	96.80
	964.000	53.30	2765.000	38.70	3937.000	96.80
	990.000	43.60	3045.000	66.20	3961.000	98.50
	1058.000	50.00	3122.000	81.50	4036.000	96.80
	1177.000	25.80	3242.000	88.80	4200.000	99.30
	1281.000	15.30	3362.000	96.80	4400.000	96.80
	1325.000	11.30	3426.000	96.80	4434.000	95.20
	1636.000	4.80	3472.000	96.00	4485.000	95.20
	1973.000	12.10	3542.000	96.00	4600.000	92.80
	2100.000	16.10	3589.000	96.00		
	2256.000	16.10	3622.000	96.80		
110	400.000	96.80	2256.000	6.45	3622.000	98.50
	662.000	95.20	2423.000	6.45	3664.000	97.60
	694.000	83.90	2590.000	10.50	3694.000	98.50
	732.000	72.60	2608.000	8.90	3732.000	97.60
	768.000	48.40	2702.000	8.90	3800.000	96.80
	846.000	32.20	2765.000	11.30	3937.000	100.90
	975.000	11.30	3045.000	42.5.80	3961.000	100.90
	1058.000	14.50	3122.000	28.20	4036.000	99.30
	1177.000	8.90	3242.000	43.60	4200.000	95.20
	1281.000	5.60	3362.000	72.60	4400.000	96.80
	1325.000	4.80	3426.000	91.80	4434.000	95.20
	1636.000	2.40	3472.000	96.00	4485.000	95.20
	1973.000	4.80	3542.000	97.60	4600.000	92.80
	2100.000	5.84	3589.000	98.50		

$dc = 1.27 \text{ cm.}$ $g = 3.81 \text{ cm.}$

$P_s = 660 \text{ N/m}^2$

$Q_s = 14.9 \times 10^{-6} \text{ m}^3/\text{sec.}$

P_c (db)	f (Hz)	P_o (N/m ²)	f (Hz)	P_o (N/m ²)	f (Hz)	P_o (N/m ²)
120	175.000	95.20	717.000	23.40	3622.000	64.60
	400.000	97.60	765.000	15.30	3664.000	74.20
	500.000	90.40	805.000	11.30	3694.000	84.70
	509.000	87.20	860.000	8.07	3732.000	90.40
	520.000	95.20	922.000	5.60	3800.000	95.20
	540.000	92.00	950.000	4.80	3937.000	71.80
	560.000	97.60	1000.000	4.00	3961.000	43.60
	575.000	88.70	1200.000	3.20	4036.000	13.70
	590.000	79.90	1500.000	3.20	4200.000	4.80
	603.000	67.80	3000.000	8.07	4400.000	11.30
	625.000	57.30	3426.000	17.80	4434.000	24.20
	643.000	48.40	3472.000	24.10	4485.000	65.40
	662.000	40.40	3542.000	40.40	4600.000	92.80
	684.000	31.50	3589.000	52.50	18000.000	95.20

 $dc = 2.54 \text{ cm.}$ $g = 1.27 \text{ cm.}$

$P_s = 660 \text{ N/m}^2$

$Q_s = 14.9 \times 10^{-6} \text{ m}^3/\text{sec.}$

90	185.000	173.00	4000.000	173.00	11000.000	173.00
	850.000	173.00	7000.000	173.00	15000.000	173.00
	1450.000	173.00	9000.000	173.00	17000.000	173.00
					18000.000	173.00
100	190.000	173.00	3000.000	173.00	10000.000	173.00
	800.000	173.00	6000.000	173.00	13000.000	173.00
	1500.000	173.00	8000.000	173.00	16000.000	173.00
					18000.000	173.00
110	180.000	173.00	773.000	166.20	1500.000	173.00
	400.000	173.00	782.000	164.60	2200.000	173.00
	600.000	173.00	789.000	166.20	4800.000	173.00
	720.000	173.00	800.000	167.40	6200.000	173.00
	743.000	173.00	828.000	169.40	12000.000	173.00
	753.000	171.10	833.000	171.10	18000.000	173.00
	759.000	169.50	840.000	173.00		
	765.000	167.90	1100.000	173.00		

dc = 2.54 cm.

g = 1.27 cm.

$$P_s = 660 \text{ N/m}^2$$

$$Q_s = 14.9 \times 10^{-6} \text{ m}^3/\text{sec.}$$

Pc (db)	f (Hz)	Po (N/m ²)	f (Hz)	Po (N/m ²)	f (Hz)	Po (N/m ²)
120	175.000	173.00	898.000	153.30	3221.000	173.00
	335.000	173.00	921.000	156.60	3412.000	173.00
	442.000	173.00	939.000	161.40	3550.000	173.00
	563.000	173.00	973.000	166.20	3656.000	173.00
	611.000	173.00	1015.000	169.50	3756.000	173.00
	684.000	171.10	1155.000	170.30	3792.000	171.10
	693.000	169.50	1338.000	171.10	3828.000	169.50
	701.000	167.90	1476.000	171.10	3858.000	167.90
	711.000	164.60	1641.000	171.10	3923.000	164.60
	723.000	159.60	1782.000	171.10	3974.000	171.10
	732.000	153.30	1852.000	171.10	4017.000	171.10
	741.000	143.60	1900.000	171.10	4039.000	171.10
	750.000	137.20	1965.000	171.10	4104.000	173.00
	761.000	129.10	2029.000	171.10	4210.000	173.00
	770.000	121.10	2154.000	171.10	4443.000	173.00
	782.000	114.40	2242.000	171.10	4584.000	173.00
	797.000	121.10	2353.000	171.10	4675.000	173.00
	811.000	122.70	2476.000	171.10	6000.000	173.00
	835.000	125.90	2700.000	171.10	8000.000	173.00
	853.000	130.70	2815.000	171.10	11000.000	173.00
	864.000	137.20	3000.000	173.00	18000.000	173.00
	879.000	148.50	3150.000	173.00		

d c = 2.54 cm.

$$P_s = 660 \text{ N/m}^2$$

g = 2.54 cm.

$$Q_s = 14.9 \times 10^{-6} \text{ m}^3/\text{sec.}$$

Pc (db)	f (Hz)	Po (N/m ²)	f (Hz)	Po (N/m ²)	f (Hz)	Po (N/m ²)
90	165.000	136.00	787.000	133.10	2300.000	136.00
	360.000	136.00	792.000	134.70	4800.000	136.00
	540.000	136.00	802.000	135.50	5600.000	136.00
	680.000	136.00	810.000	136.00	7800.000	136.00
	700.000	136.00	889.000	136.00	11500.000	136.00
	723.000	136.00	972.000	136.00	13750.000	136.00
	745.000	136.00	1031.000	136.00	16750.000	136.00
	771.000	134.70	1350.000	136.00	18000.000	136.00
	777.000	133.40	1550.000	136.00		
	781.000	133.90	1850.000	136.00		

$d_c = 2.54 \text{ cm.}$ $g = 2.54 \text{ cm.}$

$$P_s = 660 \text{ N/m}^2$$

$$Q_s = 14.9 \times 10^{-6} \text{ m}^3/\text{sec.}$$

P_c (db)	f (Hz)	P_o (N/m ²)	f (Hz)	P_o (N/m ²)	f (Hz)	P_o (N/m ²)
100	180.000	135.50	789.000	75.80	1240.000	135.50
	370.000	135.50	792.000	86.30	1308.000	135.50
	470.000	135.50	799.000	95.90	1428.000	135.50
	520.000	135.50	807.000	103.30	1540.000	135.50
	605.000	135.50	816.000	112.10	1618.000	135.50
	696.000	135.50	823.000	116.20	1822.000	135.50
	710.000	126.70	831.000	118.60	1904.000	135.50
	726.000	133.10	837.000	121.00	2090.000	135.50
	736.000	120.70	843.000	123.40	2182.000	135.50
	745.000	125.10	849.000	125.90	2318.000	135.50
	751.000	118.60	854.000	128.30	2504.000	135.50
	758.000	109.70	880.000	130.70	2733.000	135.50
	764.000	99.20	908.000	132.20	2931.000	135.50
	768.000	88.70	924.000	133.10	3600.000	135.50
	771.000	80.70	946.000	124.70	6500.000	135.50
	775.000	74.20	968.000	135.50	10500.000	135.50
	780.000	72.60	1047.000	135.50	16500.000	135.50
	783.000	70.90	1141.000	135.50	18000.000	135.50
110	175.000	136.00	867.000	43.50	2132.000	104.70
	350.000	136.00	882.000	52.40	2205.000	114.60
	450.000	136.00	898.000	62.70	2306.000	117.80
	500.000	136.00	912.000	75.80	2411.000	121.80
	600.000	136.00	929.000	81.50	2504.000	125.00
	646.000	134.70	947.000	91.20	2547.000	128.30
	661.000	132.30	966.000	95.20	2736.000	129.90
	669.000	130.70	970.000	92.80	2800.000	132.30
	682.000	125.00	1002.000	104.00	2923.000	134.90
	698.000	117.90	1030.000	108.90	3031.000	134.70
	705.000	105.70	1059.000	104.70	3191.000	134.70
	711.000	92.80	1086.000	109.70	3260.000	135.50
	717.000	79.10	1097.000	108.90	3399.000	135.50
	722.000	67.80	1121.000	108.90	3471.000	136.00
	729.000	52.40	1227.000	108.10	3668.000	136.00
	738.000	39.50	1321.000	107.30	3790.000	136.00
	748.000	29.80	1412.000	107.30	3846.000	134.70
	763.000	20.40	1473.000	105.70	3856.000	133.90
	771.000	19.30	1529.000	104.90	3900.000	135.50
	780.000	17.70	1557.000	104.00	6000.000	136.00
	792.000	18.50	1622.000	103.30	8000.000	136.00
	809.000	20.10	1733.000	104.90	12000.000	136.00
	820.000	23.40	1822.000	106.50	18000.000	136.00
	832.000	28.20	1941.000	106.50		
	849.000	36.30	2029.000	107.30		

$d_c = 2.54 \text{ cm.}$

$$P_s = 660 \text{ N/m}^2$$

 $g = 2.54 \text{ cm.}$

$$Q_s = 14.9 \times 10^{-6} \text{ m}^3/\text{sec.}$$

Pc (db)	f (Hz)	Po (N/m ²)	f (Hz)	Po (N/m ²)	f (Hz)	Po (N/m ²)
120	175.000	136.00	946.000	13.70	3171.000	99.20
	330.000	136.00	970.000	15.30	3208.000	106.50
	460.000	136.00	988.000	16.90	3249.000	113.80
	482.000	136.00	1005.000	18.50	3312.000	123.40
	505.000	135.50	1038.000	19.30	3265.000	126.70
	536.000	133.90	1098.000	19.30	3384.000	128.30
	564.000	131.50	1181.000	19.30	3432.000	130.70
	578.000	127.50	1264.000	19.30	3463.000	132.30
	600.000	114.60	1280.000	20.10	3504.000	134.70
	612.000	102.50	1482.000	20.90	3545.000	135.50
	623.000	94.40	1595.000	20.90	3620.000	136.00
	634.000	78.20	1696.000	20.10	3729.000	136.00
	642.000	66.90	1810.000	20.90	3787.000	135.50
	651.000	55.60	1933.000	21.80	3818.000	133.90
	663.000	44.40	2008.000	22.60	3835.000	128.30
	675.000	35.50	2136.000	22.60	3845.000	98.40
	683.000	28.20	2226.000	24.20	3852.000	74.20
	695.000	22.60	2341.000	24.20	3869.000	60.50
	716.000	18.50	2444.000	24.20	3875.000	80.70
	728.000	16.10	2480.000	28.20	3883.000	112.90
	744.000	13.70	2538.000	31.40	3894.000	128.30
	758.000	12.90	2562.000	36.30	3924.000	133.10
	775.000	12.00	2808.000	49.20	3945.000	135.50
	782.000	11.30	2896.000	62.90	4000.000	136.00
	813.000	11.30	2972.000	73.40	7000.000	136.00
	846.000	11.30	3060.000	78.20	11000.000	136.00
	881.000	12.00	3090.000	83.40	17500.000	136.00
	916.000	12.90	3136.000	94.40		

dc = 2.54 cm.

$$P_s = 660 \text{ N/m}^2$$

g = 3.81 cm.

$$Q_s = 14.9 \times 10^{-6} \text{ m}^3/\text{sec.}$$

f_c (db)	f (Hz)	P_o (N/m ²)	f (Hz)	P_o (N/m ²)	f (Hz)	P_o (N/m ²)
90	170.000	111.00	787.000	36.00	1536.000	108.00
	450.000	111.00	803.000	45.00	1691.000	109.00
	600.000	111.00	818.000	63.00	1780.000	109.00
	689.000	109.00	834.000	82.00	1871.000	109.00
	714.000	107.00	847.000	92.00	2023.000	110.00
	725.000	104.00	867.000	94.00	2294.000	110.00
	738.000	98.00	899.000	100.00	2544.000	111.00
	748.000	91.00	948.000	101.00	2600.000	111.00
	753.000	88.00	983.000	103.00	5500.000	111.00
	759.000	65.00	1044.000	105.00	7300.000	111.00
	762.000	61.00	1131.000	106.00	8600.000	111.00
	768.000	41.00	1222.000	107.00	11500.000	111.00
	775.000	36.00	1220.000	107.00	14500.000	111.00
	782.000	31.00	1624.000	107.00	18000.000	111.00
100	170.000	111.00	861.000	12.60	1919.000	80.00
	500.000	111.00	880.000	17.80	2018.000	86.00
	589.000	110.00	912.000	24.60	2082.000	90.00
	620.000	109.00	961.000	32.00	2154.000	91.00
	648.000	107.00	993.000	32.00	2275.000	100.00
	660.000	103.00	1028.000	40.00	2420.000	105.00
	676.000	94.00	1054.000	43.00	2499.000	107.00
	687.000	87.00	1069.000	42.00	2561.000	108.00
	699.000	70.00	1094.000	42.00	2655.000	107.00
	706.000	56.00	1190.000	41.60	2720.000	108.00
	720.000	36.00	1298.000	43.30	2760.000	109.00
	734.000	22.00	1393.000	42.30	2912.000	110.00
	753.000	7.40	1475.000	50.60	3292.000	111.00
	778.000	4.20	1581.000	57.00	6000.000	111.00
	785.000	4.20	1611.000	53.00	9000.000	111.00
	811.000	5.20	1666.000	64.00	15000.000	111.00
	842.000	8.40	1823.000	68.00	18000.000	111.00
110	170.000	112.00	720.000	5.20	1638.000	9.00
	400.000	112.00	743.000	2.90	1755.000	9.40
	500.000	111.00	758.000	1.90	1890.000	10.90
	538.000	110.00	787.000	1.60	1980.000	11.60
	558.000	107.00	858.000	1.90	2084.000	11.90
	578.000	101.00	883.000	2.90	2199.000	13.20
	603.000	90.00	974.000	4.20	2266.000	14.50
	619.000	74.00	1017.000	5.50	2374.000	15.80
	628.000	59.00	1124.000	6.10	2459.000	19.00
	644.000	42.00	1231.000	7.10	2506.000	23.20
	658.000	26.00	1312.000	7.70	2589.000	25.50
	676.000	15.00	1442.000	8.00	2603.000	22.60
	702.000	8.07	1526.000	8.40	2694.000	24.20

dc = 2.59 cm.

g = 3.81 cm.

$$P_s = 660 \text{ N/m}^2$$

$$Q_s = 14.9 \times 10^{-6} \text{ m}^3/\text{sec.}$$

Pc (db)	f (Hz)	Po (N/m ²)	f (Hz)	Po (N/m ²)	f (Hz)	Po (N/m ²)
110	2719.000	28.40	3207.000	108.00	3892.000	109.00
	2741.000	32.60	3311.000	110.00	3913.000	110.00
	2776.000	37.10	3500.000	110.00	3989.000	111.00
	2809.000	43.60	3614.000	111.00	4082.000	111.00
	2918.000	70.00	3712.000	111.00	4120.000	111.00
	2950.000	86.00	3808.000	111.00	6500.000	111.00
	2987.000	98.00	3844.000	111.00	8000.000	111.00
	3042.000	101.00	3871.000	110.00	14000.000	111.00
	3105.000	105.00	3883.000	110.00	18000.000	111.00
120	170.000	113.00	1644.000	1.90	3827.000	108.00
	251.000	111.00	1819.000	1.90	3847.000	100.00
	302.000	113.00	1915.000	2.30	3858.000	74.00
	370.000	112.00	2039.000	2.30	3866.000	34.00
	282.000	111.00	2158.000	2.60	3875.000	15.00
	405.000	111.00	2445.000	2.90	3901.000	19.00
	434.000	109.00	2544.000	3.60	3910.000	53.00
	457.000	104.00	2664.000	4.20	3913.000	64.00
	485.000	94.00	2760.000	4.80	3924.000	96.00
	501.000	80.00	2850.000	6.10	3946.000	107.00
	517.000	67.00	2965.000	8.70	3986.000	109.00
	531.000	48.00	3014.000	9.40	4027.000	110.00
	552.000	28.00	3109.000	11.90	4111.000	111.00
	587.000	15.00	3218.000	15.80	4220.000	111.00
	602.000	10.00	3247.000	19.00	4326.000	111.00
	632.000	6.00	3293.000	28.70	4425.000	111.00
	660.000	4.00	3337.000	37.40	4572.000	112.00
	701.000	2.00	3362.000	42.00	4688.000	112.00
	750.000	2.00	3398.000	55.00	4798.000	112.00
	835.000	2.00	3417.000	61.00	4964.000	112.00
	885.000	1.30	3433.000	66.00	5204.000	112.00
	914.000	0.90	3460.000	85.00	5656.000	112.00
	1000.000	1.00	3491.000	95.00	6122.000	112.00
	1122.000	1.00	3520.000	102.00	7090.000	112.00
	1225.000	1.00	3569.000	106.00	11000.000	112.00
	1328.000	1.30	3594.000	107.00	15000.000	112.00
	1435.000	1.60	3658.000	109.00	18000.000	112.00
	1546.000	1.60	3792.000	110.00		

dc = 2.54 cm.

g = 3.81 cm.

Pc = 100 db.

P_s (N/m ²)	f (Hz)	P_o (N/m ²)	f (Hz)	P_o (N/m ²)	f (Hz)	P_o (N/m ²)
834	460.000	167.90	940.000	112.90	4400.000	167.90
	560.000	167.90	1100.000	111.40	4800.000	167.90
	660.000	167.90	1300.000	92.00	5200.000	166.20
	700.000	137.20	1550.000	80.70	5200.000	167.90
	740.000	69.40	1850.000	56.90	7400.000	167.90
	760.000	24.20	2000.000	56.20	8600.000	167.90
	770.000	19.40	2200.000	50.00	10000.000	167.90
	780.000	17.80	2600.000	75.90	12000.000	167.90
	800.000	24.20	3100.000	82.90	15000.000	167.90
	840.000	62.90	3700.000	163.00	20000.000	167.90
920	460.000	201.80	940.000	167.90	3400.000	200.10
	560.000	201.80	1100.000	151.70	4800.000	201.80
	660.000	201.80	1300.000	127.50	5200.000	201.80
	700.000	129.60	1550.000	119.40	6200.000	201.80
	740.000	95.20	1850.000	72.60	7400.000	201.80
	760.000	53.30	2000.000	61.30	8600.000	201.80
	770.000	37.10	2200.000	50.00	10000.000	201.80
	780.000	32.30	2600.000	58.10	12000.000	201.80
	800.000	56.50	3100.000	54.90	15000.000	201.80
	840.000	112.90	3700.000	163.00	20000.000	201.80
1030	460.000	246.90	940.000	216.30	4400.000	177.50
	560.000	246.90	1100.000	203.40	4800.000	237.30
	660.000	246.90	1300.000	161.40	5200.000	246.90
	700.000	235.60	1550.000	146.90	6200.000	246.90
	740.000	129.10	1850.000	92.00	7400.000	246.90
	760.000	72.60	2000.000	75.90	8600.000	246.90
	770.000	64.60	2200.000	56.50	10000.000	246.90
	780.000	56.80	2600.000	55.70	12000.000	246.90
	800.000	102.30	3100.000	43.60	15000.000	246.90
	840.000	167.90	3700.000	104.90	20000.000	246.90
1120	460.000	285.00	1100.000	226.70	5200.000	177.80
	560.000	281.90	1300.000	186.30	6200.000	165.00
	660.000	284.00	1550.000	181.50	7400.000	165.00
	700.000	275.00	1850.000	111.60	8600.000	165.00
	750.000	142.50	2000.000	78.00	10000.000	165.00
	770.000	87.40	2600.000	55.00	12000.000	165.00
	780.000	73.00	3100.000	42.00	15000.000	165.00
	800.000	106.60	3700.000	66.30	18000.000	165.00
	840.000	167.80	4400.000	71.20	22000.000	165.00
	940.000	213.70	4800.000	165.00		

$d_c = 2.54 \text{ cm.}$

$g = 3.81 \text{ cm.}$

$P_c = 100 \text{ db.}$

P_s (N/m ²)	f (Hz)	P_o (N/m ²)	f (Hz)	P_o (N/m ²)	f (Hz)	P_o (N/m ²)
1220	460.000	327.60	940.000	319.60	4400.000	66.20
	560.000	327.60	1100.000	305.00	4800.000	98.50
	660.000	327.60	1300.000	264.70	5200.000	179.30
	700.000	327.60	1550.000	203.40	6200.000	319.60
	740.000	217.90	1850.000	174.30	7400.000	327.60
	760.000	167.90	2000.000	135.60	8600.000	327.60
	770.000	132.30	2200.000	98.50	10000.000	327.60
	780.000	59.70	2600.000	66.20	12000.000	327.60
	800.000	153.30	3100.000	38.70	15000.000	327.60
	840.000	222.70	3700.000	64.60	20000.000	327.60

$d_c = 0.95 \text{ cm.}$

$g = 1.27 \text{ cm.}$

$P_c = 110 \text{ db.}$

260	175.000	25.80	1600.000	25.80	6000.000	25.80
	205.000	25.80	1800.000	25.80	8000.000	25.80
	480.000	25.80	1900.000	25.80	10000.000	25.80
	680.000	25.80	2000.000	25.80	12000.000	25.80
	890.000	25.80	2200.000	25.80	14000.000	25.80
	1050.000	25.80	2600.000	25.80	16000.000	25.80
	1200.000	25.80	3700.000	25.80	18000.000	25.80
	1400.000	25.80	4800.000	25.80		
974	175.000	338.90	1925.000	209.80	2455.000	326.80
	400.000	338.90	1951.000	189.60	2490.000	330.40
	600.000	338.90	1976.000	177.50	2529.000	330.40
	800.000	338.90	1994.000	181.60	2564.000	334.40
	1000.000	338.90	2006.000	197.70	2585.000	330.40
	1200.000	338.90	2021.000	213.90	2643.000	326.80
	1400.000	338.90	2032.000	221.90	2610.000	322.80
	1600.000	338.90	2053.000	242.10	2627.000	314.70
	1650.000	338.90	2076.000	262.30	2649.000	314.70
	1710.000	334.90	2110.000	278.40	2662.000	314.70
	1771.000	330.80	2173.000	290.50	2674.000	318.80
	1821.000	318.80	2205.000	302.60	2687.000	322.80
	1843.000	306.70	2248.000	318.80	2710.000	326.80
	1865.000	286.50	2300.000	314.70	2745.000	326.80
	1879.000	262.30	2318.000	310.70	2795.000	330.90
	1890.000	246.10	2354.000	314.70	2814.000	330.90
	1915.000	221.90	2403.000	322.80	2856.000	330.90

dc = 0.95 cm.

g = 1.27 cm.

Pc = 110 db.

P _s (N/m ²)	f (Hz)	P _o (N/m ²)	f (Hz)	P _o (N/m ²)	F (Hz)	P _o (N/m ²)
974	2891.000	334.90	3494.000	338.90	4673.000	310.70
	2915.000	334.90	3523.000	338.90	4704.000	314.70
	2962.000	334.90	3600.000	338.90	4754.000	322.80
	3019.000	334.90	3700.000	338.90	4797.000	326.80
	3071.000	334.90	3800.000	338.90	4851.000	330.90
	3148.000	334.90	3900.000	338.90	4911.000	334.90
	3187.000	338.90	4000.000	338.90	4976.000	334.90
	3234.000	338.90	4143.000	338.90	5000.000	334.90
	3266.000	338.90	4204.000	338.90	5052.000	338.90
	3295.000	338.90	4294.000	338.90	6000.000	338.90
	3317.000	338.90	4348.000	330.90	8000.000	338.90
	3335.000	338.90	4426.000	326.80	12000.000	338.90
	3352.000	338.90	4521.000	322.80	15000.000	338.90
	3384.000	338.90	4575.000	314.70	18000.000	338.90
	3410.000	338.90	4619.000	306.70		
1253	168.000	524.60	2025.000	407.50	3864.000	524.60
	278.000	524.60	2041.000	427.70	4060.000	524.60
	377.000	524.60	2054.000	439.80	4165.000	520.50
	496.000	524.60	2063.000	451.90	4185.000	516.50
	564.000	524.60	2074.000	464.00	4212.000	516.50
	674.000	524.60	2096.000	480.20	4287.000	512.40
	747.000	524.60	2131.000	492.30	4366.000	508.40
	833.000	524.60	2188.000	504.40	4395.000	500.30
	908.000	524.60	2224.000	508.40	4429.000	492.30
	1070.000	524.60	2304.000	508.40	4469.000	476.10
	1128.000	524.60	2403.000	512.40	4535.000	427.70
	1176.000	524.60	2460.000	516.50	4565.000	407.50
	1328.000	524.60	2525.000	520.50	4609.000	394.10
	1400.000	524.60	2554.000	524.60	4641.000	351.00
	1533.000	524.60	2610.000	516.50	4690.000	351.00
	1600.000	524.60	2631.000	512.40	4728.000	367.20
	1703.000	524.60	2675.000	512.40	4770.000	411.60
	1742.000	520.50	2702.000	516.50	4787.000	443.90
	1785.000	516.50	2744.000	520.50	4814.000	459.90
	1815.000	512.40	2798.000	520.50	4878.000	476.10
	1880.000	496.30	2838.000	520.50	4913.000	488.20
	1897.000	464.00	2910.000	524.60	5002.000	500.30
	1917.000	439.80	3050.000	524.60	5051.000	514.40
	1939.000	407.50	3164.000	524.60	5084.000	504.40
	1972.000	379.30	3242.000	524.60	5129.000	510.30
	1997.000	383.20	3375.000	524.60	5161.000	500.30
	2008.000	387.40	3565.000	524.60	5216.000	500.30

dc = 0.95 cm.

g = 1.27 cm.

Pc = 110 db.

P_s (N/m ²)	f (Hz)	P_o (N/m ²)	f (Hz)	P_o (N/m ²)	f (Hz)	P_o (N/m ²)
1253	5267.000	504.40	5706.000	520.50	8400.000	524.60
	5326.000	504.40	5788.000	520.50	11400.000	524.60
	5490.000	504.40	5874.000	520.50	13700.000	524.60
	5541.000	508.40	5988.000	520.50	16500.000	524.60
	5599.000	516.50	6810.000	524.60	18000.000	524.60
1898	166.000	979.96	4387.000	970.20	6878.000	960.44
	205.000	979.96	4429.000	955.56	7028.000	955.56
	234.000	979.96	4477.000	901.27	7218.000	940.62
	448.000	979.96	4514.000	857.05	7288.000	930.86
	668.000	979.96	4561.000	822.58	7430.000	940.62
	808.000	979.96	4588.000	812.52	7574.000	930.86
	960.000	979.96	4660.000	812.52	7619.000	921.10
	1050.000	979.96	4714.000	802.76	7678.000	886.63
	1180.000	979.96	4757.000	812.52	7731.000	842.10
	1350.000	979.96	4783.000	822.58	7758.000	832.34
	1500.000	979.96	4818.000	842.10	7800.000	822.58
	1650.000	979.96	4857.000	871.69	7843.000	837.22
	1791.000	979.96	4889.000	886.63	7859.000	852.17
	1800.000	979.96	4929.000	911.03	7883.000	886.63
	1838.000	975.08	4997.000	935.74	7906.000	904.93
	1856.000	965.32	5078.000	945.50	7954.000	940.62
	1902.000	950.68	5173.000	940.62	7998.000	955.56
	1955.000	930.86	5265.000	945.50	8034.000	965.32
	1972.000	921.10	5360.000	935.74	8113.000	965.32
	1990.000	916.22	5515.000	940.62	8154.000	960.44
	2004.000	930.86	5596.000	950.68	8230.000	950.68
	2020.000	940.62	5721.000	955.56	8317.000	945.56
	2061.000	950.68	5891.000	950.68	8427.000	945.56
	2087.000	960.44	6026.000	935.74	8575.000	935.74
	2148.000	965.32	6043.000	930.86	8709.000	935.74
	2180.000	970.20	6071.000	925.48	8873.000	940.62
	2203.000	975.08	6095.000	940.62	9000.000	935.74
	2237.000	979.96	6141.000	950.68	9149.000	945.56
	2500.000	979.96	6210.000	935.74	9298.000	945.56
	2600.000	979.96	6231.000	925.48	9429.000	945.56
	2700.000	979.96	6331.000	935.74	9680.000	935.74
	2800.000	979.96	6355.000	935.74	9828.000	940.62
	3000.000	979.96	6458.000	930.86	9987.000	955.56
	3200.000	979.96	6518.000	925.48	10098.000	960.44
	3400.000	979.96	6544.000	935.74	10253.000	965.32
	3600.000	979.96	6578.000	955.56	10387.000	965.32
	3800.000	979.96	6631.000	955.56	10617.000	970.20
	4000.000	979.96	6663.000	940.62	10780.000	975.08
	4150.000	979.96	6711.000	945.50	10980.000	979.96
	4302.000	979.96	6790.000	955.56	11000.000	979.96
	4346.000	975.08	6827.000	965.32		

dc = 0.95 cm.

g = 1.27 cm.

Pc = 110 db.

P_s (N/m ²)	f (Hz)	P_o (N/m ²)	f (Hz)	P_o (N/m ²)	f (Hz)	P_o (N/m ²)
1898	13000.000	979.96				
	15000.000	979.96				
	18000.000	979.96				
2647	170.000	1600.90	4956.000	1594.70	9627.000	1396.10
	300.000	1600.90	5025.000	1600.90	9651.000	1352.70
	600.000	1600.90	5200.000	1600.90	9700.000	1290.60
	800.000	1600.90	5400.000	1600.90	9786.000	1383.70
	1000.000	1600.90	5800.000	1600.90	9825.000	1402.30
	1200.000	1600.90	6300.000	1600.90	9965.000	1433.40
	1400.000	1600.90	6800.000	1600.90	10068.000	1476.80
	1600.000	1600.90	7000.000	1600.90	10114.000	1501.60
	1800.000	1613.30	7200.000	1600.90	10204.000	1538.80
	1838.000	1619.50	7370.000	1569.90	10326.000	1538.80
	1897.000	1625.70	7500.000	1588.50	10472.000	1532.60
	1981.000	1576.10	7634.000	1588.50	10625.000	1526.40
	2026.000	1588.00	7654.000	1563.70	10820.000	1545.60
	2067.000	1607.00	7670.000	1538.80	11066.000	1538.80
	2081.000	1613.00	7686.000	1495.40	11267.000	1545.00
	2300.000	1600.90	7705.000	1427.20	11390.000	1538.80
	2400.000	1600.90	7716.000	1389.90	11507.000	1545.00
	2600.000	1600.90	7748.000	1303.10	11615.000	1532.60
	2800.000	1600.90	7784.000	1191.40	11873.000	1538.80
	3000.000	1600.90	7821.000	1092.10	11976.000	1545.00
	3200.000	1600.90	7859.000	1290.60	12032.000	1551.30
	3400.000	1600.90	7882.000	1493.60	12215.000	1557.50
	3800.000	1600.90	7895.000	1484.20	12312.000	1563.70
	4200.000	1600.90	7943.000	1563.70	12450.000	1569.90
	4400.000	1600.90	8002.000	1588.50	12620.000	1576.10
	4494.000	1576.10	8111.000	1594.70	12836.000	1582.30
	4530.000	1538.80	8200.000	1588.50	13032.000	1588.50
	4576.000	1433.40	8286.000	1576.10	13336.000	1594.70
	4592.000	1365.10	8400.000	1576.10	13855.000	1594.70
	4615.000	992.80	8487.000	1557.50	14152.000	1600.90
	4623.000	967.60	8567.000	1526.40	14500.000	1600.90
	4659.000	1110.70	8840.000	1495.40	15000.000	1582.30
	4687.000	1241.00	9004.000	1482.90	15069.000	1582.30
	4723.000	1340.30	9159.000	1501.60	15125.000	1588.50
	4737.000	1346.10	9294.000	1495.40	15267.000	1600.90
	4759.000	1458.20	9395.000	1464.40	16000.000	1600.90
	4791.000	1507.80	9451.000	1451.90	17000.000	1600.90
	4867.000	1557.60	9530.000	1439.60	18000.000	1500.90

$$d_c = 0.95 \text{ cm.}$$

$$g = 1.27 \text{ cm.}$$

$$P_s = 660 \text{ N/m}^2$$

$$f = 1979 \text{ Hz}$$

$$Q_s = 14.9 \times 10^{-6} \text{ m}^3/\text{sec.}$$

Pc (db)	Po (N/m ²)
90	174.3
95	171.1
100	156.6
102	146.9
105	117.8
107.5	88.8
110	61.3
112.5	41.2
115.0	30.7
120	17.8
125	15.3

APPENDIX E.3

SWITCHING TIMES

$$dc = 2.54 \text{ cm.}$$

$$g = 3.81 \text{ cm.}$$

$$P_s = 1120 \text{ N/m}^2 \quad (\text{Re} = 1244)$$

$$Q_s = 18.7 \times 10^{-6} \text{ m}^3/\text{sec.}$$

f (Hz)	Pc (db.)	T _{Q.d.} (m.sec.)	T _{f.} (m.sec.)	T _{t.d.} (m.sec.)	Tr. (m.sec.)
2200	90	2.4	0.4	2.4	0.4
2200	95	2.3	0.5	2.4	0.6
2200	100	2.2	0.4	2.8	0.9
2600	90	2.0	0.4	2.4	0.7
2600	95	2.4	0.5	2.0	0.5
2600	100	2.3	0.6	2.5	0.9
3100	90	2.4	0.5	2.2	0.5
3100	95	2.2	0.6	2.3	0.6
3100	100	2.2	0.7	2.5	0.8
3700	90	2.3	0.5	2.4	0.5
3700	95	2.2	0.3	2.2	0.5
3700	100	2.1	0.5	2.7	0.6
4400	90	2.2	0.3	2.3	0.4
4400	95	2.2	0.3	2.4	0.2
4400	100	2.1	0.7	2.6	0.5

$d_c = 2.54 \text{ cm.}$

$g = 3.81 \text{ cm.}$

$P_c = 100 \text{ db.}$

$f = 3100 \text{ Hz.}$

P_s (N/m ²)	Q_s (m ³ /sec. \times 10 ⁻⁶)	Tq.d.	Tf.	Tt.d.	Tr.
1220	23.5	2.0	0.3	2.4	0.5
1030	20.5	2.0	0.5	2.7	1.3
920	19.3	2.3	0.8	3.0	0.5
834	17.5	2.7	0.4	3.0	0.6

VITA AUCTORIS

- 1948 Born in Chatham, Ontario, Canada on April 23.
- 1965 Completed high school Chatham Kent Secondary School, Chatham, Ontario, Canada in June.
- 1968 Received the Mechanical Technologist Diploma from St. Clair College, Windsor, Ontario, Canada in May.
- 1971 Received the Degree of Bachelor of Applied Science in Mechanical Engineering from the University of Windsor, Windsor, Ontario, Canada in May.
- 1974 Currently a candidate for the Degree of Master of Applied Science in Mechanical Engineering at the University of Windsor, Windsor, Ontario, Canada.